Data Acquisition System Design and Validation to Record Interior Cabin Noise Levels of Aircraft

by

Andrew Lawrence Price

A thesis submitted to the Faculty of Graduate and Postdoctoral Affairs in partial fulfillment of the requirements for the degree of

Master of Applied Science

in

Aerospace Engineering

Carleton University
Ottawa, Ontario

Abstract

Aircraft crew members and maintenance personnel are subject to significantly high sound pressure levels. Cumulative exposure to such high levels could induce hearing loss. Therefore, choosing the optimal hearing protector is of the utmost importance. The equipment used to measure the sound levels in the aircraft cabin for helmet selection must be subjected to airworthiness regulations to be flown. This thesis documents the selection, implementation and validation of an in-flight data acquisition system. The signal route is characterized with digital signal processing theory and a comparison to LMS Test.LAB acoustic analysis software. Bell 412 in-flight data is presented to validate the measurement method. The main rotor and tail rotor harmonics were found to dominate the low frequency sound pressure levels. The analysis concluded that the SPH 5CF helmet satisfies the Canadian Labour Code Part II for in-flight occupant noise exposure limit of a maximum of 87 dBA for eight hours.

Acknowledgements

I would like to extend my deepest thanks and immeasurable appreciation to the following persons who helped make this study possible.

Firstly, to **Dr. Viresh Wickramasinghe**, who has made these life changing experiences possible for me as well as supported me throughout the entire Master's process. Any success I have achieved in this project owes credit to his level of trust and support throughout it all.

To **Dr. Fred Nitzsche**, who provided the single most life changing, research opportunity of my young life.

To **Dr. Sebastian Ghinet**, **Dr. Yong Chen**, **Brent Lawrie** and all the guys at good ol' U66A, who answered every one of my seemingly endless questions. I am so thankful for every opportunity I got to work with you on your projects. I stayed late more than once, just for the opportunity to participate in and observe your work.

To the guys at the **NRC Airworthiness**, the **Design and Fabrication** as well as the **Instrumentation** labs who quite literally got the project up and flying. Thank you for all the hours you put into helping "that student and his DAS lunchbox project".

To **Dr. Craig Merrett**, who proved a most professional mentor and guide to me on a number of unplanned occasions. Your advice was always greatly appreciated and sought after.

To **Dr. Mojtaba Ahmadi**, **Dr. Daniel Feszty** and **Dr. David Lau** for their insight and support with my thesis and defence.

To my **brother** and **friends** who supported me throughout the past two years and helped edit. Thanks for keeping things lively.

And lastly, to my mother and father: **Linda** and **Dwayne Price** who have loved and supported me to an unknowable extent these past years. I could never have gotten to where I am without you. Thank you.

Table of Contents

List of Tables

List of Figures

List of Equations

List of Appendices

Abbreviations and Nomenclature

- A/D: Analog to Digital, commonly an analog to digital converter
- AWM: Airworthiness Manual (specifically, the Canadian Airworthiness Manual)
- BNC: Bayonet Neill-Concelman (a type of coaxial quick connect connector)
- DAS: Data Acquisition System
- DAU: Data Acquisition Unit
- DFT: Discrete Fourier Transform
- DSP: Digital Signal Processing
- EMC: Electromagnetic Compatibility
- EMI: Electromagnetic Interference
- FFT: Fast Fourier Transform
- HPs: Hearing Protectors
- ICP: Integrated Circuit Piezoelectric (trademark of PCB)
- NRC: National Research Council
- OSPL: Overall Sound Pressure Level (the total sound energy within the spectrum)
- PSD: Power Spectral Density (power squared per frequency band; narrow band)
- RMS: Root Mean Square
- SD: Spectral Density (a narrow band frequency domain, data display format)
- SLF: Steady Level Flight (aircraft maintained a constant heading, pitch, roll and speed)
- SPL: Sound Pressure Level
- TTC: Teletronics Technology Corporation

Unit	Description
A	Ampere, unit of electric current
dB	Decibel, $[dB] = 20\ log_{10}(\frac{P_1}{P_0})$, ratio measure of pressure, $P_0 = 2x\ 10^{-5}\ Pa$
dBA	Decibel, altered by acoustic weighting curve A
kts	Knots, $\sim 0.514\frac{m}{s}$, unit of speed
Pa	Pascal, $\frac{N}{m^2}$, unit of pressure
RMS	Root Mean Square, $RMS = \sqrt{\frac{1}{n}\sum x^2}$
V	Volt, $\frac{kg\ m^2}{A\ s^3}$, unit of electric potential
Hz	Hertz, $\frac{1}{s}$, a rate, often used to define frequencies or sample rates

1. Introduction

Background context and the motivation for recording cabin noise exposure in aircraft are provided in this chapter. The chapter begins with a literature review of similar projects including their challenges and implemented solutions. Next the thesis objective is characterized in section 1.2.

1.1. Introduction to Helicopter Noise and Vibration

A helicopter is a type of aircraft that produces both lift and propulsion from horizontal rotating rotors. All helicopters perform basic manoeuvres such as vertical take-off and hovering in addition to straight and level flight. This versatility allows helicopters to perform unique tasks such as landing in populated areas or on buildings, emergency evacuation and surveillance. Due to these capabilities, helicopters are found in many civilian and military settings.

The signature sound of a helicopter is produced by its rotors impacting the air. These rotors generate vortices. The helicopter is unique in that as it sheds these vortices they continually impact the body of the aircraft or the next advancing rotor blade. Additionally, it is common to have helicopter rotor tips approach or surpass the speed of sound, especially when coupled with the aircraft's forward motion. Further including the aircraft engine, it can be seen that a helicopter has a multitude of noise generation sources.

These vibrations and noises can have detrimental effects on human health. Many standards begin to take precautions against noise at $85\ dBA$ (A-weighted decibel) [1],

[2]. Most aircraft operate in excess of this. Noise and vibration are distinctly linked. High frequency vibration can lead to pilot or passenger exhaustion. Low frequency vibrations may cause large load variations on the body. The neck is especially vulnerable and has been the subject of much study. The situation is compounded with the additional weight of a helmet and its accessories [3]. This study will primarily focus on noise.

1.1.1. Hearing Conservation Risks

As noted above, $85\ dBA$ is a standard limit to begin hearing conservation control [1], [2]. The Aviation Occupational Health and Safety Regulations have the following exposure limits:

Table 1: Sound pressure level exposure limits [4]

SPL (dBA)	Exp. Limit (hours)	SPL (dBA)	Exp. Limit (hours)	SPL (dBA)	Exp. Limit (hours)	SPL (dBA)	Exp. Limit (hours)
84	16.0	93	2.0	102	0.25	111	0.032
85	13.0	94	1.6	103	0.20	112	0.025
86	10.0	95	1.3	104	0.16	113	0.020
87	8.0	96	1.0	105	0.13	114	0.016
88	6.4	97	0.80	106	0.10	115	0.013
89	5.0	98	0.64	107	0.080	116	0.010
90	4.0	99	0.50	108	0.064	117	0.008
91	3.2	100	0.40	109	0.050	118	0.006
92	2.5	101	0.32	110	0.040	119	0.005

For an 8-hour workday, a noise environment of $87\ dBA$ is acceptable. The labour code also states that $74\ dBA$ is sufficiently low enough that it can be excluded from noise exposure calculations [4]. Although these limits are quite detailed, hearing loss is not so easily quantified.

Degradation in hearing can be quantified as an average $10\ dB$ change at 2, 3 and $4\ kHz$ [2]. This degradation can be classified as two forms: temporary and permanent threshold shifts. A temporary threshold shift occurs quickly to help protect one against loud noises. A permanent threshold shift is irreversible and occurs over time; there are not necessarily any immediate effects. Permanent damage is often a result of damage to the hair cells in the inner ear [5]. As hearing naturally degrades with age, this degradation is in addition to any existing hearing damage. Therefore, although hearing damage may not be a current problem, it may develop to be severe and debilitating.

Hearing protectors (HPs) are used to mitigate hearing damage. HPs are the least preferred course of action as it is often safer to reduce the amplitude of the source of noise if possible. In the case of operating aircraft, HPs are a necessity making the evaluation of HPs part of the problem to be analyzed. In fact, much research has been completed and is still being done on the performance of HPs (including the extensively used HGU-56/P helmet [6], [7] and [8]). This research is often initiated due to complaints from aircrew about excessive noise.

In addition to background noise, aircrew operators will often increase the volume of the intercom as a strong signal-to-noise ratio is important for clear communication. In reference [5], a Chinook helicopter is estimated to have radio headset communications that contribute an additional $8.6\ dBA$ to the background noise levels. Communications can significantly contribute to noise.

In extreme noise conditions with high attenuation HPs, sound may follow conduction paths directly through bone and tissue (bypassing the outer and middle

ears) [5]. MIL-STD-1474D is a design criteria standard which states that flight members shall not be exposed to levels exceeding $145\ dB$, regardless of hearing protection worn [9].

While the objective of this hearing protection project was to analyze the noise environment and to consider the attenuation of the HP, the scope of the work associated with this thesis was limited to a reproducible method for recording cabin noise onboard aircraft.

1.1.2. Quantifying Aircraft Noise Generation

Short summaries of similar projects have been provided. The equipment and measurement procedures used in each summarized project may be compared against this report's equipment characterized in sections 3.5 and 3.6.

1. Diamond D-Jet [10]

In 2007, the National Research Council (NRC) assisted Diamond Aircraft Canada to record sound onboard a D-Jet aircraft. The project aimed to characterize the noise level within the aircraft and to identify the source of an irregular "buzzing" noise. The interior cabin noise was found to be $93 - 101\ dBA$ throughout the flight.

The recording equipment included a Josephson C617 and MK221 capsule microphone configuration. This microphone had a frequency response of $10\ Hz - 20\ kHz$. The microphone was externally polarized and pre-amplified. The analog to digital converter had a 16 bit resolution with a sample rate of $44.1\ kHz$. A second channel of data was taken directly from the intercom audio (total of two channels of data). The equipment was powered with $12\ V$ batteries (independent from

aircraft power). Additional measurements were taken with a Brüel and Kjær Model 2231 sound pressure level (SPL) meter.

Both ground and in-flight measurements were completed. A variety of flight conditions were flown to characterize the normal operational window of the aircraft. The ground measurements were noted to be louder than the flight measurements at similar throttles due to the reflecting plane of the ground.

Analysis concluded that the buzzing noise was likely attributable to a structural resonance excited by the compressor shaft (as opposed to noise directly generated by the engine). The report recommended future recordings include a $96\ kHz$ sampling rate to enable observation of the fan and turbine passage frequencies.

2. CH147 Chinook [11]

In 1976, the Canadian Department of Defence made an assessment of the Chinook helicopter prior to its introduction into service with the Canadian Forces. As this is a controlled document, no results are shared but the method is reviewed.

The measurement equipment included a Brüel and Kjær Type 2209 sound level meter with a Type 1613 octave filter set. This set included 11 octaves with center frequencies ranging from $31.5\ Hz - 31.5\ kHz$. A Kudelski Nagra Type IV-SJ tape recorder and a Hewlett Packard 3590A wave analyzer provided a frequency analysis range of $20\ Hz$ to $620\ kHz$ [12]. In this instance the limiting factor would be the microphone. Unfortunately, the report does not detail the microphone set up or type.

The measurement locations included the pilot, jump seat and three passenger locations spaced along the cabin interior. There was no indication of the number of

channels or if flight conditions were repeated. A clever method of recording the intercom electrical signal to reproduce the intercom noise later in the lab was adopted.

The results concluded that the intercom headset noise was significant.

3. Various Military Vehicles Noise [5]

In October 2004, a paper encompassing many vehicles was presented at the NATO Research and Technology Organisation Symposium by Sander J. van Wijngaarden and Soo James.

Few comments were made on the method of data capture, presumably as the paper drew its data from many sources. The paper commented on the limited analyzing capability of hand-held sound level meters and their inability to measure the entire acoustic spectrum. Most sound analyzers possess real-time weighted octave and 3^{rd} octave measurements as opposed to narrow band analysis.

The results depicted jet aircraft interiors as the loudest cockpits with helicopter interiors having the loudest cabin/cargo areas. The paper discussed the importance of characterizing the interaction between the noise environment and the frequency-dependent noise attenuation characteristics of the applicable HP. Furthermore, the importance of in-situ noise dose measurements was discussed. In-situ measurements are more representative than laboratory replications, primarily due to improper helmet use, helmet deterioration and intercom communication.

Ideally, testing would involve inserting microphones into crew member ears underneath HPs during flight. While not always feasible, the point is well taken as every effort should be made to account for these details.

4. HGU-56/P Helmet Study [8]

The HGU-56/P study was unique in that the helmet was placed on live subjects who had microphones mounted in their ears. The method followed standards ANSI S12.42-1995: Microphone-in-Real-Ear and Acoustic Test Fixture Methods for the Measurement of Insertion Loss of Circumaural Hearing Protection Devices. This method was creative in that it approached the insertion loss measurement of the helmet directly. The testing was done in a reverberant sound room (not in-flight).

The results of the report discussed various helmet configurations and their associated attenuations. The helmet's best attenuation occurred in the mid to high frequency ranges.

1.1.3. Aircraft Noise Capture Challenges

A large portion of past in-flight noise measurements have been completed through the military. This is logical due to their access to, and large usage of, vehicles requiring HPs for the operators. Unfortunately, a large amount of this information is restricted.

Extensive ground testing has been done but various researchers have stressed the need for in-flight measurements. In-flight measurements are more representative and can record the different noise environments of each flight condition. Of note is that fewer papers discussed multi-channel simultaneous recording or the recording of multiple flight conditions.

In-flight data is less common than ground or laboratory based data. The difficulties of obtaining in-flight data can be primarily summarized into five points:

1. **Environment.** Aircraft have more freedom of motion in space and consequently the ability to apply inertial loads in more directions than a single horizontal plane. Furthermore, soft padding and vibration isolation are often too heavy to include. As such, measurement equipment installed on aircraft must be rugged to withstand vibrations in every axis of motion. Standard lab equipment might malfunction.
2. **Expense.** Aircraft operation is expensive. Dedicated flight time for noise measurements can be difficult to obtain.
3. **Expertise.** This is contextual based on the individual who is tasked with noise measurement. A pilot, flight engineer or aircraft technician, while highly trained and experienced, may not appreciate acoustic priorities. Hand held meters, while simple, easy and safe to use, do not provide the same level of detail and insight as a high sample rate data acquisition system (DAS).
4. **Safety.** The installation of a DAS can be disruptive to the methodical operation of aircraft. Aside from physically blocking areas of a cabin, a DAS can influence aircraft systems if care is not taken. Aircraft are governed by multiple regulations which must be adhered to.
5. **Understanding.** Hearing loss is, by nature, intangible. Without immediate symptoms and a varying degree of sensitivity depending on the occupant, hearing loss is often taken less seriously than other ailments.

It is understandable and logical for acoustic precedents to have a lower priority than vehicle performance objectives. Performance is directly linked to mission

objectives and budgeting. Therefore, it is all the more necessary to produce valid, understandable, reproducible results when taking the few measurements one can.

1.2. Thesis Objective

The previous section outlined some of the difficulties associated with obtaining in-flight acoustic measurements. This type of data is relatively sparse and difficult to obtain in comparison to ground based vehicles and laboratory measurements. Few concrete relationships between helicopter sound sources and hard data exist. The work associated with this thesis aims to quantify helicopter sound.

The intention is to record helicopter noise while relying on certain technical standards. A method compliant to international standards will be reproducible and the data more easily shared and understood by the scientific community. Furthermore, these standards have been written and agreed upon by experts in the field of acoustics as well as the aviation industry.

This thesis is part of a larger project. The NRC has been tasked with evaluating the noise levels of aircraft as well as their associated HPs. The project goal is to establish if the HPs are sufficient to prevent hearing loss. Otherwise, recommendations for ameliorating the situation will be given. The scope of this thesis, and the completed work of the author to date, has been to produce, operate and evaluate a reproducible method of noise measurement onboard a variety of aircraft. The purpose of this thesis is to explain the instrumentation and system integration work done. The results of the first in-flight measurements completed onboard a Bell 412 helicopter are used as validation for this work.

2. Standards Review

In order to ensure a reproducible procedure for the acoustic measurements completed in this hearing protection project, a variety of noise measurement standards were reviewed. This chapter contains a summary of the applicable components from four noise measurement standards. As this project also aims to compare the results to occupational health and safety standards, both types of standards are reviewed.

2.1. ISO 5129:2001(E) (Reference [13]) "Acoustic-measurement of sound pressure levels in the interior of aircraft during flight"

ISO 5129 was the primary standard followed for the establishment of measurement procedures. Some of the major parameters have been summarized below. This summary is not a complete characterization of the standard, but merely an outline of relevant aspects for the design of this project's DAS.

2.1.1. ISO 5129 Microphone System Requirements

The standard states, "The microphone system shall conform to the applicable specifications of IEC 61675-1 for random-incidence sounds." The microphone chosen for the author's project was a 378B02 and is characterized in section 3.5.1. The 378B02 is a free-field microphone as opposed to a random-incidence microphone. The difference between the two types of microphones is their frequency characteristics.

At high frequencies the presence of a microphone will increase the local measured sound pressure. As stated by a GRAS selection guide, "The frequency characteristics of a

free-field microphone are designed to compensate for this increase in pressure…" [14]. This increase in pressure occurs at higher frequencies where the dimensions of the microphone impact the wavelength. For a ½ inch (0.0127 m) microphone:

Equation 1: Speed of sound equation

$$v = \lambda f$$

- v **is the speed of sound (**$\sim 340.29\ m/s$**) at sea level**
- λ **is the wavelength (assume the** $0.0127\ m$ **microphone dimensions)**
- f **is the frequency**

$$340.29 \frac{m}{s} = (0.0127\ m)\ \boldsymbol{f}$$

$$\boldsymbol{f} = 26\ 794.5\ Hz$$

This frequency is where the maximum pressure increase will occur for a standard ½ inch microphone [14]. However, for this measurement project, the objective was to qualify noise exposure for human hearing whose commonly accepted limits are $20\ Hz$ to $20\ kHz$ [13]; more significantly, $20\ Hz$ to $10\ kHz$. Frequencies in the proximity of $26.8\ kHz$ are of lesser interest. As it is at these frequencies where the free-field and the random-incidence microphones experience differences, a free-field microphone is a valid selection for random-incidence measurements below its adjusted frequency range. This validates the 378B02 selection. Furthermore, as later discussed in section 3.1, the internal DAS low-pass filters would attenuate any microphone resonance.

2.1.2. ISO 5129 Microphone Location Requirements

The ISO 5129 standard microphone measurement locations have been summarized below:

- **Seated passenger** and **non-essential crew locations** require the microphone to be vertically mounted $0.15 \pm 0.025\,m$ from the headrest and $0.65 \pm 0.05\,m$ above the unoccupied seat cushion.
- **Standing crew locations** require the microphone to be $1.65 \pm 0.1\,m$ above the floor without the presence of the crewmember.
- **Essential crew locations** require the microphone to be within $0.1\,m$ of the typical ear position with the crewmember present and seated.

ISO 5129 states, "Measurement locations shall be chosen so as to provide a representative description of the acoustical environment… The microphone shall be held in a fixed location with a bracket or extension rod as appropriate to minimize interference and shielding effects… No person shall be seated or standing within $1\,m$ of the microphone, except at flight crew stations."

Windscreens are to be included if airflow impinges on the microphone during a test. ISO 5129 further states, "The insertion loss of the windscreen as a function of frequency and angle of sound incidence, in the absence of wind, shall be known…"

The aircraft interior is to be fully furnished with the standard acoustic and thermal insulation treatments as well as seats, carpets and cushions. All seats are to be deployed in the occupied position. The environmental control systems of the aircraft are to be set to operate normally. Any noise or vibration control systems are to be operating normally.

2.1.3. ISO 5129 Data Analysis

On the subject of data capture ISO 5129 states, “The overall acoustical sensitivity of the measurement system shall be determined, while on the ground, prior to, and after, the measurements of the sound pressure levels in the aircraft interior.”

For helicopters, 3rd octave bands from mid-band frequency $16\ Hz$ to $10\ kHz$ are to be analyzed. Data recordings must be a minimum of 30 seconds long. Adjustments for the effect of the windscreen insertion loss must be made and if background noise from the measurement system exists, it must be accounted for.

Each of the above parameters will be covered in the appropriate chapters that follow as ISO 5129 was the primary standard followed for the measurement and analysis of the BELL 412 helicopter flight.

2.2. MIL-STD-1294A (Reference [15]) “Acoustical noise limits on helicopters”

The scope of the MIL-1294 standard is more specific than that of the ISO 5129. The standard is intended to “Minimize hearing loss among personnel exposed to helicopter noise and near-field exterior noise at maintenance/service locations around the helicopter.” The standard also concerns itself with communication intelligibility and helicopter design/manufacture.

2.2.1. MIL 1294 Equipment Requirements

As read in MIL 1294, “Test instrumentation shall be electrically isolated (e.g. battery powered or isolation transformers)… Test instrumentation shall be adequately shielded

to preclude the recording of erroneous data… Precautionary measures should be taken to prevent erroneous response of the aircraft navigational systems due to the operation of on-board magnetic devices (e.g., tape recorders). A tape recording shall be made in-flight with the microphone replaced by an equivalent shielded impedance to establish an instrumentation baseline."

Certain parameters of this standard are arguably dated in their procedure. The standard is primarily concerned with two aspects:

1. Avoiding measurement of electronic signal noise from the electrical power system

2. Ensuring that all necessary flight systems remain fully operational

For the Bell 412 helicopter flight, the DAS operated under aircraft power. The power input could vary between $24\,V \pm 4\,V$ with no impact on the measurement as the DAS power module filtered all incoming power. Due to the ruggedness of this design, the measurements occurred without concern of signal noise from the power system. Furthermore, the Phase II design was modified to include a battery. This new design has been used on all subsequent tests, satisfying this standard.

Concern 2 is valid but falls under the regulating body in ownership of the aircraft to satisfy. The pilot, co-pilot and flight engineer will not fly until 100% confidence has been achieved that the aircraft is not adversely impacted by the installation of the measurement system in any way. On the day of the Bell 412 measurement (and all subsequent measurements on different aircraft) a source victim test was completed. The aircraft was started up normally with the DAS turned off. After normal start-up the

DAS was given permission to turn on and all aircraft systems were monitored for disturbances. For more details on the procedure of this test refer to section 3.2.2.

2.2.2. MIL 1294 Microphone Location Requirements

MIL 1294 states, “Noise measurements shall be made at or near the head positions of all crew stations and at a representative number of passenger stations.” Microphones shall be located $80\ cm$ above the seat reference point or $165\ cm$ above the floor for standing positions. “Whenever possible, noise measurements should be made with the crew member or passenger absent…” Either the ISO $65\ cm$ or the MIL $80\ cm$ can be followed (but not both) for microphone placement.

The different aircraft configurations to be measured include:

1. Doors and windows open with acoustic treatments installed

2. Doors and windows open without acoustic treatments installed

3. Doors and windows closed with acoustic treatments installed

2.2.3. MIL 1294 Ground Measurement Requirements

ISO 5129 focuses on measurements made in-flight and consequently was not a sufficient reference for all crew tasks subject to noise exposure around aircraft.

On the subject of ground measurements MIL 1294 reads, “… measurements shall be made at the head position at a representative number of *normal maintenance locations,* as approved by the procuring activity.” All subsystems shall be operating normally with windows and doors open. Acoustic treatments and access panels normally removed for maintenance are to be removed. The following conditions are to be measured:

1. Engines off, APU (Auxiliary Power Unit) operating

2. Engines on, rotors turning at flight-idle (minimum collective pitch) and APU operating

3. Engines on, rotors stationary, APU operating (if this condition is possible)

2.2.4. MIL 1294 Noise Limits Criteria and Data Analysis

For helicopters less than $20\,000\ lbs$ the SPL limit for each octave shall be less than:

Table 2: MIL 1294 helicopter SPL limits

Octave Band Center Frequency (Hz)	Design Limit (dB)
63	116
125	106
250	99
500	91
1000	87
2000	82
4000	80
8000	85
16000	89

It should be noted that the lowest octave band is $63\ Hz$. The Bell 412 helicopter has a nominal rotor rpm of $324\ rpm\ (5.4\ Hz)$ [16]. This frequency and its harmonics (especially the 4^{th} harmonic of $21.6\ Hz$) are major sound sources. In comparison, ISO 5129 requires 3^{rd} octave bands as low as $16\ Hz$ to be measured. These are referenced to in chapter 5.

MIL 1294 further reads, "All *steady state noise* data shall be analyzed in octave band, 1/3 octave band, A-weighted and C-weighted sound pressure levels for each of the measured stations… Data should be corrected to compensate for any non-flat frequency response of the entire measurement/analysis system including microphone and windscreen directivity characteristics."

This microphone directivity characteristic was discussed previously in 2.1.1. The windscreen insertion loss is commented on in chapter 5. The combination of ISO 5129 and MIL 1294 provided the basis for producing a repeatable noise measurement procedure. Any deviations from the standards have been discussed.

2.3. CSA-Z107.56-06 (Reference [17]) "Procedures for the measurement of occupational noise exposure"

This standard relates to an occupational health and safety perspective of noise exposure. While the previous two standards focused on aircraft, aircraft safety and single measurement fidelity, this standard was written for ground based office or shop environments. For this reason, parts of the standard are less applicable. The CSA-Z107.56-06 approach is to take many measurements for statistical analysis. This type of approach may not be feasible when operating aircraft.

2.3.1. CSA Z107 Equipment Requirements and Microphone Locations

The standard calls for a Type 2 sound level meter as outlined by ANSI S1.4: Specifications for Sound Level Meters [18]. These references to these sound level meter types are not applicable to this DAS, described in chapter 3. The data capturing method employed by this project was of a much higher fidelity and stored the data in an unaltered format. All weighting methods were applied afterwards in post calculation analysis.

This CSA Z107 standard has less regimented microphone locations than the previously discussed standards. Depending on the task, microphones should be at head

height no greater than $0.5\ m$ from the worker's ear with the worker present during the measurement. Measurement devices may be installed on the workers themselves as they move from task to task. Microphone direction may be in any upward configuration and should aim to have the flattest possible frequency response.

The stricter and more applicable aircraft measurement procedures, discussed previously with ISO 5129 and MIL 1294, were followed.

2.3.2. CSA Z107 Measurements

This standard aims for long term measurements (in the magnitude of hours) to be completed with multiple repetitions to build confidence in the results. As discussed earlier, this is not feasible for in-flight measurements. However, extrapolating the shorter measurements completed onboard the aircraft allows the application of the CSA standard's equations for equivalent sound level, should it be desired.

Equation 2: Equivalent sound level

$$L_{eq,t} = 10 \log \left[\frac{1}{100} \sum_{i} P_i 10^{\frac{L_{eq,i}}{10}} \right]$$

- $\boldsymbol{P_i}$ **is the estimated average percentage of time spent on the ith activity** $(\sum \boldsymbol{P_i} = \boldsymbol{100}\%)$
- $\boldsymbol{L_{eq,i}}$ **is the measured** $\boldsymbol{L_{eq}}$ **during the ith activity**

This method of comparison relates the normally separate aircraft measurement standards to the occupational health and safety measurements. All standards are in agreement in that the work activities and environment shall be unaltered from normal operation.

2.4. ISO 9612:2009(E) (Reference [19]) "Acoustics – Determination of occupational noise exposure – Engineering method"

Once more, this standard was written from a ground based workforce perspective. Not every component of this standard was found to be applicable for in-flight measurements.

Three measurement methods are proposed:

1. Task based measurement

2. Job based measurement

3. Full day measurement

Full day measurement would only be possible with clearance to have equipment installed in the aircraft for normal mission operation. Task based measurement was deemed the most applicable as the noise generated by aircraft is highly dependent on the specific manoeuvre being completed at that time. Minimum recordings of five minutes are required by this standard. With 28 different measurements completed on the Bell 412 helicopter flight this would correspond to over two hours of recording, not including the time between each flight condition. This would place the measurement session in excess of four hours based on previous experience. In light of this, the less stringent 30 seconds defined by ISO 5129 and MIL 1294 was deemed more applicable.

ISO 9612 requires the use of windscreens in areas of air flow, but makes little mention of the insertion loss or the requirement to record the insertion loss of said windscreens. Similarly to the CSA standard, ISO 9612 held applicable methods for extrapolating the long term exposure of a crewmember at a station.

2.5. Standards Discussion

Part of the difficulty in the end goal of this hearing protection project lay in that aircraft noise measurement data, and ground based occupational health and safety data come from different perspectives.

The ground based standards refer to various weighting methods (A-weighting, C-weighting etc.) as depicted in Figure 1 below. A-weighting in particular is intended to account for the relative loudness perceived by human hearing. In aircraft and other noisy environments HPs are mandatory. In these situations, A-weighting should be applied in addition to the insertion loss of the HP. The flat frequency response (unaltered data) should be preserved by the DAS as the ISO 5129 and MIL 1294 standards require.

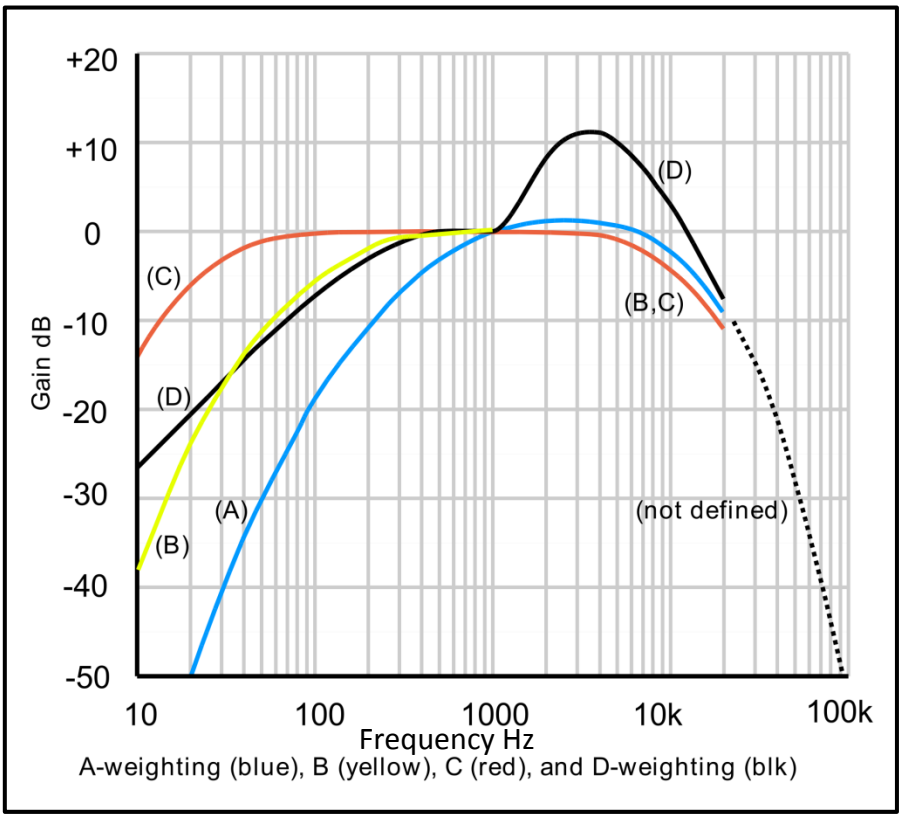

Figure 1: Acoustic weighting curves [70]

The objective of this thesis is the documentation of the instrumentation and systems integration methodology, further validated through analysis of a noise measurement completed onboard a Bell 412 aircraft. However, in the interest of providing some degree of closure to the collaborative hearing protection project as well, additional NRC work on the HPs and their associated insertion loss data will be shared in chapter 5.

3. Flight-Worthy Data Acquisition Equipment

This chapter includes a summary of the hardware and software used to record data for the hearing protection project as well as the justification for each design aspect. There were two phases to the development of the instrumentation box. The phase I instrumentation was designed and built independently by the author. Following this proof of concept, the phase II instrumentation case was built. The phase II physical housing (design and construction) was contracted out and then returned for certification, troubleshooting and integration by the author.

Various design challenges are identified and addressed. Equipment specifications are characterized in detail along with signal routing and an overview of the data importation methodology. Various sources of error are acknowledged and discussed as well.

3.1. Data Acquisition Unit Selection

As discussed in section 1.1, there are a variety of challenges associated with data capture onboard operating aircraft. The primary considerations when selecting an airworthy DAS have been summarized in Table 3.

Table 3: Considerations when selecting a DAS for in-flight measurement

#	Consideration	Description of Reasoning
1	Aviation and Military Standards	A multitude of standards must be adhered to when operating equipment onboard civilian or military aircraft.
2	Rugged Equipment	Altitude changes, high temperature variations and other environmental conditions are common in-flight.
3	Minimum 20 kHz Nyquist Sampling	A minimum sample rate of $2\,X\,20\,kHz = 40\,kHz$ is required for frequency measurements up to $20\,kHz$.

4	Multiple Microphone Channels	Multiple microphones are required to properly characterize the interior of the fuselage.
5	Autonomous Operation	Depending on the flight configuration, personnel may not be able to operate the DAU.
6	Reliable Measurements	Aircraft operation is expensive, repeated testing is to be avoided if possible.
7	Standardized Sensor Hardware	A variety of different types of sensors are required (microphones and accelerometers especially).
8	Onboard Memory	Onboard memory is required to eliminate the need for additional external equipment to be certified.
9	Size and Weight	Aircraft cargo space, weight and balance may be limited.
10	Independent Power	Using aircraft power is a safety concern.

The **TTC MCDAU-2000** from Teletronics Technology Corporation (TTC) based in Newtown, Pennsylvania, USA as seen in Figure 2 was selected.

The TTC MCDAU-2000 is a modular data acquisition unit (DAU) and data recorder. Each module is connected to a "stack" to serve a singular purpose. In this manner, only modules ideal for each type of data acquisition are used. Additional modules supply the overarching software formatting, the stack power and the memory storage.

Figure 2: TTC MCDAU-2000

The TTC MCDAU-2000 satisfies the Table 3 criteria. A detailed list of the standards the TTC MCDAU met would be impractical to include here, as each module must satisfy different standards depending on its function. For specific module details refer to the TTC interface control documents in the technical references. All modules and equipment met ANSI/ASQC Q9001-1994: "Quality Systems – Model for Quality Assurance in Design, Development, Production, Installation and Servicing" [20].

The specifications of each module can be found in Table 4. Simply stated, the TTC MCDAU-2000 can be split into two major functionalities: **1)** Data Acquisition and **2)** Data Recording. The acquisition partition acquires the data from the sensors and formats it before sending it along the internal data bus to the recording partition for storage. The data acquisition formatting instructions are controlled through the MWCI-120-2 while the data recording formatting instructions are controlled through the MSSR-110C-1. Both partitions are physically connected within a single "stack" as seen in Figure 2. For convenience, a flow chart depicting how the modules interact with one another can be seen in Figure 3.

Table 4: Specific module parameters

(A) – Module is part of the acquisition system
(R) – Module is part of the recorder system
Current system configuration as of 2014

Component	System	Identifier	Specifications/Purpose
Overhead Control Module [21]	1 module *(A)*	**MWCI-120-2**	Formats and relays instructions to data acquisition modules. Acts as the interface for user programming of the stack.
High Speed Data Acquisition Module [22]	3 modules *(A)*	**MGRC-202W-1**	2 Channels, Software low-pass filter restriction of $10\ kHz$ sampling Sampling rate up to $125\ kHz$ (12.5 X oversampling ***)

High Speed Data Acquisition Module [22]	2 modules *(A)*	**MGRC-202W-3**	2 Channels, Software low-pass filter restriction of 20 kHz sampling Sampling rate up to 125 kHz (6.25 X oversampling ***)
Low Speed Data Acquisition Modules [23]	3 modules *(A)*	**MSCD-606D-13**	6 Channels, Software low-pass filter restriction of 5 kHz Sampling rate up to 25 kHz (5 X oversampling ***)
Power Module [24]	1 module	**MPSM-2012-1**	Converts power source to the various formats required for each module. Requires $28V \pm 4V$
Power Module [25]	1 module	**MPFM-461-1**	Filters incoming power. Works in conjunction with MPSM-2012-1.
Overhead Control Module for Recorder [26]	1 module *(R)*	**MSSR-110C-1**	Formats and relays instructions to recorder modules. Acts as the interface for user programming of the unit.
Pulse Code Modulation Interface [27]	1 module *(R)*	**MPCM-102M-1**	2 Channels Receives data from the DAS and formats the data to chapter 10 format for storage.
Solid State Memory Module [26]	1 module *(R)*	**MCFM-110-1**	Contains two removable 16 GB Solid State memory cards. Continuous recording from card to card.
Video Input [28]	1 module *(R)*	**MVID-301M-1**	One HDMI, DVI, Composite, S-Video or RGB compatible channel and one stereo audio channel. This data acquisition module is part of the recorder system.
Video Input [28]	1 module *(R)*	**MVID-301MD-1**	Works in conjunction with the MVID-301M-1 (required).
IRIG Standard Time [29]	1 module *(R)*	**MIRG-220M-2**	IRIG standard timekeeper for the recorder. Capable of receiving IRIG time continuously or tracking time independently.

***** Oversampling**
Oversampling refers to the DAU sampling faster than necessary. If a 10 Hz signal was being measured, a sample rate of at least 20 Hz (Nyquist frequency) is required to characterize the signal. In ideal circumstances, sampling a 10 Hz signal at rates of 20 Hz and 40 Hz would return the same information (sampling faster would provide no additional information). In reality this is not always the case, as such oversampling can be beneficial.

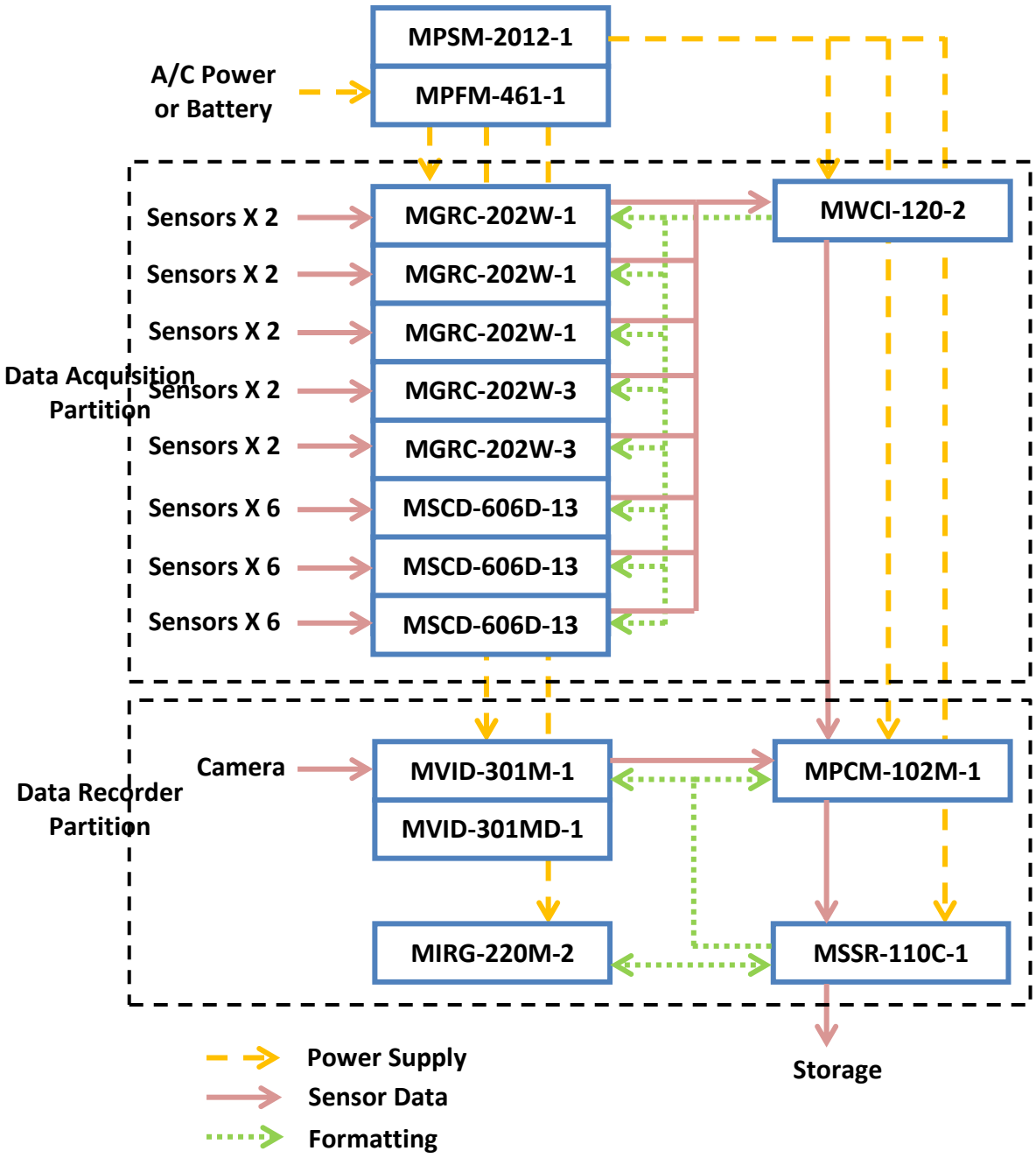

Figure 3: Module communication flow chart

The entire stack is rugged, with an operating temperature of $-35\,℃$ to $85\,℃$, $25\,g$ shock resistance, $5-95\%\,RH$ humidity operational limits and an unlimited altitude ceiling [30]. These and the aforementioned airworthiness certification made the TTC MCDAU-2000 an ideal choice for noise measurement onboard aircraft during flight.

3.2. Design of the Enclosure Box, Phase I

The DAU was placed in an enclosure box primarily for the following reasons:

Table 5: Advantages of containing the DAU in a single DAS box

#	Advantage
1	To contain the complicated multitude of wires connected to the DAU
2	To simplify the interface for an operator during flight
3	To require only a single package of equipment to be tested for airworthiness
4	To provide accommodations to strap the DAU down to any aircraft surface

The DAU was enclosed in a ZC7050 aluminum case from Zero Cases [31]. The dimensions were $14.5\ X\ 25.4\ X\ 15.0\ cm$ $(5.69\ X\ 10\ X\ 5.91\ inches)$. The aluminum case was selected as a heat sink for the DAU and to provide electromagnetic shielding.

The zero case may be seen in Figure 4.

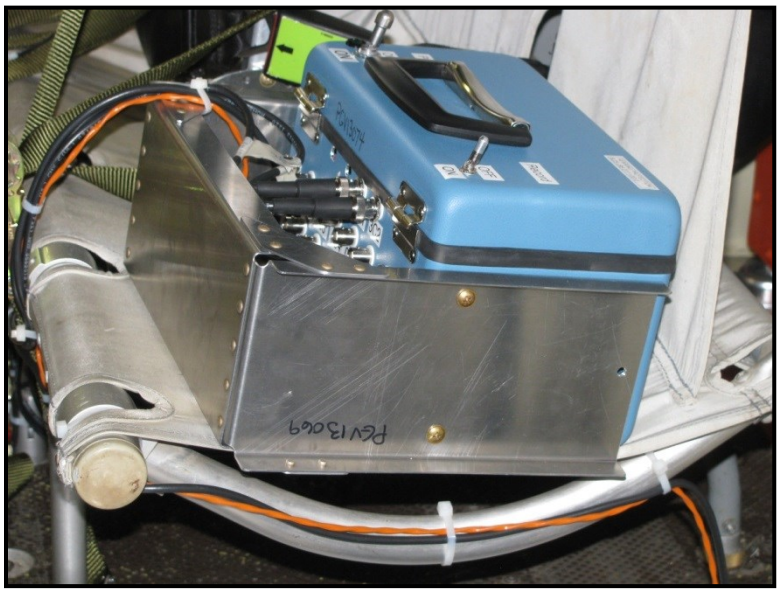

Figure 4: Phase I enclosure box

Holes were punctured in the casing for BNC style connectors to simplify the wiring to standard quick connectors for various sensors. An additional hole was punctured for a military style connector to pass $28\ V$ of power to the box from either a battery or

aircraft power [32]. The top of the casing had three holes to include a power indicator LED, a power switch and a recording switch. These may be viewed in Figure 5 and Figure 6. An exterior casing was also added to protect the exposed BNC connectors from any external loading as BNC connectors are not designed for physical loading and would be prone to snapping under such circumstances.

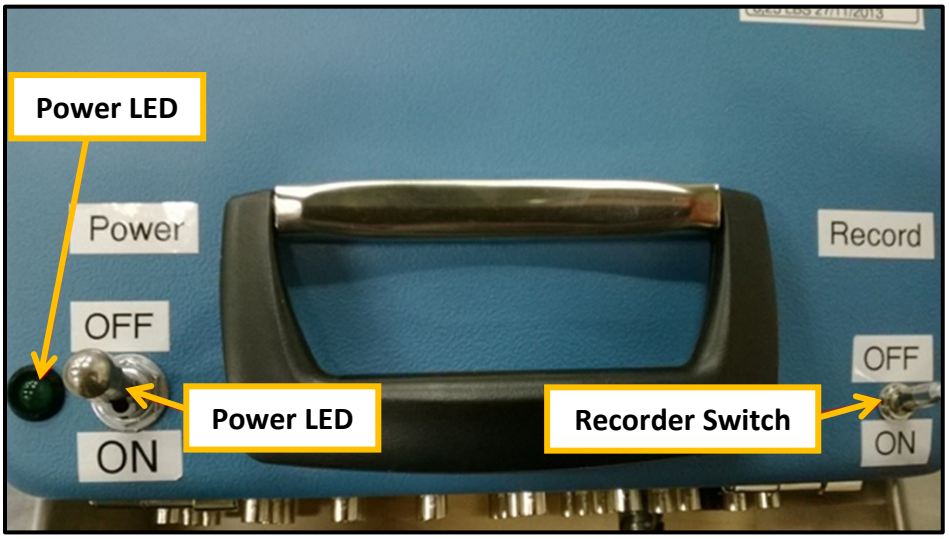

Figure 5: Top view of the Phase I enclosure box

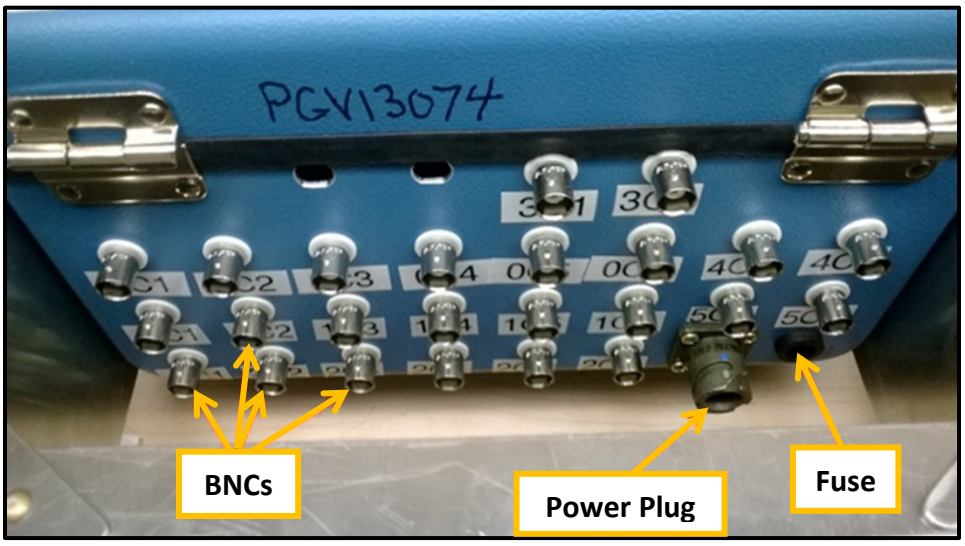

Figure 6: Frontal view of the Phase I enclosure box

Wiring diagrams detailing the interior wiring may be found in reference [32].

Many design aspects of this enclosure box were selected to meet certain airworthiness considerations discussed below. The major airworthiness considerations for installing foreign equipment on an aircraft may be categorized as:

1. Electrical Compatibility

2. Electromagnetic Interference

3. Emergency Landing Conditions

4. Aircraft Egress

5. Fire Protection

6. Aircraft Weight and Centre of Gravity

7. Common Reliability Practices

3.2.1. Electrical Compatibility

Section 529.1353 of the Transport Canada Airworthiness Manual (AWM) states: "(a) Electrical equipment, controls and wiring shall be installed so that the operation of any one unit or system of units will not adversely affect the simultaneous operation of any other electrical unit or system essential to safe operation." [33].

The intent to connect the DAU to the aircraft's internal power has safety implications for an airworthiness engineer. The aircraft must be certified to operate simultaneously with the foreign equipment. Proving compliance and gaining confidence in this arrangement is possible and often put into practice. However, the nature of this project had the DAU designed to be installed in a variety of different aircraft for data measurements. Therefore, powering the DAU with portable batteries was optimal.

However, for the initial flight with the Phase I enclosure; the DAU was connected to aircraft power. The electrical compatibility validation was facilitated by the fact that the NRC Bell 412 helicopter was run under an experimental license. As the project progressed with non-experimental aircraft, a battery solution was implemented as can be seen in section 3.3.

3.2.2. Electromagnetic Interference Testing

Electromagnetic Interference (EMI) could be considered a subsection of Electrical Compatibility, however, whereas certain electrical concerns may be avoided by isolating the DAU electrical system from the aircraft, EMI is always a concern that must be accounted for.

Aircraft EMI is defined as "…the phenomenon occurring when electromagnetic energy present in the intended operational environment interacts with the electrical or electronic equipment causing unacceptable or undesirable responses, malfunctions, interruptions, or degradations in its performance." [34].

After installing electronic equipment in an aircraft, the equipment must be proven to be compliant. For more details and specifics on the means of compliance, refer to the Transport Canada Electromagnetic Compatibility (EMC) Circular [34]. Summarizing the circular, one of the most widely accepted means of compliance is by EMC test. An EMC test matrix is drafted and each impacted electronic system ("victim") is tested to ensure compatibility with the source of electromagnetic interference. Naturally, the systems native to the aircraft are compliant amongst themselves. Therefore, adding a single piece of equipment to the aircraft will result in the simple test matrix seen in Table 6.

Each victim is checked for abnormal operation while the source is powered and operating normally. In the event that all equipment is functioning normally, an EMC test report is written and the equipment is deemed electromagnetically compliant and consequently safe for operation during flight.

Table 6: Example EMI test matrix for the NRC Bell 412 helicopter

Equipment denoted with * are unique to the NRC Bell 412 helicopter**

Impacted System ("victim")	TTC MCDAU-2000 Source
Navigation System • **Multiple redundant navigation systems**	EMC Test Results
Communications System • **Radio** • **Transponder**	EMC Test Results
Ancillary Equipment • **Air conditioning and heating system** • **Wipers and window defrost** • **Nav lights and land lights**	EMC Test Results
Fly-by-wire System *** • **The software suit,** • **Force feel system,** • **Health monitoring** • **FFC flight control**	EMC Test Results
Sensor Suite *** • **Radar altimeter** • **Inertial measurement system** • **Air data measurement**	EMC Test Results

3.2.3. Emergency Landing Conditions

As described by subsection 529.605 of the Transport Canada AWM, "…each occupant and each **item of mass** inside the cabin that could injure an occupant is restrained when subjected to the following ultimate inertial load factors relative to the surrounding structure: (i) Upward-4 g (ii) Forward-16 g (iii) Sideward-8 g (iv) Downward-20 g (v) Rearward-1.5 g" [33].

Later sections describe in more detail the significance of all cargo being safely and appropriately stowed so as to avoid harming any occupants or vital equipment in the event of an emergency. The forward ultimate inertial loading of $16\,g$ is especially stringent in this regard.

The DAU enclosure box was designed to use the existing personnel safety strapping for each seat. As the DAU system weighs less than a person, the ultimate inertial loading consideration is met as the aircraft safety strapping was designed for heavier loads. Additional cargo ratchet straps were used to securely tie the DAU enclosure box to avoid unnecessary vibration.

3.2.4. Aircraft Egress

Egress is defined as the "way out" [35]. In aerospace vernacular, egress refers to the route that a particular occupant of the aircraft will take to exit the aircraft during an emergency. This is frequently determined by the pilot, loadmaster or flight engineer before flight. The route of each occupant is checked for obstructions and alternative routes are considered in the event of the aircraft rolling to one side, or other obstacles.

The DAU enclosure was intended to be installed in an unoccupied seat. In this manner, the system will be isolated from any traffic or walkways in the event of an emergency. Each individual installation is further reviewed contextually as well.

3.2.5. Fire Protection

Fire protection is primarily discussed in AWM subsections 529.851 to 529.864 [33]. The installed equipment should not contribute to the spreading of a fire in the event of an emergency. Therefore, all chosen material should be fire resistant. "…except for

electrical wire and cable insulation… [materials] shall not have a burn rate greater than 4 inches per minute when tested horizontally." [33]. The DAU and its aluminum casing satisfied these requirements.

3.2.6. Aircraft Weight and Centre of Gravity

The weight limits are discussed in AWM subsection 529.25, while the centre of gravity is discussed in subsection 529.27 [33]. Pilots and other crew members are familiar with their specific aircraft and its centre of gravity limits. In this instance the DAS and its sensors did not contain such a significant mass as to produce any abnormal weight distributions. The system fell well within the aircraft's normal cargo limits.

The DAU enclosure box has a mass of $2.7\ kg\ (6\ lbs)$ while the DAU stack itself has a mass of $1.2\ kg\ (2.6\ lbs)$. This mass depends on the modules configured within the DAU. These weights are commonly acceptable as cargo for the vast majority of aircraft.

3.2.7. Common Reliability Practices

This subsection is not strictly an airworthiness consideration governed directly by the AWM. Instead it is a summary of important practices that were followed during fabrication of the DAU enclosure box under the supervision of an avionics technician.

- **Lead flux soldering was used.** While the majority of industries have discontinued the practice of using lead flux due to health concerns, the aviation industry continues the practice as lead flux has proven to be more reliable and enduring.
- **All soldering was sealed within clear plastic shrink tubing.** This allowed each soldering point to be observed for deterioration.

- **All wire was Mil-Spec.** Allied Wire and Cable states, “Mil-Spec wire is built in accordance with military specifications. The wire is specially designed for the harshest environments” [36]. This DAS was wired with 22 gauge wire which follows the MIL-W-5086/2 standard (an aircraft wire standard).
- **Cables were soldered as 1 wire to 1 terminal.** If multiple wires go to one terminal, they were soldered together at an earlier independent junction.
- **Any open or unused wiring or terminals were sealed with shrink tubing.** This avoided short circuiting and sparking.
- **Wires were bundled and tie wrapped.** This served two purposes: **1)** To provide support to the wiring to avoid unnecessary movement which could cause the wire to fray and **2)** To organize the wiring for debugging; see Figure 7.

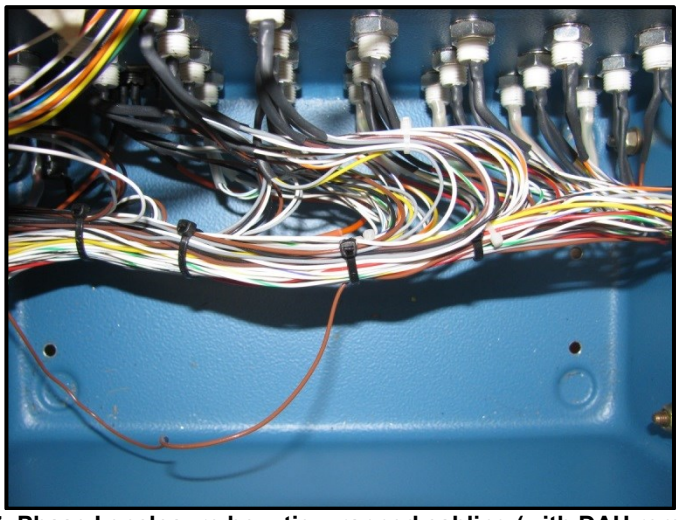

Figure 7: Phase I enclosure box, tie-wrapped cabling (with DAU removed)

All data presented in chapter 5 was recorded with the Phase I DAU; however, there remained a number of challenges to be optimized for future measurements:

1. Although ideal for electromagnetic shielding, the aluminum box needed to be electrically isolated to avoid static buildup with the aircraft.

2. The DAS was only operable if the user was within reach of the enclosure box.

3. The DAU was challenging to access for troubleshooting.

4. The small box provided little surface area for switches and connectors.

5. The DAS was not designed to incorporate a battery for independent power.

These difficulties were addressed and are discussed in Section 3.3.

3.3. Design of the Enclosure Box, Phase II

As the project progressed, the decision to install the DAU in a new enclosure box was made to improve a few design considerations for certification onboard other aircraft (especially military aircraft). The DAU was enclosed in an iM2450 plastic pelican case with dimensions $50\ X\ 38.5\ X\ 23\ cm\ (19.7\ X\ 15.2\ X\ 9\ in)$ as seen in Figure 8. The design alterations are discussed below.

Figure 8: Phase II enclosure box and remote

3.3.1. Design Alterations

1. **Plastic casing**. The transition to plastic was driven by the need to isolate the DAS from the aircraft electrically (to avoid grounding issues) and because the pelican case plastic was nonreactive and durable.
2. **Remote trigger**. An additional remote was included (as seen in the forefront of Figure 8). This remote was $18\ ft.$ long and allowed the operator to operate the DAU with *OR LOGIC* as shown in Table 7.

Table 7: DAU and remote power switch logic

Box Power Switch	Trigger Power Switch	System Operation
OFF	OFF	Not powered up
ON	OFF	Powered up
OFF	**ON**	Powered up
ON	**ON**	Powered up

3. **Data Transfer**. As can be seen in Figure 9, the DAU was wired to have external RS-232 connectors for programming, USB ports for data downloading and a BNC connector for live data streaming.

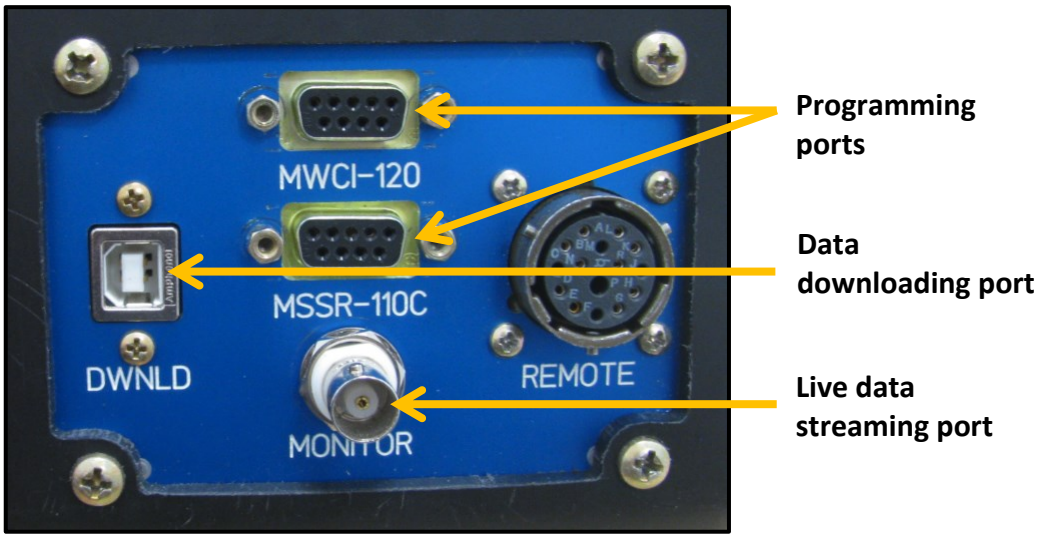

Figure 9: Phase II enclosure box data transfer ports

4. **Surface Area**. As can be seen in Figure 6, the majority of the Phase I real estate was used for BNC connectors. In the second phase, two additional modules were purchased which required four additional BNC connectors. The operational switches and new ports mentioned in ***3*** also required additional space. Furthermore, the BNC connectors were exposed on the Phase I enclosure. This exposure could cause unintentional grounding and loss of signal if a metal component touched a BNC; or a BNC could snap if force was applied directly to it. As can be seen in Figure 10, the BNCs were encased within the pelican case wherein all the wiring could exit through a side port.

Figure 10: Phase II enclosure box BNC sensor ports and wire exit port

5. **Battery.** The largest singular alteration to the new enclosure was the inclusion of a $28.8\,V$ lithium ion battery. With its own power source, the DAS no longer interacted with the aircraft electronically (excluding electromagnetic interference). This stand-alone approach allowed the DAS to be considered as non-essential, non-required "cargo". This was ideal for certifying equipment on various aircraft.

3.3.2. Battery Safety Considerations

Installing a battery introduced new challenges in addition to the advantages. Mention is made of “Flammable Fluid Prevention” in AWM 529.863 [33]; however, a battery’s dangers go beyond mere fluid leaks and prevention of ignition sources. Advisory Circular 43.13-1B gives strong precautions when working with batteries, “…Routine pre-flight and post-flight inspection procedures should include observation of physical damage, loose connections, and electrolyte loss.” [37]. The worst case scenario is battery combustion leading to a chemical fire.

Specific to lithium ion batteries is their unique combustion process. The circular states, “Lithium ion cells become dangerous when internal temperature reaches $177\,℃\ (350\,℉)$ (thermal runaway). A cell in thermal runaway gets extremely hot, then over pressurizes, releasing flammable liquid electrolyte.” [38]. Once thermal runaway has begun in one cell it will overheat other cells as well. Extinguishing methods are limited as smothering the fire is not sufficient. The battery cells will reignite unless they are cooled. In fact, every recommended method in the “Extinguishing In-Flight Laptop Computer Fires” video supplied by the Federal Aviation Administration involves the use of water (or other non-alcoholic liquids) to pour over the battery cells to convey away the heat to cool the cells (preventing further thermal runaway). The video asserts, “Avoid the use of ice or other covering materials. These will insulate the laptop, making it more likely that more cells will reach thermal runaway.” [38].

While a battery explosion is a highly unlikely scenario, a number of safety features in the design were included for good measure.

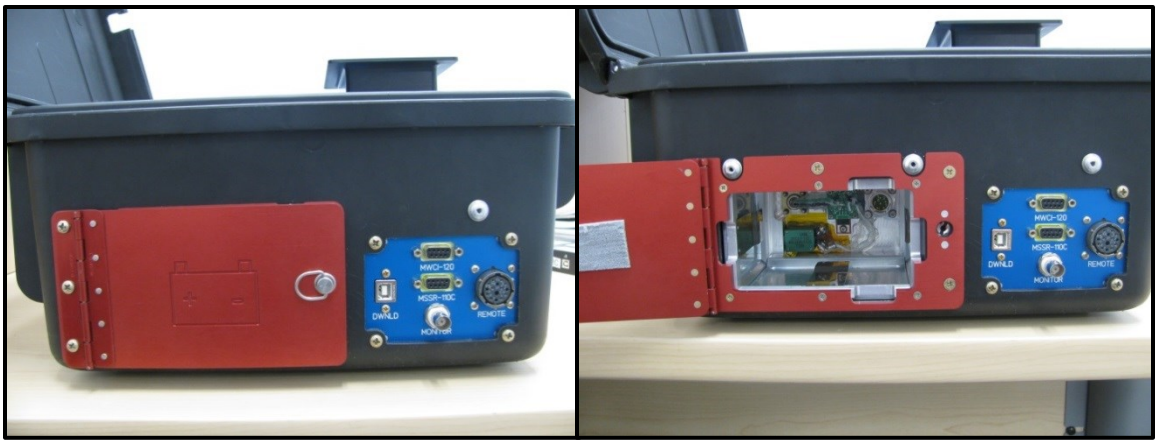

Figure 11: Phase II enclosure battery casing

1. The battery was housed within the enclosure box which protects the battery from foreign objects that might puncture or deform the battery casing, see Figure 11.
2. The battery housing was clasped with a single motion twist and release mechanism. This allowed for easy battery inspection and removal for jettison from the aircraft in the event of an emergency.
3. The circuitry included a $7\ A$ breaker to limit the battery discharge to a $6\ A$ discharge rate. A maximum voltage shutoff of $17.4\ V$ and a minimum voltage shut off of $11\ V$ were installed for each cell to limit battery loading. An installed internal temperature fuse ceases the battery's operation at $70\ ℃\ \pm\ 5\ ℃$ [39] to prevent thermal runaway.

3.3.3. Internal Wiring

As this is the current box configuration, the internal wiring will be discussed to some extent [40]. This reference has been included in appendix A1 for convenience.

Appendix A1, Sheet 1/14 is a block diagram of the various hardware components and the cables interconnecting them. The central box labelled IG14023 is the main internal circuit board. This overall layout replaced many soldered connections with

snap-in connectors facilitating debugging and maintenance. Everything not contained within the dashed/dotted line are components not physically contained within the pelican casing. Sheets 2/14 to 14/14 describe each particular cable. Refer back to Figure 3 for a more simplistic understanding of the module interconnections.

The cabling viewable on sheet 2/14 (IG14022-200) and 6/14 (IG14022-600) in drawing IG14022, are the cables running between the DAS and the BNC sensor connectors. These cables were wired for ICP type sensors.

Drawings IG14023, IG14024 and IG14025 have also been included in appendix A1 for convenience. In order, they depict the main interface circuit board, the accelerometer interface circuit boards and the microphone interface circuit boards.

The 5EHMS4S is a power line filter for external power when no battery is used. The external power accepts standard North American wall outlet power at $60\ Hz, 120\ V$. The SCS120PW30 is an AC to DC power converter (as the DAU requires $28\ \pm\ 4\ V\ DC$). In the event that external power is required, a switch located directly on the 5EHMS4S can be toggled. Additional precautions have been taken such as tie wrapping the cabling for organizational purposes and vibration resistance, as well as gluing any connector without a snap fixture.

This concludes the hardware description of the DAU and its enclosure box.

3.4. Design of the Microphone Stand

Microphone stands were designed in accordance with the standards discussed in chapter 2. The purpose of these stands was to simplify the installation of each microphone in the aircraft interior while satisfying the height requirements of the

measurement standards and the relevant airworthiness regulations. The stands were designed and built in-house with the NRC Design and Fabrication department.

The microphone was to be located $0.65 \pm 0.1\,m$ above a seated unoccupied crew member station according to ISO 5129 [13] and $0.8\,m$ above a seated unoccupied crew member station according to MIL 1294 [15]. As $0.65\,m$ and $0.8\,m$ are not the same height, the microphone stand had to accommodate either standard. Chapter 2 contains the description of these standards.

Concurrently with the DAU enclosure box phase I and phase II, a phase I and phase II were completed with the seated microphone stands. The phase I stand may be seen in Figure 12. As seen in the right of the figure, the microphone was installed vertically by using two Adel clamps attached together. The stand satisfied ISO 5129, and was thin enough in structure to avoid producing any noticeable acoustic reflections.

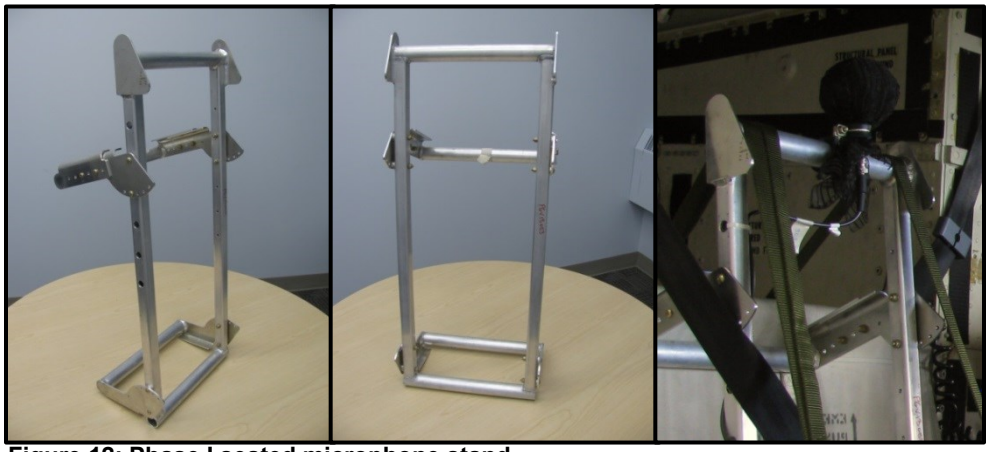

Figure 12: Phase I seated microphone stand

There remained, however, a number of features to be improved upon:

1. **Damping**. The frame was constructed out of aluminum and would emit a "ringing" when struck. The noise was audible and would be picked up by the microphones.

2. **Measurement Standards**. As discussed in chapter 2, there are two main measurement standards which should both be accounted for. This stand was able to only satisfy the more recent of the two standards: ISO 5129.
3. **Seat Stability**. The bottom section of the microphone stand was primarily a structure of two aluminum rods. For the majority of aircraft seat types this was sufficient, however, various “rag and tube” seat designs (an example of which can be seen in Figure 13) proved challenging.

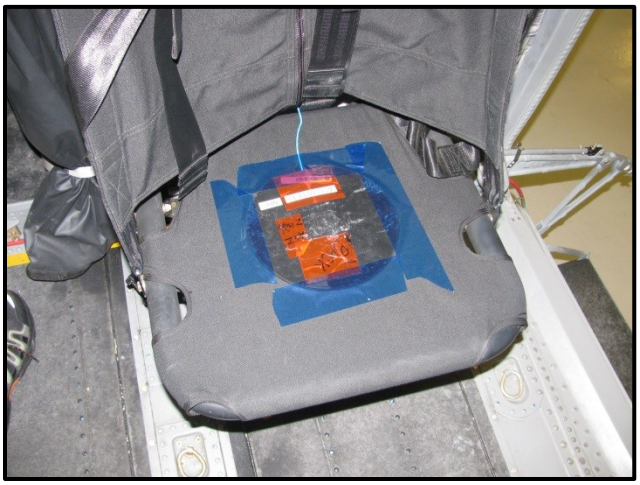

Figure 13: Example of a rag and tube seat

For the reasons stated above a second phase of microphone stands were designed. This stand had a base constructed of a cylindrical hollow metal cage as seen in Figure 14. An attachment rod for microphone mounting was connected to the top of the stand. Various rod lengths were accommodated. Finally, the entire stand was coated in a LINE-X SE-500 polyurethane coating [41].

1. **Increased damping**. The polyurethane coating was intended for reduced noise transmission and also increased the damping properties of the stand. The stand no longer held an audible ring when struck.

2. **Variable microphone height**. The attachment rod is adjustable. The $0.65\ m$ and the $0.8\ m$ heights could each be met individually.
3. **Increased seat stability**. The cylinder more closely matched the seated position of a human pelvis / hips. Additional hooks were added for secure use of the aircraft seat straps. Ratchet straps were no longer always required. Furthermore, the additional polyurethane coating had a higher coefficient of friction than aluminum, making it unlikely to slide across seat fabric.

Figure 14: Phase 2 microphone stand strapped into a seat

On December 9th, 2014 the second phase stands were used successfully onboard a Canadian Forces CH147F Chinook for a separate noise measurement. The results from that flight are not shared here, but the data gathered was of high fidelity.

3.5. Microphone Selection

This section includes a discussion the type of sensors used in conjunction with the DAS and some of their properties, focusing primarily on the microphone.

While the DAU supported charge type and voltage type sensors, only Integrated Circuit Piezoelectric (ICP) sensors have been used in conjunction with this project. The DAU enclosure has been wired to support ICP sensors only. ICP sensors are ideal for their low impedance signal is highly resistant to environmental noise and they do not require an external preamplifier (additional external equipment to be certified). The sensors implemented in this project may be viewed in Table 8.

Table 8: Primary sensors used with the DAS

Type of Measurement	Manfct.	Model #	Nominal Sensitivity	Comments
Acceleration	PCB	352C22	10 mV/g	Single axis ICP accel, [42]
Acceleration	PCB	356B41	100 mV/g	Tri-axial ICP cushion accel, [43]
Pressure	PCB	378B02	50 mV/Pa	½ in. free-field microphone, [44]

3.5.1. PCB 378B02 Microphone Specifications

The 378B02 microphone is depicted below in Figure 15. The specifications have been included for convenience in Table 9. The 378B02 is a standard ½ in. free-field ICP pre-polarized condenser microphone. The operational temperature range is $-40\,℃$ to $+80\,℃$ with a temperature sensitivity coefficient of $0.009\,dB/℃$. For the entire operational temperature range the sensitivity variation is $1.08\,dB$. This was ideal for this project as the experienced temperature spectrum involved during in-flight testing could be large. The spectrum may range from extremely hot jet engines running with closed doors on the ground to open door flight at high altitudes in winter (chapter 4 will include the latter condition).

Figure 15: PCB 378B02 ½ inch ICP free-field microphone

Table 9: PCB 378B02 ½ inch ICP free-field microphone specifications, [44]

Specification	SI
Performance	
Nominal Microphone Diameter	**1.27 cm (1/2 inch)**
Frequency Response Characteristic (at 0° incidence)	**Free-Field**
Open Circuit Sensitivity	**50 mV/Pa**
Open Circuit Sensitivity (+/-1.5 dB)	**-26 dB re 1 V/Pa**
Frequency Range (+/-1 dB)	**7 to 10 000 Hz**
Frequency Range (+/-2 dB)	**3.75 to 20 000 Hz**
Lower Limiting Frequency (3 dB)	**1.0 to 3.0 Hz**
Inherent Noise (linear)	**<18.5 dB re 20 µPa**
Inherent Noise	**<16.5 dB(A) re 20 µPa**
Dynamic Range (3% distortion limit)	**>135 dB re 20 µPa**
Dynamic Range (maximum without clipping)	**138 dB re 20 µPa**
TEDS Compliant	**Yes**
Environmental	
Temperature Range (Operating)	**-40 to +80 °C**
Temperature Sensitivity Coefficient (-10 to +70°C)	**0.009 dB/°C**
Static Pressure Coefficient	**-0.013 dB/kPa**
Humidity Sensitivity Coefficient (0 to 100%, non-condensing)	**±0.001 dB/%RH**
Influence of Axial Vibration (0.1g (1 m/s²))	**63 dB re 20 µPa**
Electrical	
Polarization Voltage	**0 V**
Excitation Voltage	**20 to 30 VDC**
Constant Current Excitation	**2 to 20 mA**
Output Bias Voltage	**10 to 14 VDC**
Maximum Output Voltage	**+/-7 Vpk**
Output Impedance	**<50 Ohm**
Physical	
Housing Material	**Stainless Alloy**
Venting	**Rear**
Electrical Connector	**BNC Jack**
Mounting Thread (grid)	**0.5 - 60 UNS**
Size - Diameter (with grid)	**13.2 mm**
Size - Diameter (without grid)	**12.7 mm**
Size - Height (with grid)	**91.9 mm**
Size - Height (without grid)	**90.9 mm**
Weight	**45.8 gm**

The DAU satisfied the electrical requirements of the microphone and the microphone dynamic range was above the expected SPL to be recorded on the Bell 412.

These parameters are referenced again in section 3.6, when possible sources of erroneous data are discussed.

3.5.2. Review of Microphone Functionality

It was important to have an understanding of the functionality of a microphone to be able to recognize erroneous data sources.

Condenser microphones convert acoustical energy into electrical energy through a vibrating capacitor as depicted in Figure 16 below.

The front plate of the capacitor vibrates when struck by sound waves. As the plates move closer together capacitance increases and the current charges. As the plates move further apart, capacitance decreases and the current discharges. In this way, condenser type microphones are sensitive and will often respond faster than the traditional dynamic type microphone. Additionally, condenser microphones usually have a flatter frequency response (they are uniformly sensitive to different frequencies) than dynamic microphones [45].

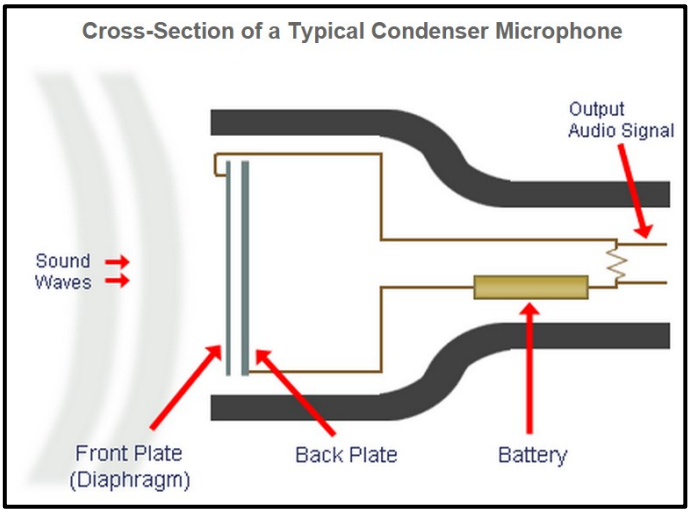

Figure 16: Cross-section of a typical condenser microphone [46]

Within the sensor itself, high impedance circuitry is preferred (ideally infinite impedance). Once the microphone capacitor develops a charge, the capacitor will immediately begin to discharge said charge. The discharge is a logarithmic decay as depicted in Figure 17 [46]. The circuit impedance must be as high as feasibly possible to slow this decay. With a high-speed decay the microphone will output many "pressure fluctuations" due to capacitor charge decay as opposed to actual pressure fluctuations.

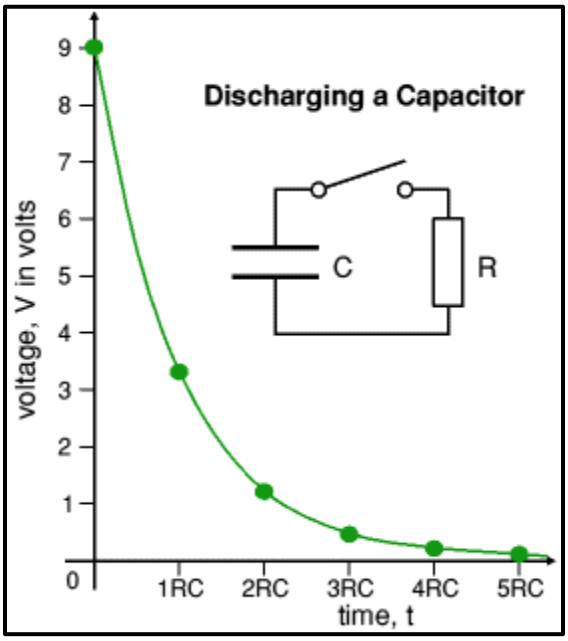

Figure 17: Example logarithmic decay of a discharging capacitor [47]

However, high impedance signals are not ideal for long distance data transfer. The high impedance will limit the current and a large voltage drop will be experienced along the cable length. High impedance cable lines are adversely affected by the inherent capacitance in the cable and behave as undesirable low-pass filters in these instances [47].

For these reason, the selected sensors were all ICP type [48]. Standard condenser microphones are normally charge type sensors (the charge is developed across the

previously mentioned capacitor). Additional internal circuitry converts the high-impedance charge signal into a low-impedance signal suitable for transmission across any feasibly long, low impedance cable length.

3.5.3. Erroneous Data Sources

Having discussed the workings of the 378B02 microphone, possible error sources can now be discussed. Table 9 stated three important error coefficients:

1. Temperature Sensitivity Coefficient, $c_T = 0.009 \frac{dB}{℃}$

2. Static Pressure Coefficient, $c_P = -0.013 \frac{dB}{kPa}$

3. Humidity Sensitivity Coefficient, $c_H = \pm 0.001 \frac{dB}{\%RH}$

Chapter 4 describes the noise measurement completed on the Bell 412 helicopter during December, 2013. For the present error analysis, environmental data from that flight and date will be used.

The following table contains the original microphone calibration conditions [49] and the Ottawa International Airport (CYOW) weather station climate data for December 3rd at 13:00 [50] on the **ground**. The error was calculated by:

Equation 3: Simple error calculation equation

$$e_x = (\Delta_x)(c_x)$$

- ***x*** **is a subscript replacement for *T*, *P* and *H*, the three error sources noted above**

Table 10: Microphone error information for <u>on the ground</u>; Dec 3rd, 2013

Condition	Calibration [49]	Dec 3rd, Airport [50]	Delta (Δ)	Error
Temperature	$21\,℃$	$-0.2\,℃$	$21.2\,℃$	$+0.190\ dB$
Static Pressure	$99.2\ kPa$	$100.09\ kPa$	$0.89\ kPa$	$-0.012\ dB$
Rel. Humidity	$46\ \%RH$	$89\ \%RH$	$43\ \%RH$	$\pm 0.043\ dB$

The following table contains the original microphone calibration conditions [49] and estimations made with empirical relations [51], [52] using the Ottawa International Airport (CYOW) weather station climate data for December 3rd, at 13:00 [50] as a baseline for the highest recorded in-flight **altitude of $556\ \boldsymbol{m}$** $[1825\ ft.]$.

Table 11: Microphone error information for 556 m altitude; Dec 3rd, 2013

Condition	Calibration [49]	Dec 3rd, Airport Estimation	Delta (Δ)	Error
Temperature	$21\ ℃$	$-3.1\ ℃$ [51]	$24.1\ ℃$	$+0.217\ dB$
Static Pressure	$99.2\ kPa$	$94.89\ kPa$ [52]	$4.31\ kPa$	$-0.056\ dB$
Rel. Humidity	$46\ \%RH$	$89\ \%RH$ [50]	$43\ \%RH$	$\pm 0.043\ dB$

It is common to use the root mean square (RMS) of such errors to estimate the total error [53]. In this instance a worst case scenario approach is used wherein all errors will be assumed to be positive or negative errors.

Equation 4: RMS error

$$e_{RMS} = \sqrt{\frac{1}{3}\left({c_T}^2 + {c_P}^2 + {c_H}^2\right)}$$

Equation 5: Decibels

$$[dB] = 20\log_{10}\left(\frac{p_{RMS}}{p_{REF}}\right)$$

The **ground $\boldsymbol{e_{RMS}} = \pm 0.08\ dB$**, while the **in air $\boldsymbol{e_{RMS}} = \pm 0.11\ dB$**. A change of $0.08\ dB$ is an increase of $0.93\ \%$ in pressure and a change of $0.11\ dB$ is an increase of $1.27\ \%$ in pressure. In most acoustics applications this is considered small. These numbers are referred to again in section 5.2.5 when the flight data is discussed.

Two additional microphone error sources are the capacitor discharge decay error source and white noise transmitted throughout the microphone cabling. It can be noted

that according to Table 9, the $\pm 2\ dB$ frequency range is 3.75 to $20\ 000\ Hz$. Therefore, for a fluctuation slower than seven times a second, a noticeable data loss should be present. As the typical human hearing range is arguably between $20\ Hz$ to $20\ kHz$, this type of error was negligible for this study. As seen in chapter 5, common 3rd octave charts do not go below 12.5 or $16\ Hz$.

3.6. Digital Signal Analysis Methodology

The final section of this chapter serves to characterize the signal path. The previous section explains how a microphone produces an analog signal from dynamic SPL. For this DAU, work was required to transform the data into a format readable by commercial software for analysis (such as LMS Test.Lab).

3.6.1. Sound Pressure Level Signal Path

The block diagram shown in Figure 18 depicts the signal path from the microphone to the eventual display of data on a computer.

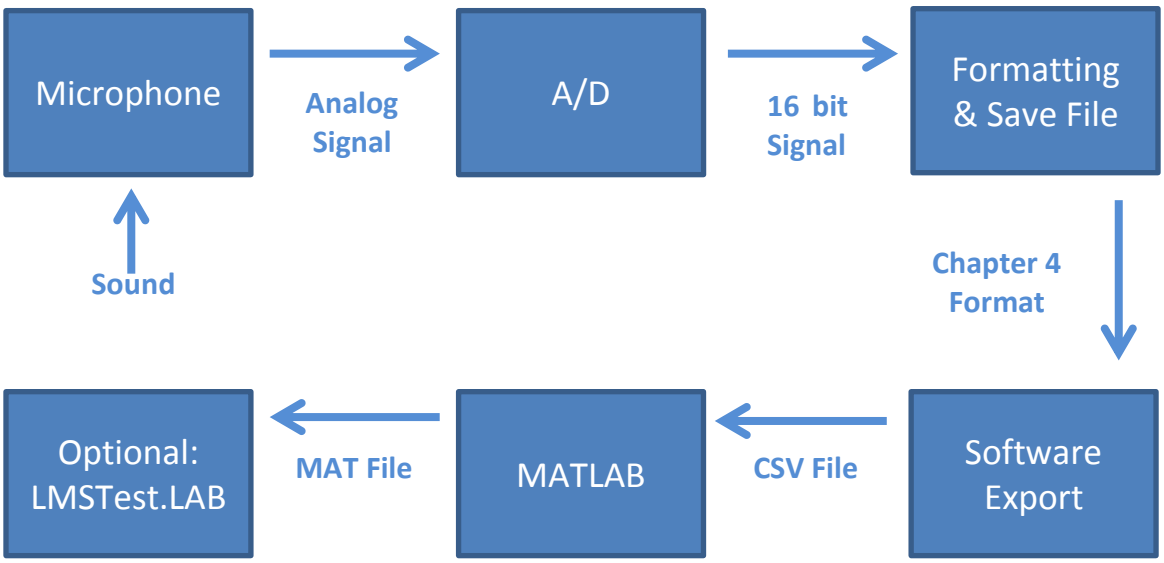

Figure 18: Sound pressure level signal path for the TTC DAS

3.6.2. Analog to Digital Conversion

The analog to digital converter is a component built into the MGRC-202W-1 module. The device samples the analog signal to record a new value. The MGRC can sample up to $125\,000\ Hz$. For the Bell 412 helicopter flight recording, the MGRC was programmed to sample at $50\,000\ Hz$.

Figure 19 contains an example of analog to digital (A/D) conversion with a 3 bit converter so there are $2^3 = 8$ possible outputs (quantization levels). For this DAU, the data samples are written in 16 bit "words" with 4 bits reserved for formatting instructions for a functional data sample of 12 bits ($2^{12} = 4096$ possible outputs). Therefore, every $1/50\,000 = 0.000\,02$ seconds the A/D converter would record another 12 bit "word". The significance of this conversion as well as other potential error sources is discussed at the end of this section. The DAU was formatted to receive voltage signals from the microphone in the range of $-10\ V$ to $+10\ V$.

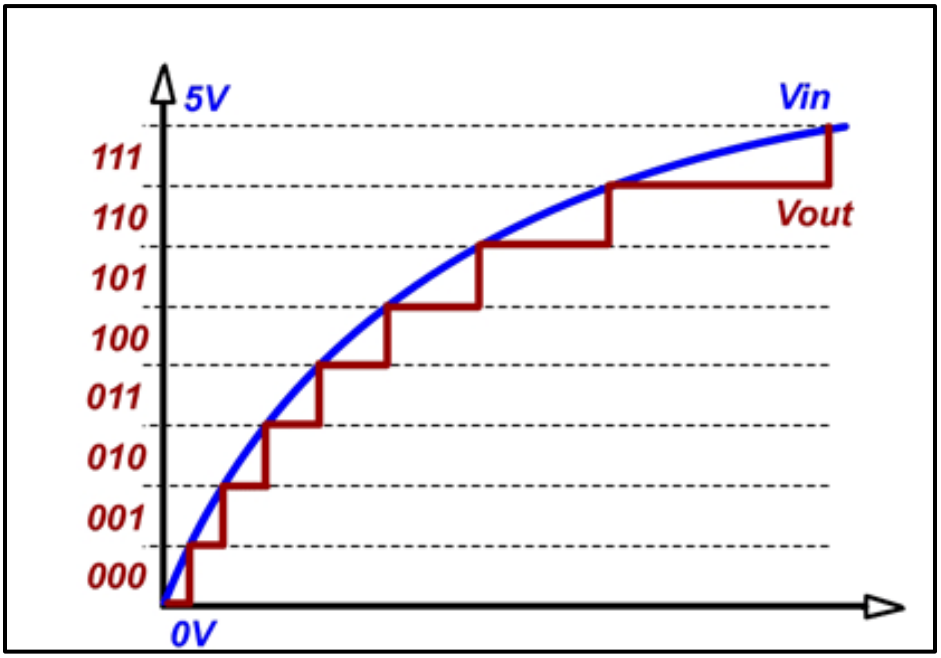

Figure 19: Quantization of an analog signal [67]

Next the data is saved in Chapter 4 format (a TTC software bit format); this format has 16 bit words. The 12 bit words are converted into 16 bit words (but still maintain the resolution of a 12 bit word). Using the TTC ground station software, the data can be exported in a decimal format for reading into MATLAB or other software.

It should be commented on that 12 bit resolution would be considered low in this era of 32 and 64 bit desktop computers. Although the TTC MCDAU is competitive hardware, some of the technology would be considered old. The certification process for various airworthy digital signal processing (DSP) formats is time consuming and expensive. For this reason, standardized airworthy equipment may lag behind the competitive high speed technology market.

3.6.3. MATLAB Conversion

The MATLAB conversion step is a simple "compression" of the data. An example Chapter 4 CSV export can be seen below in Table 12.

Table 12: Sample chapter 4 format CSV export

Time	Channel 1	Time	Channel 2	Time	Channel 3
Time Data	Bit Value				
		Time Data	Bit Value		
				Time Data	Bit Value
Time Data	Bit Value				
		Time Data	Bit Value		
				Time Data	Bit Value
…	…	…	…	…	…

The MATLAB conversion simply removes all the empty cells and assumes each channel reading occurs at identical times. In reality each channel is reading 800 ns apart. Therefore, the process is essentially shifting each successive channel in time by an

additional $800\,ns$. While insignificant for this study, it is important to note, as depending on the type of analysis done and how many channels there are, this could grow to be an important factor. The measurements were not precisely simultaneous.

Some minor data conversions are completed at the same time for convenience. The bit value is converted to a voltage which is then converted into pressure using calibration sensitivities (sensitivities found through calibration). One sample MATLAB import script may be found in appendix A2. An example calculation for a single data point is shown below. The example will assume the DAU measured a voltage of $0.280\,V$ from the microphone, which would be saved as a bit value of 33684.

Table 13: Example calculation for a data point

Equation	Example	Explanation
$V = \frac{Bit\ Value}{3276.8}$	$\frac{33684\ bits}{3276.8\frac{bits}{V}} = 10.280\ V$	First the bit is converted back into a voltage. *$3276.8 = 2^{16}/20$ (# bits divided by voltage range)
$Centered\ V = V - 10$	$10.280\ V - 10\ V = 0.280\ V$	The range is -10 V to +10 V, not 0 V to 20 V
$mV = V * 1000$	$0.280\ V * 1000 = 280\ mV$	Conversion to mV
$Pa = mV/sens$	$\frac{280\ mV}{217.3\frac{mV}{Pa}} = 1.29\ Pa$	The channel sensitivity was found earlier from calibration

***3276.8 is a conversion of volts to bits. With a 16 bit storage format ($2^{16} = 65536$) and a voltage range of $-10\ V\ to + 10\ V$ $(20\ V\ total)$ each volt has 3276.8 possible bit values contained within it.**

While simple, the process becomes time consuming and memory intensive for long duration files sampling at $50\,kHz$. For nine channels sampling at $50\,kHz$, 27 million "words" are recorded in one minute. For longer files or additional channels, the MATLAB code would need to be optimized.

To determine the sensitivity of each channel (from calibration) mentioned earlier, the same process as seen in Table 13 may be followed with the exception of the last step. Instead, the milliVolt value is compared to the known calibration pressure input. The ratio is written as the sensitivity. While completing this calibration, it is important to approximate the test conditions in every way possible. For the Bell 412 helicopter measurement (and subsequent measurements) calibration files were created in dry runs in a secure indoor testing location as well as in the loud hanger environment before takeoff. Standard ISO 5129 requires a post calibration to be completed after the test to ensure the sensitivity of a channel has not changed during flight (a common indicator of noise, interference or signal route degradation).

For the Bell 412 helicopter flight, a post calibration was completed. In the aircraft hangar it was difficult to secure a perfect calibration for each channel. Due to this, some low frequency, high amplitude noise was generated which needed to be manually removed (the calibrator emits only one frequency and thus could be isolated).

A simple script was written to compare various methods of removing the low frequency components (for calibration files; NOT data files). The methods were:

1. Periodic Re-Centering

2. High-pass Butterworth Filter, stop-band 100 Hz

3. High-pass Chebyshev Type 1 Filter, stop-band 100 Hz

4. High-pass Chebyshev Type 2 Filter, stop-band 100 Hz

The calibrator used for the Bell 412 helicopter flight measurement was a type 4230, $1\,000\,Hz$, $94\,dB$ Piston phone manufactured by Brüel & Kjær. For specifics on the MATLAB filter generation refer to appendix A3.

Figure 20 contains a visual comparison of these methods. The darker blue is the original signal and the lighter red is the filtered signal overlaid the original signal. Notably, the *Chebyshev Type I* filter had a significant decrease in amplitude, perhaps due to the ripple in the pass-band that *Chebyshev Type I* filters have. The *periodic re-centering* was noisy as the resolution used for the re-centering was limited to a single period in size. However, it worked as a proof of concept and closely matched the *Butterworth* and *Chebyshev Type II* filters. Figure 21 is a magnification of the *Chebyshev Type II* filter. The slow blue waveform oscillations are filtered out to produce the uniform red waveform.

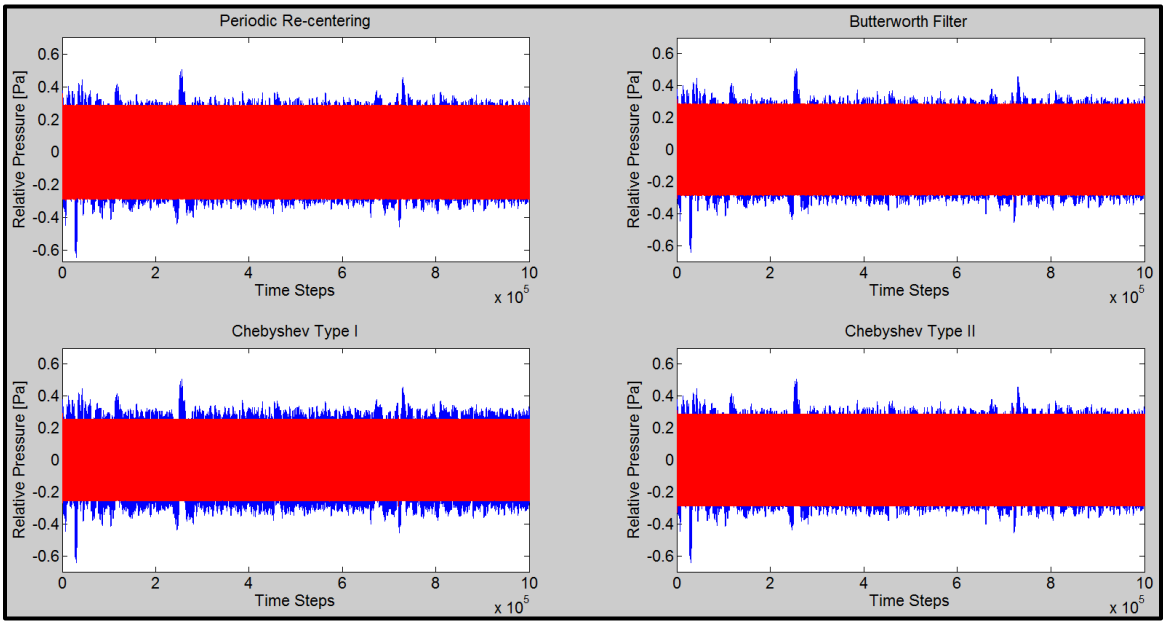

Figure 20: Visual comparison of the filter methods

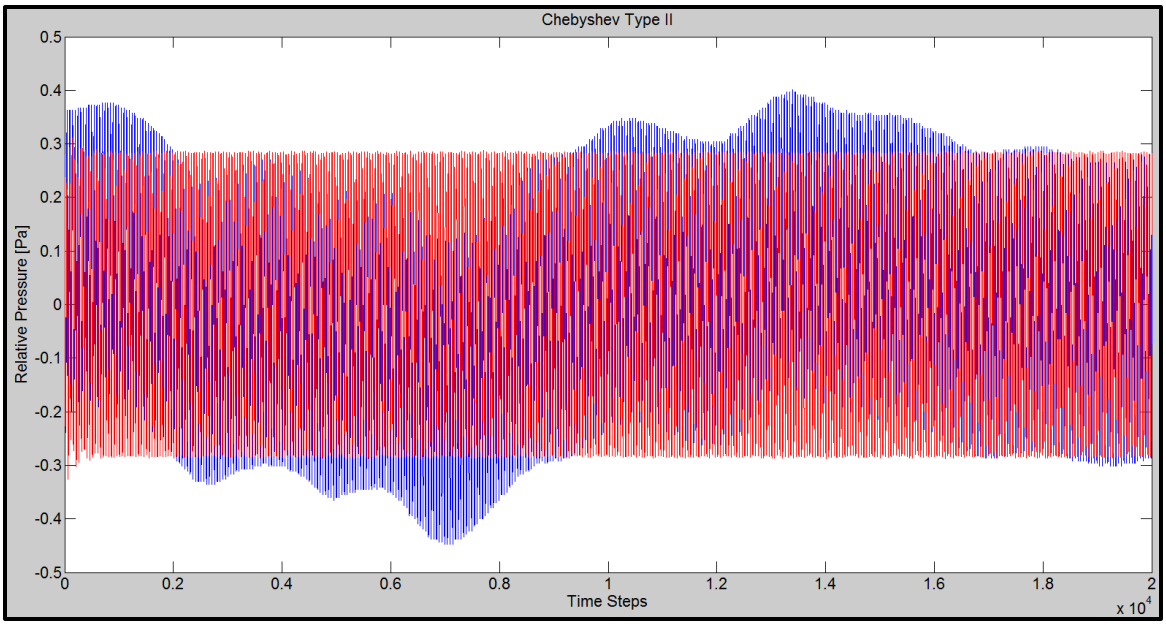

Figure 21: Magnification of Chebyshev Type II Filter

The RMS values for each method were found as:

1. 0.1995 for Periodic Re-Centering
2. 0.1995 for the Butterworth Filter
3. 0.1784 for the Chebyshev Type I Filter
4. 0.1995 for the Chebyshev Type II Filter

Having established confidence in the *Butterworth* and *Chebyshev Type II* filters, the sensitivities of the microphone channels were then calculated.

3.6.4. Sources of Erroneous Data

Calibrating the microphones for every test reduces the likelihood of signal route degradation. Error sources include:

1. **Quantization of the analog signal**. The DAU $20\ V$ range divided by the 2^{12} possible bit value outputs is a voltage of $4.88\ X\ 10^{-3}\ V$, which corresponds to approximately $0.024\ Pa$ with the settings used for the Bell 412 flight. Therefore, the measurement

resolution was $0.024\ Pa$ (an error of $\pm 0.012\ Pa$). This is small for loud measurements (such as the $\sim 130\ dB$ recordings discussed in chapter 5).

2. **Computer rounding**. This is standard for all digital post-processing results. MATLAB's default number storage is "double" which is a 64 bit number. This resolution is many orders of magnitude larger than the DAS and therefore not of concern.
3. **Calibration validity**. Likely of primary concern, significant errors can be produced by calibrator movement during calibration (largely affecting the small enclosed pressure volume). A calibration is also sensitive to local atmospheric pressure. These errors can be mitigated with multiple calibration files and documentation of sensitivities from previous tests.

This concludes the summary of the flight-worthy data acquisition equipment used for the Bell 412 flight measurement and all subsequent measurements performed to date. Chapter 4 discusses the test measurement completed with the use of the previously summarized hardware and software.

4. Bell 412 Noise Measurement

This chapter outlines the measurement procedure for the Bell 412 helicopter flight. A summary of the various activities that were completed on the measurement day as well as relevant details on hardware installation are included. The in-flight measurements and ground measurements procedure in particular are characterized. For the in-flight data and sound pressure data, refer to chapter 5.

4.1. Flight and Ground Measurements Test Objective

The objective of this flight measurement was to measure noise at representative stations for aircrew during standard aircraft manoeuvres to determine the noise level exposure of crew and maintenance personnel, both interior and exterior of the aircraft.

4.2. Bell 412 Aircraft Specification

The Bell 412 is a dual-engine utility helicopter from the Bell Helicopter company. For convenience, some major specifications and a photo have been included in Table 14 and Figure 22.

Table 14: Default Bell 412 specifications [16]

Empty Weight	3 084 kg (6 800 lbs)	**Max Range**	766 km (414 nmi)
Max Gross Weight	5 398 kg (11 900 lbs)	**Max Endurance**	4.5 hours
Engine	Pratt and Whitney PT6T-3D Twin Pac	**Max Continuous Speed**	244 km/h (130 kts)
		Rotor Blades	4

The NRC Bell 412 helicopter is unique in that it is maintained under an experimental aircraft license and an additional sensor suite and a fly-by-wire system were added. The sensor suite supplied air data during flight. This data is summarized in section 5.2.1.

Figure 22: NRC Bell 412 helicopter

Standard operational crew for the NRC Bell 412 is a pilot, co-pilot and a flight engineer; however additional rag and tube seating may seat up to two additional passengers. An equipment rack containing hardware for an unrelated experiment was installed on the aircraft portside interior. This equipment was located further than a metre from the measurement locations.

4.3. Equipment Installation

Two sets of equipment were used. The TTC DAS was used for the in-flight measurement while an LMS Test.LAB and front end were used for exterior ground measurements. The following sections discuss both.

4.3.1. In-Flight Measurement

As discussed in section 3.3 and 3.4, standard aircraft seat restraints were used to secure the microphone stands and the DAS. Figure 23 below contains the locations of the crewmembers and microphones. Figure 24 depicts the interior of the NRC Bell 412 from the starboard side. Three measurement locations have been highlighted with circles.

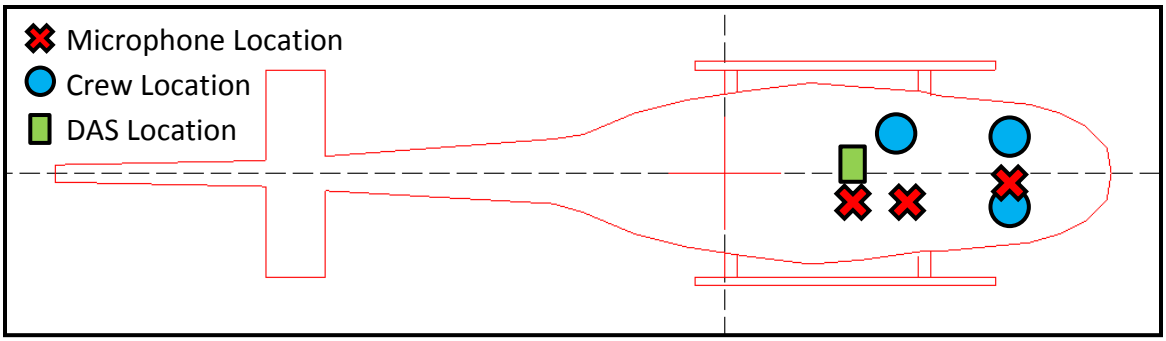

Figure 23: Bell 412 measurement sensor and crew locations

Figure 24: Interior of the NRC Bell 412 as seen from the starboard side

The microphone installations from bow to stern were:

1. The **pilot location** was approximately $10\ cm$ away from the helmet left ear of the pilot at head height facing horizontal towards the bow.
2. The **standing location** was not at the full $1.65\ m$ height required by ISO 5129 as this would not be applicable for this cabin height (due to the proximity to the roof).

3. The **seated passenger location** was within the required distance of the headrest and met the ISO requirement of $0.65\ m$ above the seat.

Figure 25 depicts additional cargo ratchet straps used to reduce the vibration of the stands.

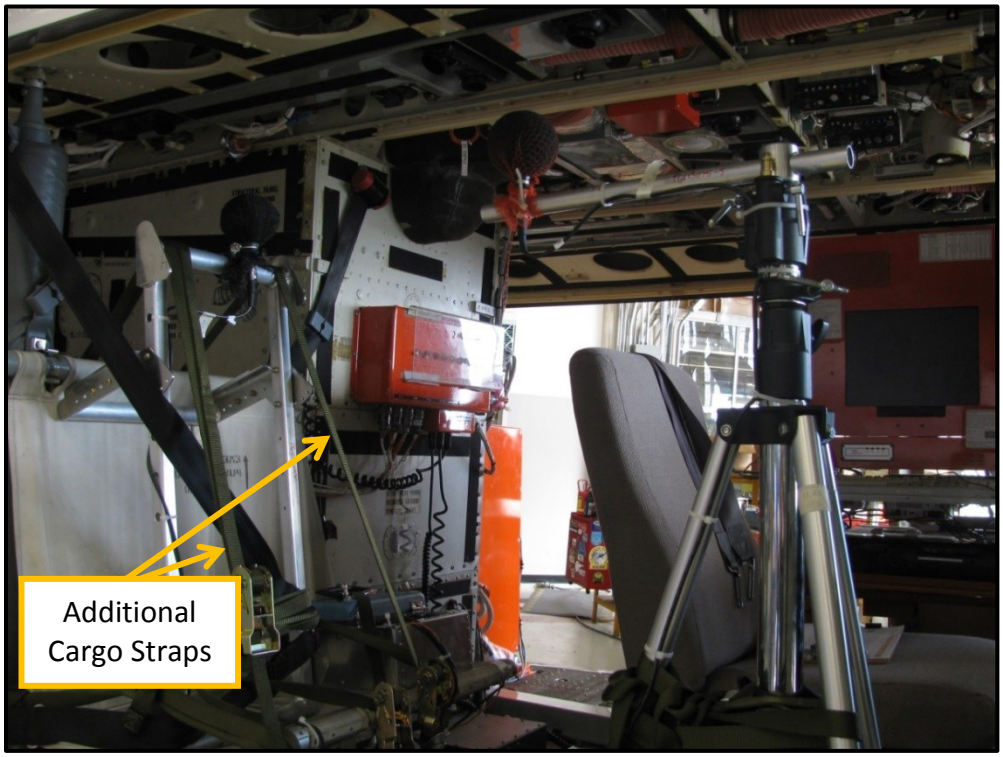

Figure 25: Bell 412 rear interior

The locations satisfied the requirements set out by standards ISO 5129 and MIL 1294 as discussed in chapter 2. Spacing the sensors along the entire interior span of the cabin was important to characterize the entire cabin space (as seen in chapter 5). It should be noted once again that free field microphones were used instead of the ISO 5129 random incidence microphones. For further details on mounting procedures and the validity of the selected microphones, refer to ISO 5129.

4.4. Equipment Validation and Testing

To ensure measurement validity, the sensitivity of the DAS system was determined on the ground before and after the flight while the equipment was installed in the aircraft. This procedure accommodates ISO 5129 as well as being appropriate for the overarching ISO 9001 Quality Standard that the NRC operates under.

Calibration before and after a test enables the user to verify that the sensitivity of the system did not change (a sign of signal degradation), and ensures the signal route was not damaged during a test. This procedure was followed for the Bell 412 helicopter measurement and it was found that each channel's sensitivity remained static.

However, as mentioned in section 3.2, the Phase I DAU box (the equipment set up used for the Bell 412 helicopter flight) was incapable of live-streaming the data, making onsite troubleshooting difficult and requiring that the data be downloaded to an external computer for preliminary analysis. Particular data had to be recorded twice due to an unexpected power loss. These experiences directly influenced the design of the Phase II DAS to include live-streaming.

From these experiences, the following signal route validation methodology was developed to ensure the fidelity of future measurements:

1. A space as large as the interior of the aircraft being measured is reserved.
2. Microphones are placed at the expected locations.
3. Cables are selected and run to each location (to ensure cables are sufficiently long on test day).

4. Each cable, microphone and channel ID are labelled and calibrated together. On the test day, the same cables, channels and microphones are used together and calibrated again.
5. The equipment is disconnected and stowed for shipping to the aircraft hangar.
6. On the test day, the equipment is installed and recalibrated.
7. After the test, the equipment is recalibrated a third time and uninstalled.

This number of calibrations ensured a signal route history that could be reviewed after the flight measurement to ensure data validity.

4.5. Flight Measurement Procedure

Once the equipment was installed, the measurement procedure was reviewed with the aircrew before flight. A later revision of the measurement procedure is recorded as reference [54]. In summary: "According to ISO 5129, aircraft flight conditions shall be those for steady flight, with aircraft Mach number or indicated airspeed, or both, and engine power setting or shaft rotational speeds, or both, stabilized to specified values within specified tolerance limits." [54] The flight conditions for the Bell 412 helicopter measurement have been summarized in Table 15.

Table 15: Bell 412 measurement conditions [54]

CLOSED DOORS				OPEN DOORS			
ID	**Condition**	**ID**	**Condition**	**ID**	**Condition**	**ID**	**Condition**
1	Ground	**8**	60 kt Climb	**1**	Ground	**8**	60 kt Climb
2	50 ft. Hover	**9**	100 kt SLF	**2**	50 ft. Hover	**9**	60 kt SLF
3	Landing	**10**	120 kt SLF	**3**	Landing	**10**	80 kt SLF
4	60 kt Climb	**11**	140 kt Descent	**4**	60 kt Climb	**11**	80 kt Descent
5	100 kt SLF	**12**	50 ft. Hover	**5**	60 kt SLF	**12**	50 ft. Hover
6	120 kt SLF	**13**	Landing	**6**	80 kt SLF	**13**	Landing
7	140 kt Descent	**14**	Ground	**7**	80 kt Descent	**14**	Ground

Both the open doors and the closed doors configurations had the applicable acoustical/thermal insulation treatments and furnishings in place. Both open doors and closed doors used the same equipment configuration. Apart from the installation of the recording equipment, the aircraft was flown with its normal configuration.

Once discussed, the pilot, co-pilot and flight engineer may rearrange or cancel any flight conditions depending on the weather and aircraft configuration. Notably, for this flight measurement, the open door flight segments were slowed to $60\ kts$ and $80\ kts$ as certain equipment cables from a separate experiment were vulnerable to the high wind velocities associated with open door flight.

The crew members included a pilot, co-pilot and DAS operator. With a total of 28 measurement conditions (each lasting one minute), the flight duration was approximately two hours. The co-pilot announced each measurement condition over the aircraft intercom and the DAS operator pressed record and wrote down the times for later comparison (to redundantly match the internal DAS time with the local time).

The summarized testing procedure was as follows:

1. Installation and calibration of equipment
2. Crew meeting and procedure review
3. Aircraft start-up
4. Ground measurement (as described in section 4.6)
5. Removal of ground measurement equipment; flight crew boarded the aircraft
6. Closed door flight segment
7. Landing and conversion to open door flight segment

8. Open door flight segment

9. Landing and shut down

10. Post calibration and removal of equipment

Microphone calibration is explained in more detail in section 3.6.

4.6. Ground Measurement Procedure

For the ground measurement, additional personnel were required to handle microphones, to restrict cables motion in the wind, and to secure each microphone stand. Before recording, a concise measurement procedure was organized between the crew members and ground personnel. This procedure will vary for each aircraft.

For the Bell 412 helicopter measurement the pilot remained in the aircraft while the co-pilot exited the aircraft to supervise the ground crew. There were a total of 5 crewmembers:

1. Pilot remained in the aircraft

2. Co-pilot exited the aircraft and directed the measurement to ensure aircraft safety

3. Ground crew 1 held the microphone stand and moved it from location to location

4. Ground crew 2 ensured no excess cabling was free to move in the rotor wash

5. Ground crew 3 manned the DAS

ISO 5129 states for interior standing locations, "The measurements are made with the helicopter on the ground at standing locations with the microphones at $1.65 \pm 0.1\,m$ above the ground. All subsystems which are normally operated during ground maintenance (generators, hydraulics, environmental control unit, etc.) shall be operating." [19]

An LMS Test.LAB front end, a laptop and a single 378B02 microphone were used for this measurement. Once the Bell 412 helicopter was brought to idle, ten different measurement locations were recorded consecutively (location one was recorded twice).

The measurement locations were measured with respect to the helicopter and have been recorded in Table 16 for convenience. Note the distance to the hanger door in schematic Figure 26. Figure 27 is a photo taken during the ground measurements.

Table 16: Exterior ground measurement locations

ID	X Position [m (in)]	Y Position [m (in)]
1	7.18 (282.76)	6.39 (251.54)
2	0.20 (7.78)	7.53 (296.43)
3	2.34 (92.31)	6.81 (268.06)
4	3.78 (148.92)	5.08 (200.14)
5	4.33 (170.57)	3.04 (119.77)
6	4.11 (161.64)	1.57 (61.90)
7	4.32 (170.00)	0.016 (0.63)
8	3.88 (152.70)	-1.64 (-64.63)
9	3.23 (127.18)	-3.09 (-121.69)
10	7.16 (281.79)	-0.25 (-9.72)
11	7.18 (282.76)	6.39 (251.54)

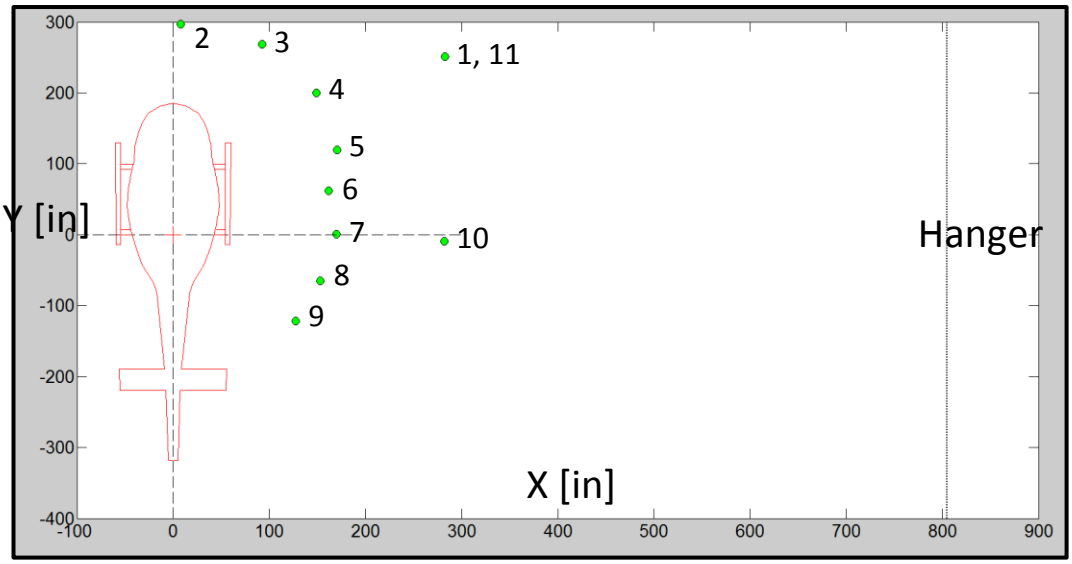

Figure 26: Exterior ground measurement locations

Figure 27: Exterior ground measurements of the Bell 412

4.7. Measurement Summary

The measurement took place on December 3rd, 2013. The temperature was approximately $-15°C$, clear skies and an atmospheric pressure of approximately $101\ kPa$ [50]. Cold temperatures are optimal for microphone usage as microphone sensitivity is consistent at the lower limits [55]. The temperature was well within the operational range of the microphone, the cabling and the DAS. While temperature and pressure will affect the SPL readings, this is accounted for with the calibrations done before and after the flight on the day of the flight as well as the microphone environmental adjustments discussed in section 5.2.5. Condensation is not of great concern for pre-polarized microphones, as opposed to externally polarized microphones [55]. No icicles formed on the microphones during flight and therefore did not impact the measurements.

The entire measurement campaign duration was less than three hours. All hardware performed optimally. For measurement results please continue to chapter 5.

5. Data Analysis and Results

The cabin noise measurement results performed on the Bell 412 helicopter on Dec 3rd, 2013 are presented in this chapter. Colour plots are recommended for interpretation of the following figures as a large quantity of data has been presented.

In order to better comprehend the functionality of the commercial acoustic analysis software LMS Test.LAB, the DSP procedures were first implemented in MATLAB for comparison. These comparisons are presented at this start of this chapter.

The descent and climb flight segments are compared to demonstrate the differences in their associated cabin noise measurements. Further comparisons between closed door and open door noise spectrums are completed in narrow band and 3rd octave formats. Finally, A-weighted results are contrasted to non-weighted results as per the standards discussed in chapter 2.

A discussion on windscreen insertion loss, microphone environmental adjustments, additional work completed by the NRC on HPs attenuation, and a summary of the exterior maintenance crew SPL measurements concludes the chapter.

5.1. Data Processing Theory

In order to understand the implemented algorithms used in LMS Test.LAB acoustic analysis, the theory was reviewed and implemented in MATLAB. This section is a summary of that work.

5.1.1. The Frequency Domain

As discussed in section 3.6, the DAS is a digital device that stores a finite number of measurements during a finite recording period. Assuming that this finite signal is periodic wherein the data captured coincidentally lines up with one period of the signal, the signal can be expanded into a finite set of sinusoidal waves similar to Figure 28.

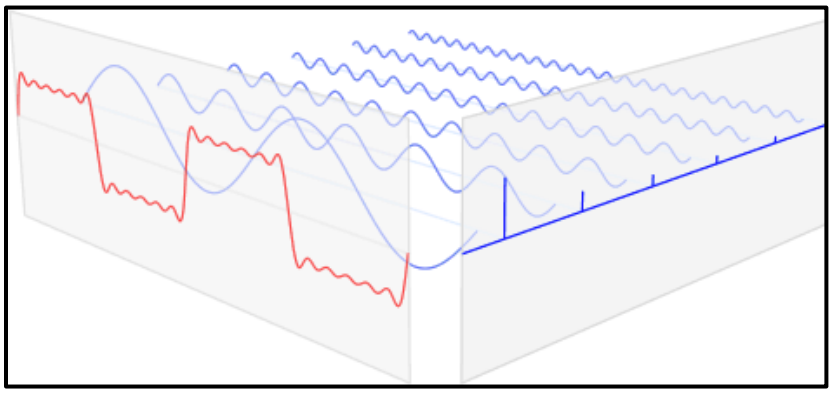

Figure 28: Summation of sinusoidal waves [68]

For a discrete signal, the decomposition to sinusoidal waves is mathematically exact. Notably, in Figure 28 above, the various blue sinusoidal waves have different amplitudes. A higher amplitude for a sinusoidal wave indicates a higher correlation between the time domain data and that particular sinusoid. This process of determining the amplitude for each frequency of wave is labelled the Fourier Transform [56].

The bandwidth of the data (the range of frequencies in the frequency domain) is related to the sampling rate of the DAS and the resolution of the data is related to the duration of the signal measured. Therefore, longer measurements will allow a higher resolution to accurately determine the frequency of a particular correlated sinusoid, while a faster sampling rate will allow a broader range of sinusoids to be considered. This determined the reason the DAS was programmed to have $50\,kHz$ sampling

(allowing analysis to include the $20\,kHz$ hearing domain) and the reason for the measurement duration of approximately 60 seconds (for resolution).

The Discrete Fourier Transform (DFT) may be written as:

Equation 6: The "real" discrete Fourier transform [56]

$$X_C[k] = \sum_{i=0}^{N-1} x[i]\, cos\left(\frac{2\pi k i}{N}\right)$$

$$X_S[k] = -\sum_{i=0}^{N-1} x[i]\, sin\left(\frac{2\pi k i}{N}\right)$$

- **i is a time sample step in the time domain**
- **k is a frequency step in the frequency domain**
- **$x[i]$ is the time domain signal being analyzed**
- **$X_{C,S}[k]$ are the cosine (C) and sine (S) frequency domain signals being calculated**
- **N is the total number of data points sampled (N = sampling rate X duration)**
- **The i index runs from 0 to $N-1$, the k index runs from 0 to $\frac{N}{2}$**

This equation is simple to implement as seen in appendix A4. This equation is the "real" DFT. The true DFT equation contains imaginary numbers which account for the phase of each sinusoidal wave in addition to their amplitude. For this noise analysis only the respective amplitude for each sinusoidal wave is required. Therefore, the "real" DFT is calculated. In effect, the DFT is methodically correlating the input signal with sequential sinusoidal waves. The higher the correlation between the signal and a particular sinusoidal wave, the higher the amplitude that sinusoid will have in the frequency domain.

A plot of **Equation 6** for a closed door climb flight segment of the Bell 412 is shown at the top of Figure 29. In comparison, the **MATLAB FFT** for the same flight segment has been presented in the bottom of Figure 29. The results are identical. The two circled

peaks have significant “tails” sloping downwards from the peak, which is termed spectral leakage.

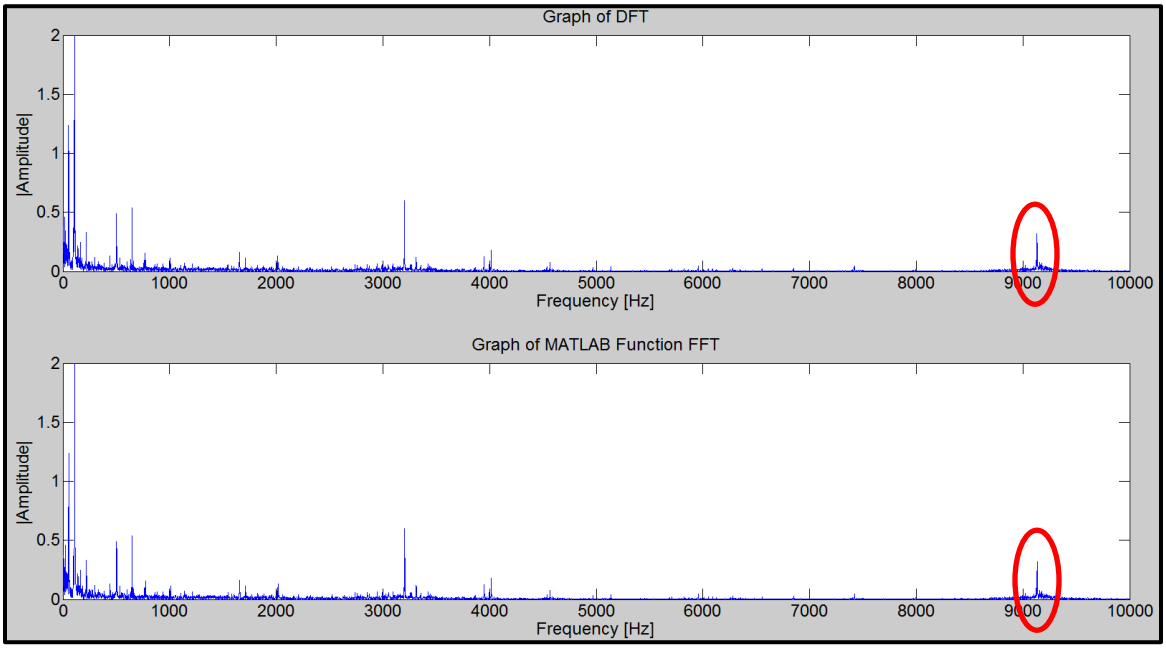

Figure 29: DFT compared to MATLAB FFT

Furthermore, one can observe that the x-axis runs to $10\ kHz$. The actual data was sampled at $50\ kHz$ allowing for a bandwidth of $25\ kHz$. However, as discussed in section 3.1, some of the microphone modules have an internal low-pass software filter of $10\ kHz$. All data past $10\ kHz$ was zero for this recording and therefore is not shown. Methods of accounting for spectral leakage and other nuisances are discussed in section 5.1.2 below.

5.1.2. Optimizing Frequency Domain Results

Two issues that are commonly dealt with in frequency domain analysis are spectral leakage and noise.

Spectral leakage is the result of a sinusoid present in the signal, existing between two different frequency bands in the frequency domain. The energy associated with this

sinusoid will be divided amongst adjacent frequency bands. Wording it another way, the energy will “leak” into adjacent frequency bands.

The solution is to convolve a window onto the signal, consequently broadening the frequency domain peaks while attenuating the energy leakage into adjacent bands. This is effectively a trade-off of frequency resolution for reduced spectral leakage [56]. Figure 30 shows the advantage of using a Hanning window. The peak occurring at $5.5\,Hz$ has been enlarged. The blue peak corresponds to the original FFT of the time domain signal, while the shorter red peak corresponds to the FFT of the time domain signal convolved with a Hanning window. The “tails” have been significantly reduced making the peak associated with the $5.5\,Hz$ sinusoid more pronounced. Disadvantageously, the amplitude of this sinusoid has also diminished (the energy was attenuated).

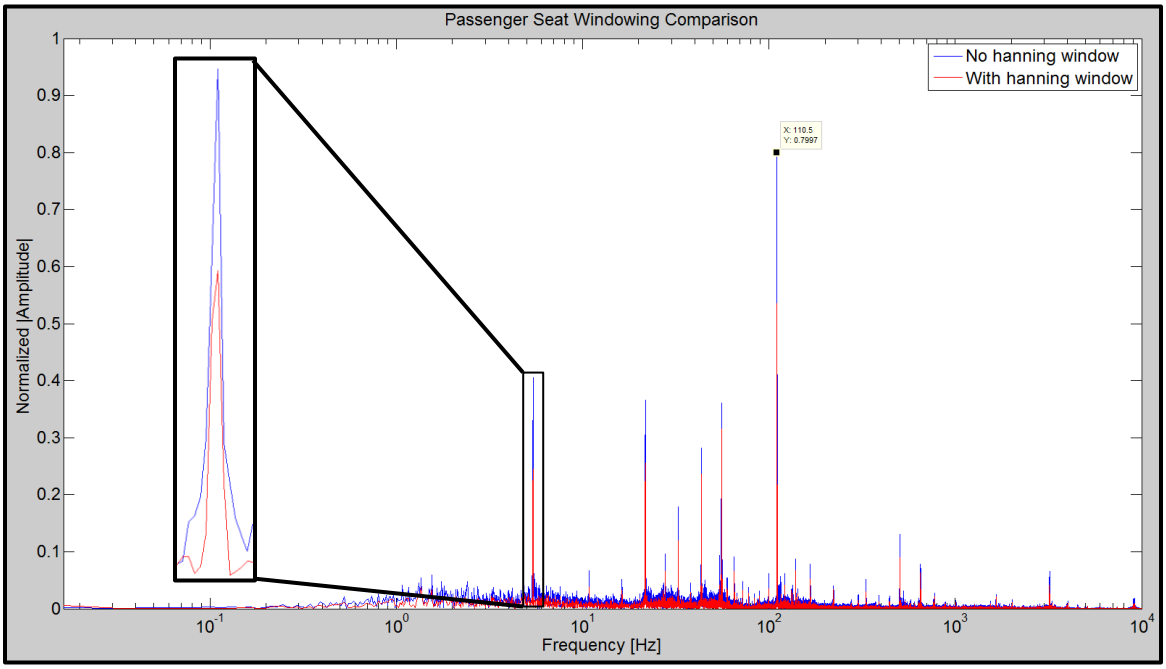

Figure 30: Hanning window comparison

The drop in amplitude is accounted for with correction factors. LMS Test.LAB automatically accounts for this. The LMS correction factors may be viewed in Table 17.

Table 17: LMS windowing correction factors [57]

Window Type	Amplitude	Energy
Uniform	1	1
Hanning x1	2	1.63
Hanning x2	2.67	1.91
Hanning x3	3.2	2.11
Blackman	2.8	1.97
Hamming	1.85	1.59
Kaiser-Bessel	2.49	1.86
Flattop	4.18	2.26

The second issue: noise; is naturally generated from background noise in an electronic system (the random motion of the electrons), as well as a variety of other sources contextually based on the location of the measurement. Noise is time signal data uncorrelated to any specific sinusoid. To reduce the presence of noise in the frequency domain, multiple averages are taken. In essence, a single time domain signal is split into multiple segments, a DFT of each signal segment is completed and these multiple DFTs are averaged together. Sinusoids that are present in each DFT then become more prevalent.

Finally, a **MATLAB DFT** was combined with a Hanning window, a correction factor of 1.63 and **no averaging**, which can be seen in Figure 31. This was compared against an **LMS DFT** with a Hanning window and **50 averages**. Without averaging, the MATLAB DFT is noisier and the peak associated with $110.5\ Hz$ has been significantly attenuated while various low amplitude peaks such as the $12.5\ Hz$ sinusoid disappear entirely. Without averaging, information is lost.

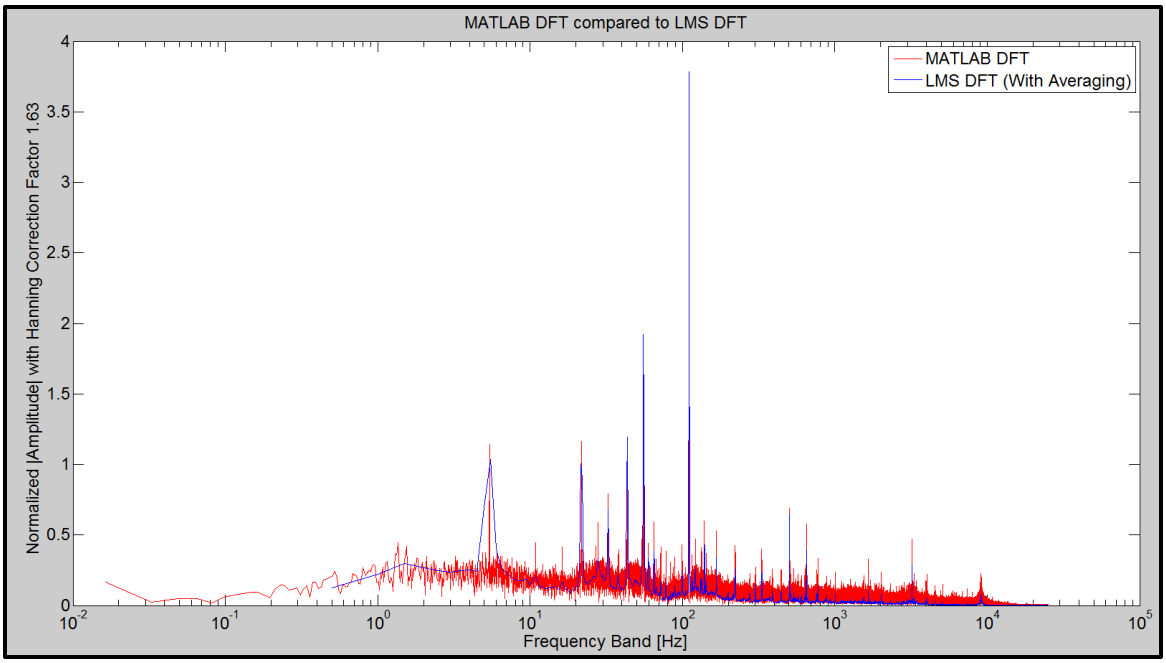

Figure 31: MATLAB DFT validation

After a thorough understanding of the LMS Test.LAB algorithms was established the Bell 412 helicopter in-flight measurements were analyzed using LMS Test.LAB and have been included in Section 5.2.

5.2. Flight Test Results

The Bell 412 helicopter in-flight measurements produced large quantities of data. A concentrated effort has been made to summarize characteristics of interest, as well as to isolate aircraft sound sources. Refer to section 4.5, Table 15 for the description and explanation of the flight conditions.

5.2.1. Flight Data Parameters

The NRC Bell 412 was equipped with a custom air DAS. Applicable flight condition parameters for the **closed door** flight segments have been recorded and are shown in the flight segment order, in Table 18 below.

Table 18: Closed door Bell 412 aircraft flight data

Event	ALT (m)	IAS (kts)	TAS (kts)	Pitch (Deg)	Roll (Deg)	HDG (Deg)	MRRPM (RPM)	TRRPM (RPM)	TQ M (%)
GRD. RUN A	115.8	8.14	14.52	3.61	-0.21	278.40	323.71	1658.51	23.81
HOVER A	132.3	10.05	15.72	6.15	-0.84	279.71	324.15	1660.78	72.60
CLIMB A	318.1	54.86	58.10	4.10	-2.38	37.60	325.04	1665.35	67.01
SLF 100 A	423.9	91.96	96.67	0.04	-1.44	57.43	326.35	1672.06	59.70
SLF 120 A	407.8	109.69	115.23	-0.08	-2.21	58.97	323.32	1656.52	78.22
DESCENT A	343.5	129.19	135.31	-3.10	-1.94	78.57	323.00	1654.90	80.64
CLIMB B	391.8	53.22	56.74	3.83	-2.18	241.35	324.95	1664.85	61.66
SLF 100 B	543.2	92.21	97.65	0.29	-0.65	288.28	325.11	1665.69	63.16
SLF 120 B	556.3	110.45	116.89	-0.81	-1.77	251.70	323.48	1657.31	78.23
DESCENT B	402.5	128.57	134.87	-3.43	-2.39	239.64	323.08	1655.28	83.29
HOVER B	131.1	8.31	14.61	5.42	-2.20	281.87	324.04	1660.21	73.02
GRD. RUN B	115.4	7.82	14.34	3.41	0.05	286.59	322.79	1653.83	24.40

- **ALT is the Altitude in meters**
- **IAS is the Indicated Airspeed in knots**
- **TAS is the True Airspeed in knots**
- **HDG is the Heading in degrees**
- **MRRPM is the Main Rotor RPM in revolutions per minute (RPM)**
- **TRRPM is the Tail Rotor RPM in revolutions per minute (RPM)**
- **TQ M is the Main Rotor Mast Torque in percent of maximum rated torque**
- **GRD. RUN is a Ground Run (aircraft was stationary on the ground)**
- **SLF is Steady Level Flight in knots**
- **A and B are separate measurements of the same flight condition**

For the **closed door** flight segment, the maximum altitude of $556.3\ m$ occurred during the steady level flight 120 knot B segment. This corresponds to an approximate decrease in pressure of $5\ kPa$ [58]. The maximum true airspeed was $135\ kts$ during descent A. The highest torque on the main rotor mast occurred during descent B. This parameter is significant for high frequency noise generation. Stable flight conditions were achieved as the pitch attitude did not exceed 6 degrees, roll attitude did not exceed 3 degrees and the baseline rotor speed remained within 1% of $324\ RPM$ for the entire flight duration.

The **open door** flight condition parameters have been presented in Table 19.

Table 19: Open door Bell 412 aircraft flight data

Event	ALT (m)	IAS (kts)	TAS (kts)	Pitch (Deg)	Roll (Deg)	HDG (Deg)	MRRPM (RPM)	TRRPM (RPM)	TQ M (%)
GRD. RUN A	116.3	7.38	14.12	3.50	-0.29	287.10	323.42	1657.01	24.501
HOVER A	131.7	8.64	14.90	6.16	-1.38	268.44	319.96	1639.32	70.458
CLIMB A	310.2	53.61	56.83	4.45	-1.47	39.64	320.56	1642.38	63.930
SLF 60 A	433.2	55.71	59.29	3.09	-0.93	47.37	323.85	1659.23	39.591
SLF 80 A	431.7	74.94	79.10	1.83	-0.72	45.47	322.90	1654.36	45.377
DESCENT A	299.2	75.22	78.95	1.37	-1.66	47.25	326.06	1670.56	26.354
CLIMB B	398.2	55.34	58.87	4.01	-2.78	229.32	321.32	1646.27	61.316
SLF 60 B	477.9	55.38	59.09	3.14	-1.88	232.91	325.64	1668.43	40.278
SLF 80 B	470.6	75.22	79.50	1.70	-0.63	246.28	324.77	1663.94	46.808
DESCENT B	349.7	73.60	77.55	1.39	-1.50	246.01	328.03	1680.65	27.873
HOVER B	129.7	8.64	14.80	6.10	-1.47	280.15	321.21	1645.70	69.399
GRD. RUN B	113.5	8.09	14.47	3.50	-0.14	274.20	324.77	1663.92	24.839

Refer to Table 18 footnotes for abbreviations

For the **open door** flight segment, the maximum altitude of $477.9\ m$ occurred during the steady level flight 60 knot B segment. This corresponds to an approximate decrease in pressure of $4\ kPa$ [58]. The maximum true airspeed was $79.5\ kts$ during the same segment. The highest torque on the main rotor occurred during hover A. The pitch did not exceed 6 degrees, the roll did not exceed 3 degrees and the baseline rotor speed remained within 2% of $324\ RPM$ for the entire flight duration.

The air conditions based on the Ottawa International Airport (CYOW) weather station climate data have been presented in Table 20 for convenience.

Table 20: Ottawa International Airport (CYOW) weather station climate data [50]

Condition	Dec 3rd, Airport Ground	Dec 3rd, Airport 556 m
Temperature	$-0.2\ ℃$	$-3.1\ ℃$
Static Pressure	$100.09\ kPa$	$94.89\ kPa$
Rel. Humidity	$89\ \%RH$	$89\ \%RH$

The Bell 412 helicopter in-flight noise measurements are discussed in sections 5.2.2 to 5.2.4. Additionally, 3rd octave band results that have not been altered by windscreen sound insertion loss or microphone environmental effects are presented in appendix A5.

5.2.2. Flight Measurement Spectral Density Comparison

As can be seen in Table 18, during the **closed door climb** flight segment, the main rotor RPM was measured as $25.04\ RPM$ $(5.42\ Hz)$ for segment A and $324.95\ RPM$ $(5.42\ Hz)$ for segment B. The tail rotor RPM was respectively measured as $1665.35\ RPM$ $(27.76\ Hz)$ and $1664.85\ RPM$ $(27.75\ Hz)$.

In Figure 32, a narrowband spectral density (SD) analysis of the **closed door climb** flight segment depicts several acoustic sinusoids related to the aforementioned rotor harmonics. Solid vertical lines have been overlaid on Figure 32 to depict the frequencies associated with the main rotor's fundamental frequency and its associated harmonics. Dashed lines have similarly been drawn for the tail rotor's associated harmonics.

The main rotor's 4th and 8th harmonics (MRH) as well as the tail rotor's 2nd and 4th harmonics (TRH) have been identified with arrows. A large peak occurred at $21.5\ Hz$ (main rotor's 4th harmonic). This is logical as the Bell 412 helicopter has a four bladed main rotor and it dominated the lower frequencies. The peak with the largest amplitude occurred at $110.5\ Hz$ (tail rotor's 4th harmonic, although the tail rotor is a two-bladed rotor). This indicated that the tail rotor was a significant source of noise for the **climb** segments.

Figure 32 contains many additional sinusoid peaks with smaller amplitudes. It can be observed that the majority of these sinusoidal waves are aligned with higher main rotor harmonics and higher tail rotor harmonics as opposed to independent sound sources.

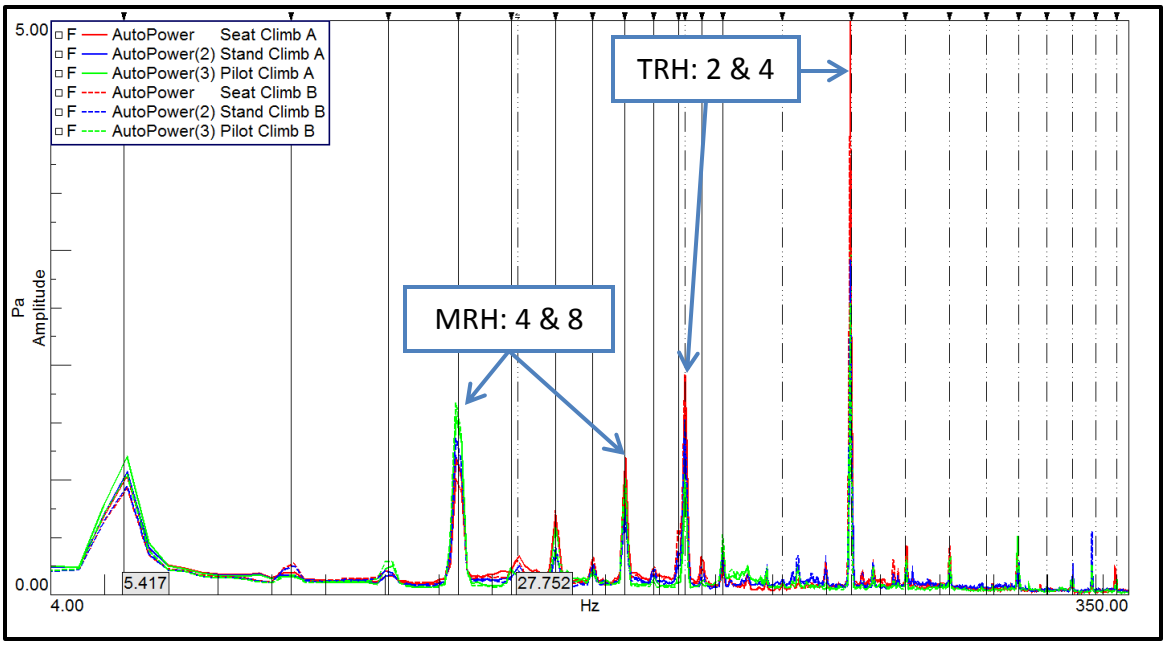

Figure 32: Spectral density of all closed door climb segment microphone positions

For the **closed door descent** segments, as depicted in Figure 33 below, the measured main rotor RPM averaged $323.4\ RPM\ (5.39\ Hz)$ while the measured tail rotor RPM averaged $1656.9\ RPM\ (27.62\ Hz)$. Once again, the main rotor's 4^{th} and 8^{th} and the tail rotor's 2^{nd} and 4^{th} harmonics have been labelled. For this **descent** flight segment, the largest peak occurred at the main rotor's 8^{th} harmonic of $43\ Hz$ (as opposed to the tail rotor's 4^{th} harmonic previously discussed for the **climb** flight segment). The main rotor's 4^{th} harmonic $(21.5\ Hz)$ also increased in amplitude (it should be noted that the Figure 33 y-axis scaling is larger than Figure 32). These results indicated that during a **descent** flight segment the main rotor became the dominant source of noise.

Furthermore, the amplitudes of the peaks associated with the tail rotor harmonics retained a similar level as during the **climb** segment while the peaks associated with the main rotor harmonics increased. Therefore, the **descent** flight segment was louder.

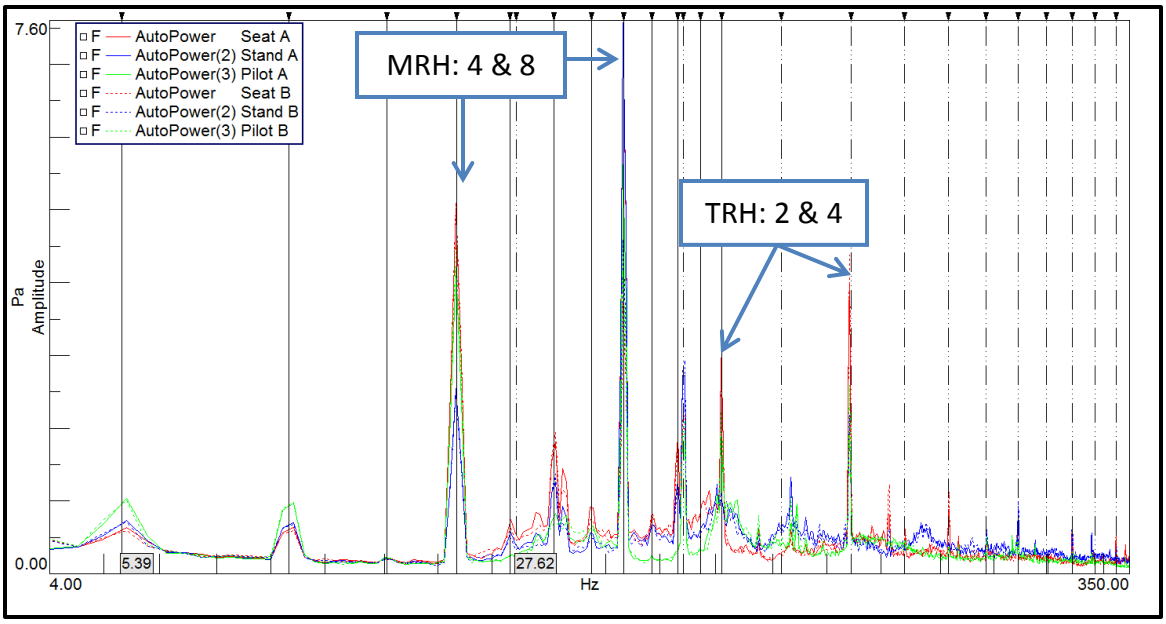

Figure 33: Spectral density of all closed door descent segment microphone positions

The overall sound pressure level (OSPL) values for the **climb** and **descent closed door** flight segments have been calculated and presented in Table 21.

Table 21: OSPL values for the closed door climb and descent flight segments

Position	Climb A	Climb B	Descent A	Descent B
Seated Position	107.00 dB	108.36 dB	114.40 dB	113.34 dB
Standing Position	104.92 dB	105.02 dB	113.74 dB	112.61 dB
Pilot Position	104.38 dB	103.91 dB	112.08 dB	111.77 dB

The values in Table 21 depict an average increase of $7.29\,dB$ from the **climb** segment to the **descent** segment corresponding to an increase of 31%.

Figure 34 below contains a narrow band analysis of all the **closed door** flight segments and a narrow band analysis of all the **open door** flight segments. The **closed door** results have been placed above the **open door** results in order to line up their abscissas. Translucent vertical lines have been overlaid on the figure at specific frequencies associated with main rotor and tail rotor harmonics.

This figure contains all 28 in-flight measurements recorded onboard the NRC Bell 412 helicopter. The depicted frequency range is 4 to $350\ Hz$ with a resolution of $0.5\ Hz$.

The largest peaks in the **closed door** spectral density analysis were associated with the main rotor's 4^{th} harmonic, the main rotor's 8^{th} harmonic and the tail rotor's 4^{th} harmonic. The largest peaks in the **open door** spectral density analysis were primarily associated with the main rotor's 4^{th} harmonic. The SPL amplitudes associated with the 4^{th} harmonic is expected to be substantial for a four bladed rotor system. However, during certain flight conditions the SPL amplitude associated with the 8^{th} harmonic was observed to be the largest. This is a characteristic response of a non-linear system presumptively dependent on the aircraft configuration and flight conditions.

The OSPL was calculated and averaged across the **closed door** flight conditions as $108.88\ dB$ while the OSPL averaged across the **open door** flight conditions was $114.02\ dB$. This $5.14\ dB$ difference corresponds to an increase of 81% in the averaged OSPL. While, these two OSPL values are not intrinsically attached to a single physical feature, they provide an excellent single number comparison for cabin noise. The **open door** flight segments are much louder despite the lowered **SLF** and **descent** flight aircraft speeds.

Furthermore, the narrow band analysis depicted in Figure 34 contains many tones. The majority of the acoustic energy represented in this narrow band analysis is closely correlated to the noise generated by the main and tail rotors.

The next section includes comparisons of the flight segments using 3^{rd} octave bands. This type of analysis satisfies the standards discussed in chapter 2.

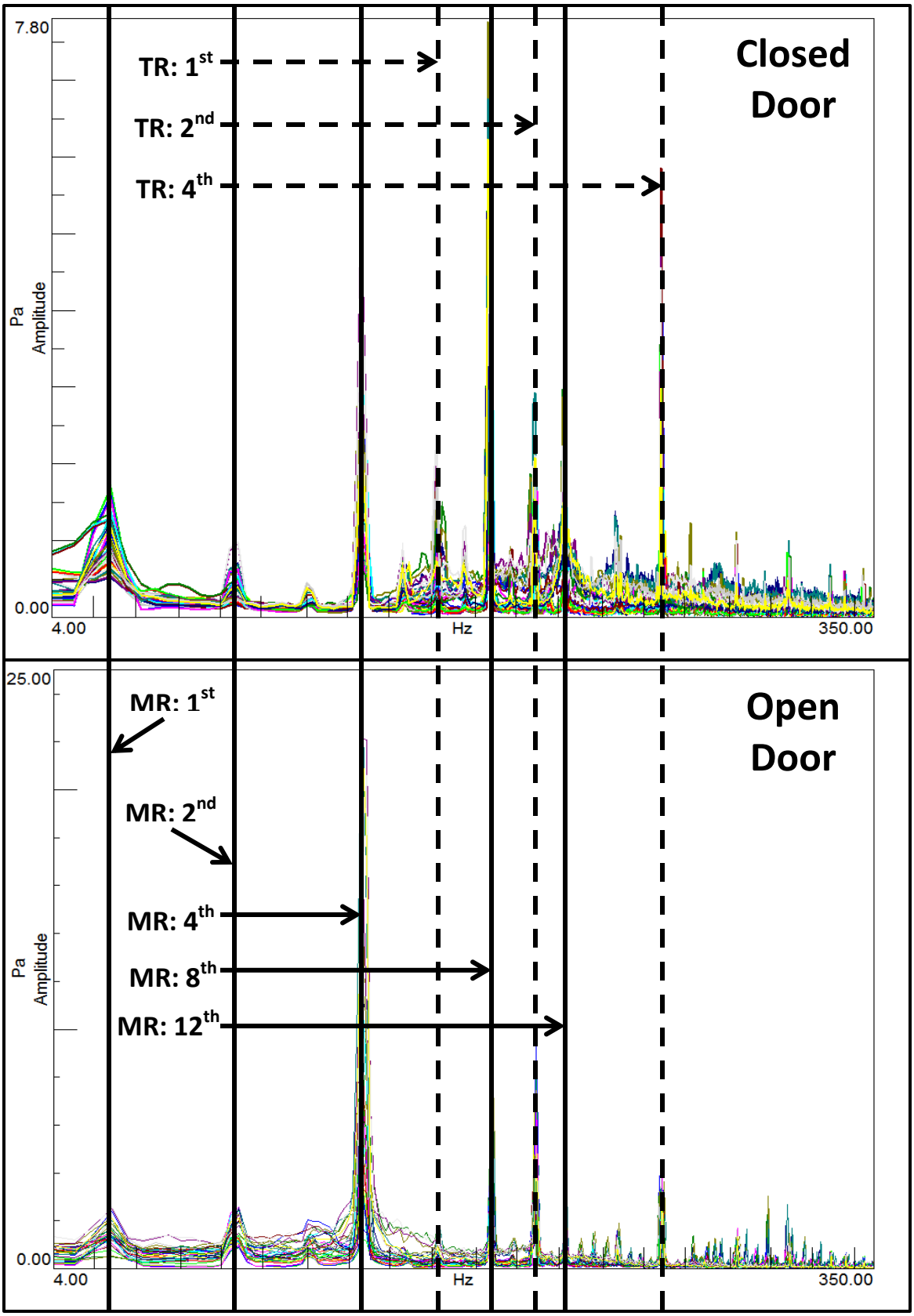

Figure 34: Closed door and open door spectral density comparison

5.2.3. Flight Measurement 3rd Octave Band Comparison

For the **closed** door flight segment, the SPL measured at the **seated** position tended to be the highest. Each of the different **closed** door flight conditions (ex. Ground, Hover, Climb, SLF etc.) have been shown for comparison in Figure 35 as measured at the **seated** location. Standard deviations have not been included to avoid cluttering the figures.

The major main rotor and tail rotor harmonics have been overlaid on Figure 35. The highest peak occurred within the $40\ Hz$ band (correlated to the 8th harmonic of the main rotor). The most consistently high peak (consistent with respect to the different flight segments) was within the $100\ Hz$ band (correlated to the 4th harmonic of the tail rotor). As the aircraft speed increased the tail rotor produced less of the total acoustic energy for the flight segment.

The **descent**, **SLF 100** and **SLF 120** flight segments were the fastest flight segments and consequently contained the largest peak amplitudes associated with the main rotor's 8th harmonic (the $40\ Hz$ band). These flight segments all contained speeds in excess of $100\ kts$. The remaining flight segments contained speeds below $100\ kts$. Furthermore, the **descent** flight segment was consistently the loudest in addition to having the highest aircraft velocity. It can be concluded that there was a large correlation between noise and aircraft velocity across the frequency bands below $1\ kHz$.

The single largest amplitude of $109.28\ dB$ for the **closed door** configuration occurred during the **descent** flight segment within the $40\ Hz$ band. This band was associated with the 8th harmonic of the main rotor.

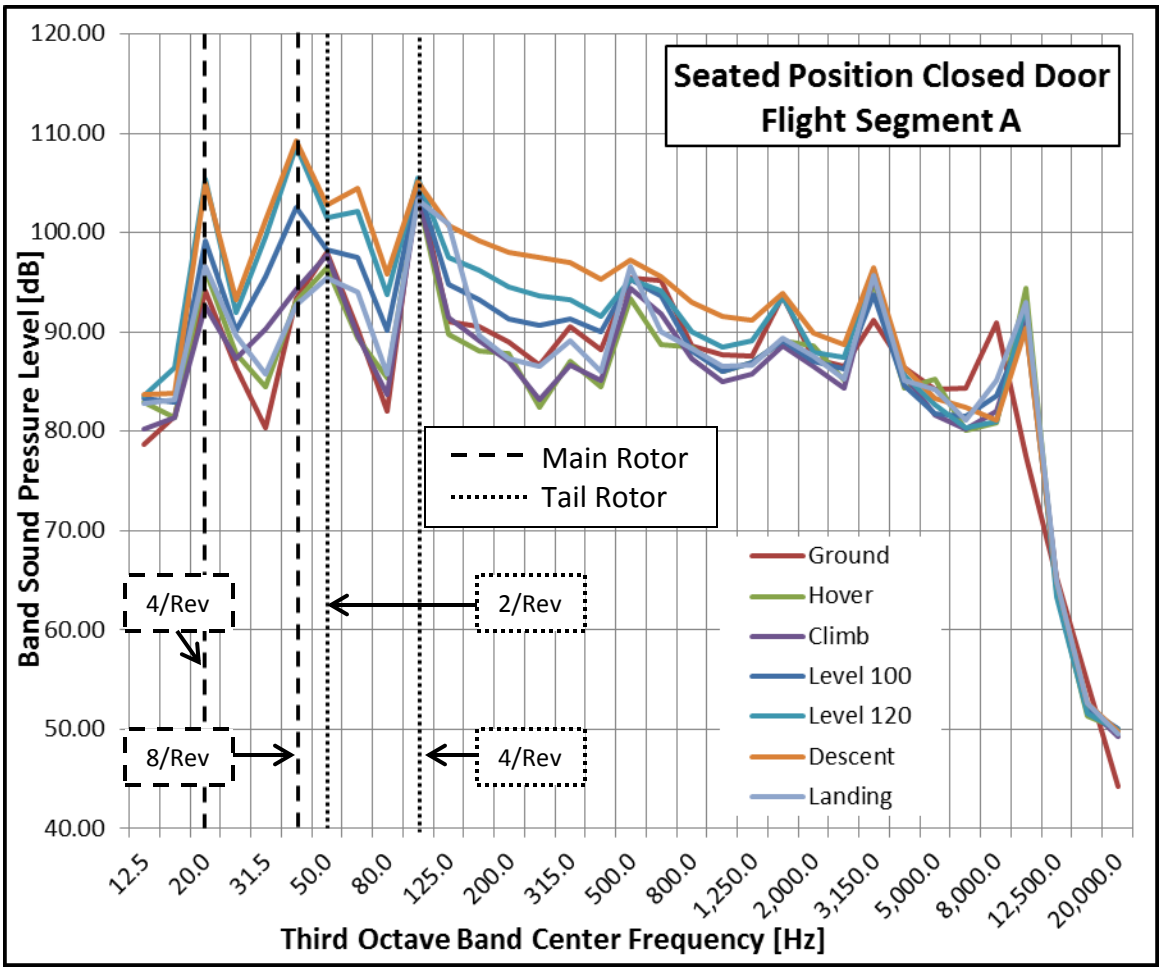

Figure 35: 3rd octave closed door seated position flight segments comparison

For comparison, Figure 36 contains the **open door seated position** 3rd octave analysis of the sound data for all flight segments. The **open door descent** flight segment was no longer consistently the loudest segment as was the case for the **closed door descent** flight segment discussed previously.

Below $500\ Hz$, the **descent** and **level 80** flight segments were the loudest. Above $500\ Hz$ the **ground** and **landing** segments were the loudest. The fact that the **open door SLF** and **descent** segments were not completed at the same speeds as the **closed door** segments is an important consideration. The **closed door** Figure 35 indicated a large correlation between noise and speed. This explains the reason the **open door descent**

segment was no longer consistently the loudest (it did not contain the highest aircraft velocity).

Above $500\ Hz$ the **ground** and **landing** segments are the loudest. This indicated that acoustic reflections present while in ground effect were largely attenuated by the closed door configuration.

Primarily, the peaks with the largest amplitudes were similar between the **closed door** and **open door** configurations. The single largest amplitude of $116.75\ dB$ for the **open door** configuration occurred during the **SLF 80** flight segment within the $20\ Hz$ 3rd octave band. This band was associated with the 4th harmonic of the main rotor.

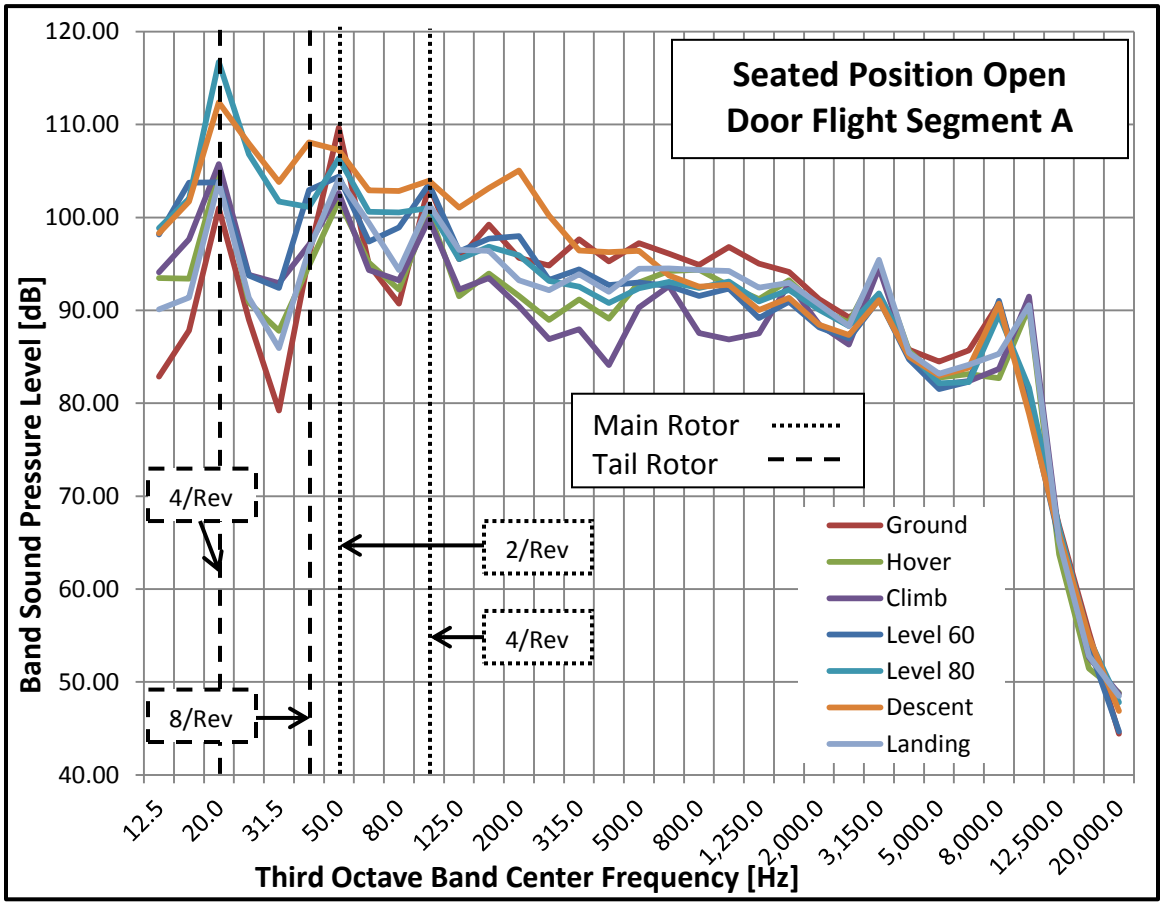

Figure 36: 3rd octave open door seated position for all flight segments comparison

Not shown in Figure 36 (**seated position**), for the **open doors,** the **pilot position** became the most predominantly loud.

The **open doors SLF 80** flight segment was the single loudest flight measurement and a 3rd octave analysis is shown in Figure 37. The microphone position OSPL were:

1. Seated Position: $117.93\ dB$
2. Standing Position: $116.46\ dB$
3. Pilot Position: $119.73\ dB$

Perhaps counterintuitively, the **standing position** microphone was the quietest notwithstanding its proximity to the open door. This indicated that the acoustic reflections off of the interior surfaces played a dominant role in the noise level. As the **pilot** SPL was consistently the loudest position, this point is further validated, since the pilot position was surrounded by the most surfaces.

It should be noted that the error bars in the following Figure 37 indicate the standard deviations from the multiple averages completed during the DFT. It was only feasible to complete each measurement recording run twice (segment A and B), which was not a sufficient population for statistical analysis. Above the $125\ Hz$ band the errors are consistently below $1\ dB$. At $125\ Hz$ and below, standard deviations reached as high as $4.8\ dB$. Similar error values were found for each flight segment discussed previously. Above $100\ Hz$ the analysis' standard deviations were smaller.

A large quantity of data was collected; thus more extensive analysis is possible. In the interest of comparing the data to the standards discussed in chapter 2, certain weighting methods were incorporated into the data.

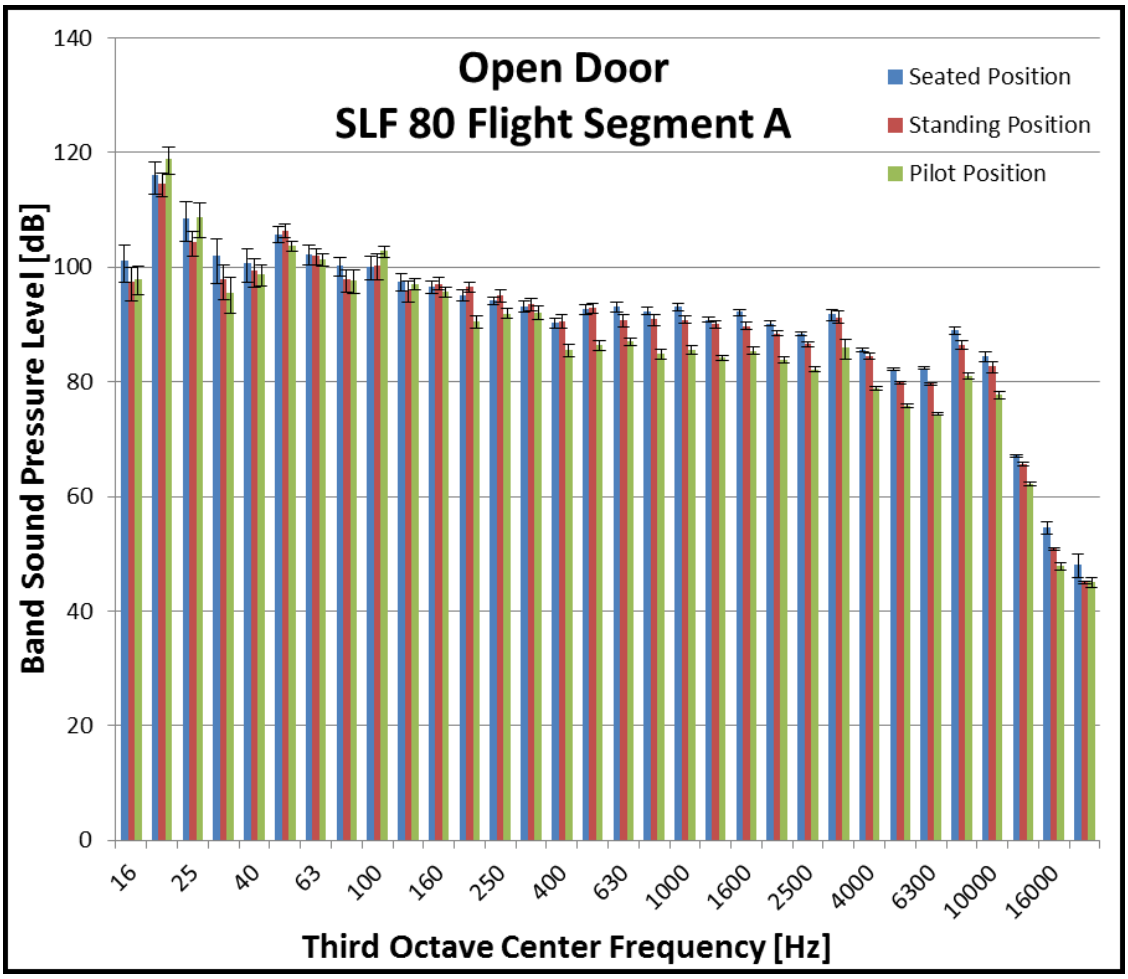

Figure 37: 3rd octave open door SLF 80 flight segment A

5.2.4. Acoustic Weighting Curves Comparison

As discussed in chapter 2, acoustic weighting curves are applied to approximate the sensitivity of human hearing. Following the workplace safety standards discussed in chapter 2, A-weighting was applied to the data. Note that this weighting was not compliant with the latest 2014 update of ISO 226 (Acoustics: Normal equal-loudness-level contours) but the standard previous to that.

Figure 38 below, contains the A-weighted 3rd octave data from the previous Figure 37 (**open door SLF 80** segment). As per A-weighting, a large portion of the energy in the lower frequency bands has been attenuated. The A-weighted OSPL were calculated as:

1. Seated Position: $102.32\ dBA$ (decrease of $15.61\ dB$)

2. Standing Position: $101.10\ dBA$ (decrease of $15.36\ dB$)

3. Pilot Position: $96.69\ dBA$ (decrease of $23.04\ dB$)

The pilot position could then be considered the quietest position in the aircraft by a considerable margin.

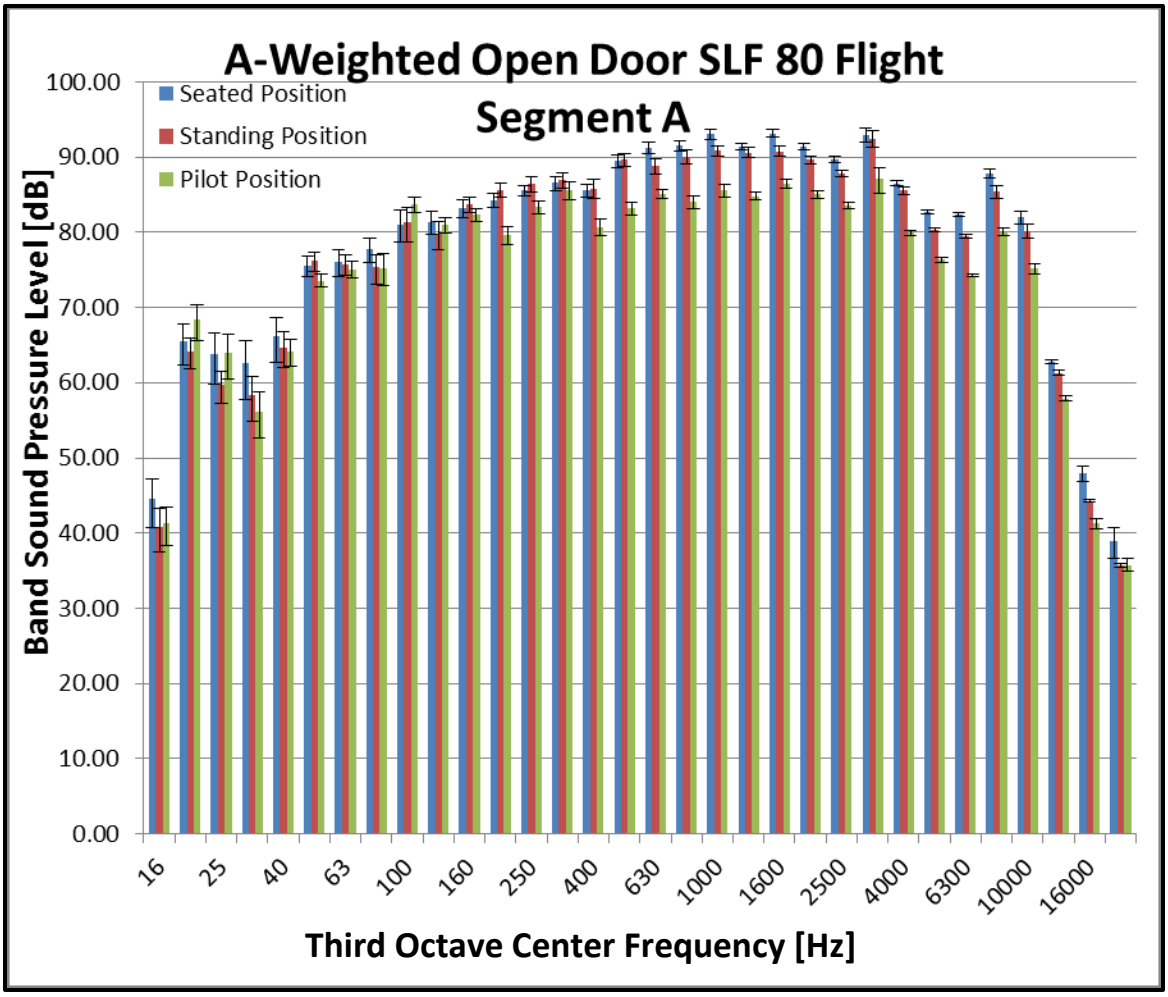

Figure 38: A-weighted 3rd octave open door SLF 80 flight segment A

Figure 39 below, contains the **A-weighted** seated position open door flight segment sound data for comparison to Figure 36 (the **un-weighted** seated position open door flight segment). Once more, the low frequency bands were the most attenuated by A-weighting. As discussed in chapter 2, the validity of A-weighting when applied to high SPL is questionable. However, the majority of the workplace safety standards have chosen exposure limits on the basis of A-weighting and therefore it was adopted here.

The single largest amplitude of $96.64\ dBA$ for the **open door seated position** occurred during the **landing** flight segment within the $3150\ Hz$ 3rd octave band. This band is not associated with any rotor harmonics.

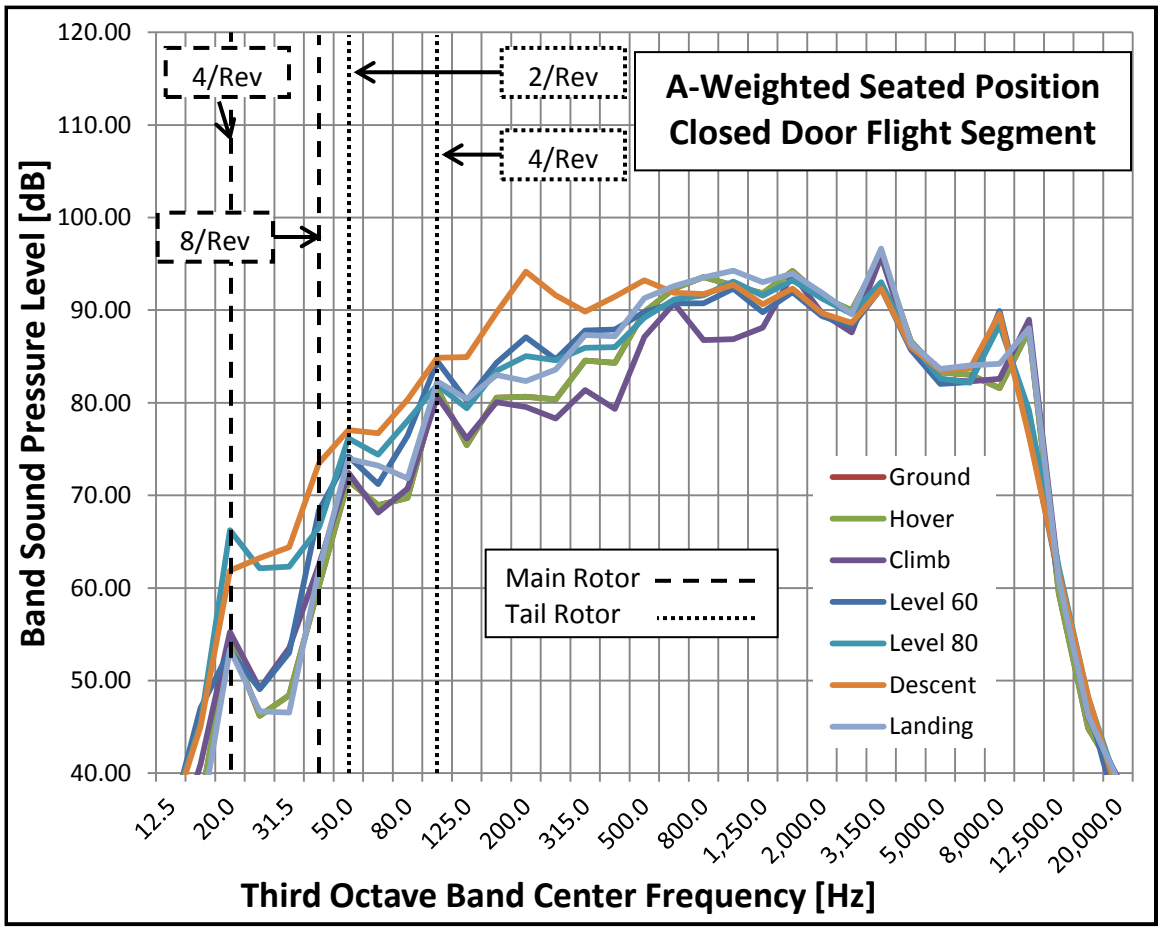

Figure 39: A-weighted 3rd octave open door seated position comparison

5.2.5. Microphone and Windscreen Adjustments

This section includes discussions of the microphone environment and windscreen sound adjustments that were accounted for in the above 3rd octave charts. Recall in section 3.5.3 and Table 11 the maximum microphone adjustments required:

Table 22: Maximum microphone adjustments required

Adjustment Parameter	Adjustment Value
Temperature	$0.217\ dB$
Pressure Change (due to altitude)	$-0.056\ dB$
Relative Humidity Change	$\pm 0.043\ dB$

The temperature and pressure changes were applied directly to the 3rd octave band amplitude while the humidity change was applied to the standard deviation.

Additionally the sound insertion loss spectrum of the windscreens has been measured. This measurement was completed in the NRC small reverberant room. Six microphones were used to record the chamber SPL, simultaneously. Three microphones were used as references while three microphones were used to measure the sound insertion loss of the windscreens. White noise was generated and controlled to the same levels for four runs. The test runs have been recorded in Table 23 for clarity.

Table 23: Windscreen insertion loss test procedure

Microphone	Test Run 1	Test Run 2	Test Run 3	Test Run 4
1 (Reference)	Windscreen OFF	Windscreen OFF	Windscreen OFF	Windscreen OFF
2 (Test)	Windscreen ON	Windscreen ON	Windscreen OFF	Windscreen OFF
3 (Reference)	Windscreen OFF	Windscreen OFF	Windscreen OFF	Windscreen OFF
4 (Test)	Windscreen ON	Windscreen ON	Windscreen OFF	Windscreen OFF
5 (Test)	Windscreen ON	Windscreen ON	Windscreen OFF	Windscreen OFF
6 (Reference)	Windscreen OFF	Windscreen OFF	Windscreen OFF	Windscreen OFF

Figure 41 is an image of the test configuration with the windscreens and without the windscreens.

Figure 40: Windscreen insertion loss test setup (Left: Run 1/2, Right: Run 3/4)

The results indicated that the sound insertion loss of the windscreens was on the order of magnitude of $0.5\ dB$ with the single largest deviation of $0.6\ dB$ occurring in the $3150\ Hz$ 3rd octave band. Unfortunately, the test run results did not achieve the desired level of consistency. It was suspected that the acoustic field was not sufficiently diffuse. As can be seen in the right side of the above images, a test window fixture was installed for an independent ongoing experiment (transmission loss testing). As the transmission loss testing setup was still in place (and had to remain so for the duration of the testing), the window was suspected of absorbing significant noise energy. Originally, the windscreen insertion loss measurement aimed to account for this window by using an excess of reference microphones; however this was not validated by the results. The insertion loss testing has been postponed until the transmission loss testing project has been completed and the window removed.

5.3. Health and Safety Standards Assessment

The purpose of the hearing protection project was to assess the Bell 412 helicopter cabin noise for aircrew noise exposure. The cabin noise measurements discussed previously were not sufficient for this assessment as all aircrew wear HPs during flight. The HP noise attenuation must be accounted for. While the measurement of the HPs and the transfer function of the ear canal are beyond the scope of this thesis, further analysis has been completed by the NRC. In the interest of providing some degree of closure to this project, a short summary of the results from subsequent analysis is reviewed here.

5.3.1. Bell 412 Hearing Protection Papers

Two short papers were presented on the Bell 412 helicopter cabin noise exposure at the Canadian Acoustics Association Conference in October 2014 [59], [60]. Insertion loss data was collected for the SPH 5CF flight helmet in the NRC small reverberant room. The maximum estimated SPL exposure for a pilot was found to be $71\ dBA$ for the **closed door** and $72\ dBA$ for the **open door** flight segments. The Canada Labour Code Part II specifies $87\ dBA$ or less is required for an eight hour exposure [4]. Therefore, a Pilot wearing an appropriately fitted SPH 5CF helmet satisfies the Canadian Labour Code for work onboard the Bell 412 aircraft.

Figure 41 contains the measured mean insertion loss of the SPH 5CF helmet. The helmet performed more proficiently at higher frequencies while the Bell 412 helicopter noise was dominated by lower frequencies. This helmet's noise attenuation ranged from as low as $12\ dB$ within the $100\ Hz$ 3rd octave band to as high as $48\ dB$ in the $5\ 000\ Hz$

3rd octave band. With such a large variation in noise attenuation it becomes important to select the appropriate helmet for each particular aircraft.

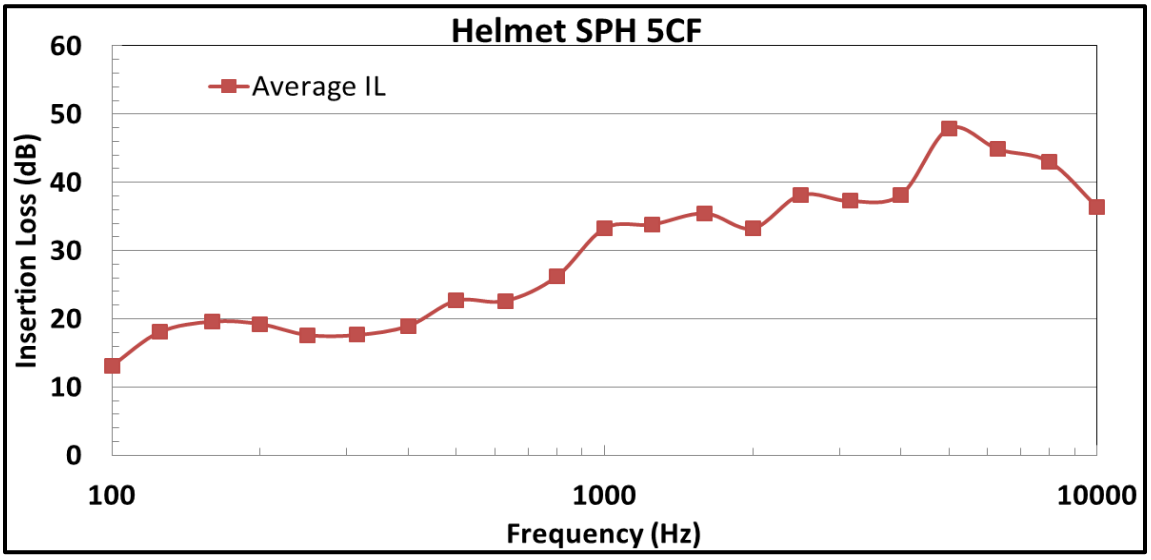

Figure 41 : Insertion loss of the SPH 5CF flight helmet [60]

The results show the satisfaction of the Canadian Labour Code Part II; however the use of A-weighting for this high SPL remains a subject of debate (as mentioned in chapter 2).

This concludes the presentation of data collected by the TTC DAS while throughout the Bell 412 helicopter flight measurement. The following section includes a summary of the **exterior ground** noise measurements recorded on December 3rd, 2013.

5.4. Ground Crew Exterior Noise Measurements

As characterized in section 4.6, an LMS Test.LAB and front end were used for exterior noise measurements of standard ground maintenance crew locations. These measurements were completed with a single roaming microphone as seen in Figure 26 on page 66. While this data was not collected with the TTC DAS discussed in this paper,

some of the exterior measurement results have been included here to complement the interior cabin noise measurement results discussed previously in sections 5.2 and 5.3.

The 3rd octave sound pressure levels for the aircraft exterior roaming microphone measurements may be seen in Figure 42 below. These measurements were not taken simultaneously; the helicopter was left to run at idle in steady state conditions while the measurement microphone moved from position to position.

The y-axis extends from $80\ dB$ to $120\ dB$. The SPL was consistent across each of the measured locations. The largest discrepancy occurred in the $40\ Hz$ band with a difference of $14.08\ dB$ from the position 2 value of $108.30\ dB$ to the position 8 value of $94.22\ dB$. This was potentially due to the fact that the 8th harmonic of the main rotor was near the upper limit of the $40\ Hz$ band. A rotor RPM of $335\ RPM$ would rest directly between the $40\ Hz$ and $50\ Hz$ 3rd octave band limits. This RPM is a little higher than the standard speed the NRC Bell 412 is commonly run at however (on average $324\ RPM$). Unfortunately, the rotor speed was not directly measured during the ground measurements, therefore this is merely speculation.

As the microphone roamed towards the rear of the helicopter (towards the tail rotor) the 3rd octave bands associated with the tail rotor harmonics increased in SPL (depicted in Figure 42 with dotted lines).

Position 9 recorded the highest SPLs of $110.64\ dB$ and $110.86\ dB$ in the $40\ Hz$ and $100\ Hz$ 3rd octave bands respectively. This is logical as position 9 was the most closely situated to the tail rotor. The OSPL varied from $116.38\ dB$ measured at position 11 to $117.79\ dB$ measured at position 4.

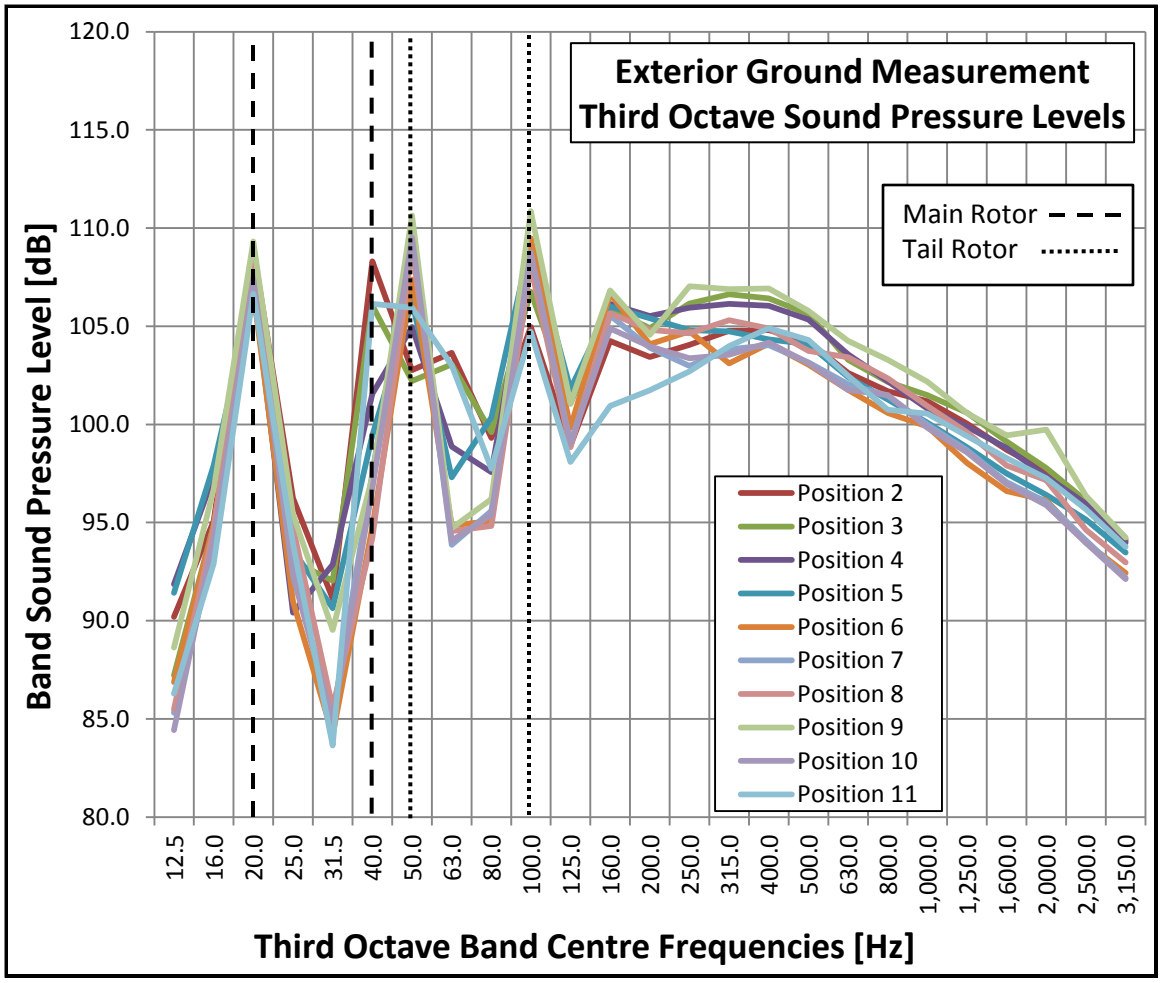

Figure 42: Exterior ground measurement 3rd octave sound pressure levels

This concludes the presentation of results from the Bell 412 cabin and exterior noise measurements completed on December 3rd 2013.

6. Conclusion and Continuing Work

For perspective, a summary of work is included at the beginning of this chapter. Section 6.2 further contains insight as to where the project is headed.

6.1. Summary

The previous 5 chapters contain an explanation of the methodology used in the development of an acoustic DAS for use onboard aircraft. This work was done in collaboration with the NRC hearing protection project.

1. **Motivation.** The initial hearing protection project was motivated by increased expenditures of the Canadian Department of Defense on aircrew hearing loss. Literature of similar projects and hearing loss prevention programs were reviewed.
2. **Standards.** Health and safety standards were characterized to provide insight into safe operating conditions as well as set a benchmark for the results to be compared against. Aircraft safety standards and procedures contain stringent requirements that must be adhered to, especially when working on military aircraft. A set of requirements were drafted for an appropriate DAS.
3. **DAS Design.** An airworthy DAU was purchased from TTC. The specific modules were selected as appropriate for acoustical analysis. Although the DAU itself had gone through significant certification for use onboard aircraft, the external equipment (microphone, stands, battery power, operating case, etc.) had to be adjusted for certification. Furthermore, a detailed understanding of the route from the analog microphone signal to post-analysis data was achieved.

4. **Flight Measurement.** The first measurement for this project was completed on the NRC Bell 412 helicopter on Dec 3rd, 2013. This test measurement served as a validation exercise for the DAS. The test procedure has been recorded in detail to facilitate future measurement reproduction.
5. **Data Analysis.** Flight measurement results were analyzed with commercial LMS Test.LAB acoustic software. The software theory was understood using original written MATLAB code to comprehend the DSP methodology. A-weighting was applied for comparison to the workplace health and safety standards. The microphone environmental adjustments as well as the insertion loss of the windscreens were discussed. Statistics of the various averages taken with LMS Test.LAB software were considered. Finally, acknowledging further NRC work, the Bell 412 was deemed compliant with the Canadian Labour Code Part II when occupants used appropriately fitted SPH 5CF helmets.

It is the author's opinion that the SPH 5CF helmet is sufficient for hearing protection onboard the Bell 412. With this statement come a few caveats:

- When a helmet is used inappropriately (chin strap left undone, ear cups not fully seated against the ear, etc.) the attenuation discussed with Figure 41 is not valid. In fact, depending on how the helmet is resting against the ear, certain frequencies may resonate between the occupant's ear and the helmet (increasing exposure).
- Helmet comfort is important but difficult to quantify. An uncomfortable helmet is less likely to be worn correctly for extended periods of time.
- These results are only applicable to Bell 412 aircraft.

- The validity of A-weighting at high levels has become the object of much debate. It is the author's firm opinion that A-weighting is not appropriate for low frequency noise spectrums at high amplitudes (such as those created from helicopters). While in this instance the noise levels are not of such a significant level to warrant excessive concern, other aircraft such as the Canadian Forces CH147F Chinook produce low frequency spectrums with more acoustic energy.

6.2. Hearing Protection Project

As mentioned previously, the NRC hearing protection project is a large scale project currently underway. The development of the DAS was an important step to facilitate the project. The Bell 412 aircraft measurement was a validation of this DAS. Since that time, the DAS has been used successfully onboard the Canadian Forces CH147F Chinook. Future aircraft measurements may include the CH-149 Cormorant aircraft used for search and rescue. While significant steps have been made, there are many areas of analysis to improve upon.

- Initial helmet sound attenuation levels were measured in the NRC small reverberant room. The dimensions of the room did not permit measurements at the low end of the frequency spectrum. Analysis has shown that the majority of helicopter sound spectra experience very high energy low frequency noise. Therefore, new measurements for the lower frequency spectrum would be to great benefit.
- Inclusion of intercom noise: It would be prudent to facilitate the measurement of intercom radio communications onboard the aircraft. Various literature reviewed in chapter 1 indicates intercommunication may be a considerable noise generator.

- Vibration and acoustic measurements are strongly correlated. The CH147F measurement campaign made the first use of the TTC DAS accelerometer modules. 24 accelerometer channels were recorded. The data has yet to be analyzed. No vibration data was taken simultaneously with the Bell 412 aircraft measurements.

6.3. Future Research

The completed measurements onboard the Bell 412 aircraft and Canadian Forces CH-147F aircraft inspired future potentially conducive research avenues:

- **Cockpit "sound absorber"**: It may be constructive to include a foam block similar to an anechoic chamber wall insulator within the cockpit. With multiple sound reflective surfaces, a single surface for energy to dissipate on might produce noticeable benefits.
- **Aircraft specific helmets**: For the helicopters measured, it was determined that the primary noise sources are correlated to specific frequencies. The noise attenuation characteristics of the helmet could be optimized for each aircraft.
- **Active noise cancelation**: Already an active field of research, the benefits of noise cancelation are apparent here. The tonal frequency characteristics of helicopters were observed to remain static through the majority of flight conditions. Actively attenuating certain frequencies could be capable of large noise energy reductions without degrading communication clarity.
- **Intercom communications**: With the progression of this project, intercom communications noise contributions to overall noise levels will be observed.

6.4. Conclusion

This concludes the summary of work completed on the TTC DAS and subsequent flight measurements. The procedure followed has been recorded in detail for future data and test reproduction. Extreme care was taken to comprehend the precise mathematical applications applied to the analog signal provided by the microphone to produce the results shared here. This procedure was designed in accordance with aircraft noise measurement standards (ex. ISO 5129), aircraft operational procedures (ex. AWM) as well as health and safety standards (ex. Canadian Labour Code). This thesis contains details on an important field of study: protecting vehicle occupant's hearing. Aircraft measurements are extremely expensive and as such, the amount of research in this field is significantly less than that of ground based vehicles.

Bell 412 helicopter in-flight measurements depicted a significant increase in noise for the occupants with open doors. Narrow band analysis showed high correlation between the noise spectrum and the Bell 412 main rotor's 2^{nd} and 4^{th} harmonics as well as the tail rotor's 4^{th} harmonic. A-weighting decreased the spectrum OSPL consistently by $15\,dB$ or more dependent on the microphone position. A decrease of $15\,dB$ corresponds to a decrease in magnitude by a factor of 5.62.

As per the Canadian Labour Code Part II, occupants of the Bell 412 satisfy the $87\ dBA$ limit for an eight hour exposure with the use of the SPH 5CF helmet.

The author hopes that this thesis served to provide the data to the scientific community in such a way that it can be trusted and further used.

Technical References

[1] University of Toronto, "Noise Control and Hearing Conservation Program," University of Toronto, Toronto, 2012.

[2] G. Cook, "An Overview of the Occupational Hearing Conservation Programs," *American Speech, Language and Hearing Association, Special Interest Group Newsletter,* April 2004.

[3] J. Adam, "Results of the NVG-induced neck strain questionnaire study in CH-146 Griffon aircrew," Defence R&D Canada, Toronto, 2004.

[4] Canada Labour Code, "Aviation Occupational Health and Safety Regulations," Minister of Justice, 2012.

[5] S. J. Sander Winjngaarden, "Protecting Crew Members against Military Vehicle Noise," in *RTO AVT Symposium on "Habitability of Combat and Transport Vehicles: Noise, Vibration and Motion"*, Prague, Czech Republic, 2004.

[6] Y. Steinman, *Evaluation of HGU-56/P Flight Helmet (Presentation),* Soesterberg, Netherlands: Royal Netherlands Air Force.

[7] R. Williams, "Assessment of the Applicability of ANSI S12.42-2010 as a General MEasure of Protection from Impulsive Noise by Measurement of Impulsive and Continuous Noise Insertion Loss of the HGU-56/P and the CEP," United States Army Aeromedical Research Laboratory: Sensory Research Division, 2012.

[8] W. Ahroon, "Insertion Loss of the HGU-56/P Aircrew Integrated Helmet System with Oregon Aero Earcup Replacement Products," U.S. Army Aeromedical Research Laboratory: Warfighter Protection Division, 2006.

[9] Department of Defense Design Criteria Standard, "MIL-STD-1474D: Noise Limits," Department of Defence, 1997.

[10] NRC, "Diamond Flight Test Report final," NRC (internal document), Ottawa, 2007.

[11] R. S. S.E. Forshaw, "Noise Levels in the CH147 Chinook Helicopter," Department of National Defence: Canada, Defence and Civil Institute of Environmental Medicine, Downsview, Ontario, 1976.

[12] Hewlett Packard, "Wave Analyzer 3590A: Operating and Service Manual," Hewlett-Packard Company, Loveland, Colorado, USA, 1970.

[13] ISO, "Acoustics - Measurement of sound pressure levels in the interior of aircraft during flight," International Organization for Standardization, Geneva, Switzerland, 2001.

[14] National Instruments, "G.R.A.S. Selection Guide for Microphones and Preamplifiers," 10 October 2012. [Online]. Available: http://www.ni.com/white-paper/14044/en/. [Accessed 15 January 2015].

[15] MIL-STD-1294A, "Acoustical Noise Limits in Helicopters," Military Standard, Department of Defense, United States of America, Washington, D.C., 1985.

[16] Bell Helicopter, "Bell Helicopter," 2014. [Online]. Available: http://www.bellhelicopter.com/MungoBlobs/704/120/412EP_SPCP_2014v02_EN_WEB.pdf. [Accessed 13 January 2015].

[17] Canadian Standards Association, "Procedures for the measurement of occupational noise exposure," Canadian Standards Association, Standards Council of Canada, 2006.

[18] Acoustical Society of America, "Specifiication for Sound Level Meters," American National Standards Institute, New York, 1983.

[19] International Standard, "Acoustics - Determination of occupational noise exposure - Engineering Method," The International Organization for Standardization, 2009.

[20] ASQC, "ASQC Q9001: Quality Assurance in Design, Development, Production, Installation and Servicing," American Society for Quality Control, Milwaukee, WI, USA, 1994.

[21] B. Ricker, TTC, "Interface Control Document, MWCI-120," Teletronics Technology Corporation, Newtown, PA, USA, 2002.

[22] S. Pellarin, TTC, "Interface Control Document, MGRC-202W," Teletronics Technology Corporation, Newtown, PA, USA, 2002.

[23] H. Grossman, TTC, "Interface Control Document, MSCD-606D-13," Teletronics Technology Corporation, Newtown, PA, USA, 2011.

[24] W. Stevens, TTC, "Interface Control Document, MPSM-2012-1," Teletronics Technology Corporation, Newtown, PA, USA, 2006.

[25] B. Ricker, TTC, "Interface Control Document, MPFM-461," Teletronics Technology Corporation, Newtown, PA, USA, 1999.

[26] J. Samuels, TTC, "Interface Control Document, MSSR-110C," Teletronics Technology Corporation, Newtown, PA, USA, 2009.

[27] G. Barnstead, TTC, "Interface Control Document, MPCM-102M-X," Teletronics Technology Corporation, Newtown, PA, USA, 2009.

[28] B. Xiao, TTC, "Interface Control Document, MVID-301M," Teletronics Technology Corporation, Newtown, PA, USA, 2011.

[29] R. Hearne, TTC, "Interface Control Document, MIRG-220M," Teletronics Technology Corporation, Newtown, PA, USA, 2009.

[30] B. Ricker, TTC, "Manual Section - Specification Appendix: MCDAU-2000 Wideband/CAIS Remote Unit," Teletronics Technology Corporation, Newtown, PA, USA, 2002.

[31] Zero Cases, "Valuline Aluminum Cases," Zero Cases, North Salt Lake, Utah, USA, 2013.

[32] A. Price, "Teletronics Data Acquisition System," Aero-Acoustics Laboratory Internal Document, Ottawa, ON, Canada, January, 2014.

[33] Transport Canada, "Canadian Aviation Regulations - Part V: Airworthiness Manual," Government of Canada, Ottawa, 2014.

[34] Transport Canada Standards, Civil Aviation, "Advisory Circular: Electromagnetic Compatibility Testing of Electrical and Electronic Equipment," Transport Canada, 2008.

[35] E. B. J. B. Sykes, The Concise Oxford Dictionary, Oxford: Oxford University Press, 1988.

[36] Allied Wire & Cable, "Mil-Spec Wire and Cable Frequently Asked Questions," Allied Wire & Cable, 2014. [Online]. Available: http://www.awcwire.com/faq-mil-spec-wire.aspx. [Accessed 3 November 2014].

[37] Federal Aviation Administration, "Acceptable Methods, Techniques, and Practices - Aircraft Inspection and Repair," U.S. Department of Transportation, 1998.

[38] *Extinguishing In-Flight Laptop Computer Fires.* [Film]. USA: Federal Aviation Administration, 2007.

[39] J. Guendelsberger, "Manual, RBP-2072-1," Teletronics Technology Corportation, Newtown, PA, USA, 2013.

[40] J. Arajo, "Hearing Protection Evaluation System - Drawing IG14022," National Research Council, Flight Research Laboratory, Ottawa, 2014.

[41] LINE-X Protective Coatings, "Product List," LINE-X, 2010. [Online]. Available: http://www.linex.com/pages/2010/light_industrial/product_list.php. [Accessed 8 January 2015].

[42] PCB Piezotronics, "Model: 352C22 Specifications," 2014. [Online]. Available: http://www.pcb.com/Products.aspx?m=352C22. [Accessed 4 November 2014].

[43] PCB Piezotronics, "Model: 356B41 Specifications," 2014. [Online]. Available: http://www.pcb.com/Products.aspx?m=356B41. [Accessed 4 November 2014].

[44] PCB Piezotronics, "Model: 378B02 Specifications," 2014. [Online]. Available: http://www.pcb.com/Products.aspx?m=378B02. [Accessed 4 November 2014].

[45] Wavelength Media, "Condenser Microphones," MediaCollege.com, [Online]. Available: http://www.mediacollege.com/audio/microphones/condenser.html. [Accessed 20 May 2014].

[46] J. Hewes, "Capacitance and Uses of Capacitors," Electronics Club, 2014. [Online]. Available: http://electronicsclub.info/capacitance.htm. [Accessed 5 November 2014].

[47] A. Keltz, "High and Low Impedance Signals," Whirlwind Music Distributors, Inc., 2014. [Online]. Available: http://whirlwindusa.com/support/tech-articles/high-and-low-impedance-signals/. [Accessed 5 November 2014].

[48] PCB Piezotronics, "Signal Conditioning Basics for ICP (R) & Charge Output Sensors," PCB Piezotronics, 2014. [Online]. Available: http://www.pcb.com/TechSupport/tech_signal. [Accessed 5 November 2014].

[49] M. Munger, "Calibration Report," PCB Piezotronics Vibration Division, Walden Avenue, Depew, New York, USA, April 29, 2014.

[50] Ottawa International Airport (CYOW), "Hourly Data Report for December 03,

2013," Government of Canada, 3 December 2013. [Online]. Available: http://climate.weather.gc.ca/climateData/hourlydata_e.html?timeframe=1&Prov=ON&StationID=49568&hlyRange=2011-12-14|2014-11-04&Year=2013&Month=12&Day=3. [Accessed 5 November 2014].

[51] Encycopedia Britannica, "Lapse rate," Encyclopedia Britannica, 2014. [Online]. Available: http://www.britannica.com/EBchecked/topic/330402/lapse-rate. [Accessed 5 November 2014].

[52] Encyclopedia Britannica, "Atmospheric pressure," Encyclopedia Britannica, 8 July 2014. [Online]. Available: http://www.britannica.com/EBchecked/topic/41486/atmospheric-pressure. [Accessed 5 November 2014].

[53] M. Hayes, *MECH 4804: Measurement and Data Systems,* Ottawa: Carleton University Undergraduate Course, 2014.

[54] S. Ghinet, V. Wickramasinghe and A. Grewal, "Flight Test Procedure on selected Canadian Forces Aircrafts to Investigate the Exposure to Helicopter Noise of Canadian Forces Crew and Maintenance Personnel," NRC, Ottawa, July 15th, 2014.

[55] PCB Piezotronics INC, "Microphone Handbook," [Online]. Available: http://www.pcb.com/Linked_Documents/Vibration/Microphone_Handbook.pdf. [Accessed 14 January 2015].

[56] S. Smith., The Scientist and Engineer's Guide to Digital Signal Processing, San Diego: California Technical Publishing, 1999.

[57] Siemens LMS, *Window Correction Factors,* Plano, USA: Theory Documents - LMS Test.LAB 13A, 2013.

[58] K. Baillie, "Altitude air pressure calculator," Apex (altitude physiology expeditions) Charity, April 2010. [Online]. Available: http://www.altitude.org/air_pressure.php. [Accessed 12 February 2015].

[59] S. Ghinet, A. Price and M. Alexander, "Closed Door Flight Test Investigation of Cabin Noise Exposure in the NRC Bell 412 Helicopter," in *Canadian Acoustics Association*, Winnipeg, October, 2014.

[60] S. Ghinet, A. Price and M. Alexander, "Open Door Flight Investigation of Cabin Noise Exposure in the NRC Bell 412 Helicopter," in *Canadian Acoustics Association*, Winnipeg, October, 2014.

[61] R. Stevens, TTC, "Interface Control Document, MCFM-100," Teletronics Technology Corporation, Newtown, PA, USA, 2006.

[62] W. Stevens, TTC, "Interface Control Document, MPSM-2515-4," Teletronics Technology Corporation, Newtown, PA, USA, 2006.

[63] G. Barnstead, TTC, "Interface Control Document, HDC-200-1," Teletronics Technology Corporation, Newtown, PA, USA, 2012.

[64] National Instruments, "Microphone Handbook," National Instruments, 28 February 2012. [Online]. Available: http://www.ni.com/white-paper/7059/en/.

[Accessed 4 November 2014].

[65] Technical Committee ISO/TC 43, Acoustics, Subcommittee SC 1, Noise, "Acoustics - Measurement of sound pressure levels in the interior of aircraft during flight," International Organization for Standardization, ISO 5129:2001(E), 2001.

[66] J. Guendelsberger, TTC, "Manual, RBP-2072-1," Teletronics Technology Corporation, Newtown, PA, USA, 2014.

[67] J. Guendelsberger, TTC, "Manual, BCU-2072-1," Teletronics, Technology Corporation, Newtown, PA, USA, 2014.

[68] Microcontroller Board Blog, "PIC Analog to Digital Converter Tutorial," MicrocontrollerBoard.com, 2015. [Online]. Available: http://www.microcontrollerboard.com/analog-to-digital-converter.html. [Accessed 8 January 2015].

[69] S. Cao, "Replicate the Fourier transform time-frequency correspondance in illusatration using TikZ," 8 August 2013. [Online]. Available: http://tex.stackexchange.com/questions/127375/replicate-the-fourier-transform-time-frequency-domains-correspondence-illustrati. [Accessed 11 February 2015].

[70] Aldem, "Hydrogen Audio," 17 January 2015. [Online]. Available: http://upload.wikimedia.org/wikipedia/commons/thumb/3/39/Acoustic_weighting_curves_(1).svg/2000px-Acoustic_weighting_curves_(1).svg.png. [Accessed 27 April 2015].

Appendices

A 1: Reference [40]: Hearing protection evaluation system – drawings

The following appendix A1 drawings include:

- IG14022: System block diagram and cable wiring
- IG14023: Main circuit interface board
- IG14024: Accelerometer circuit interface board
- IG14025: Microphone circuit interface board

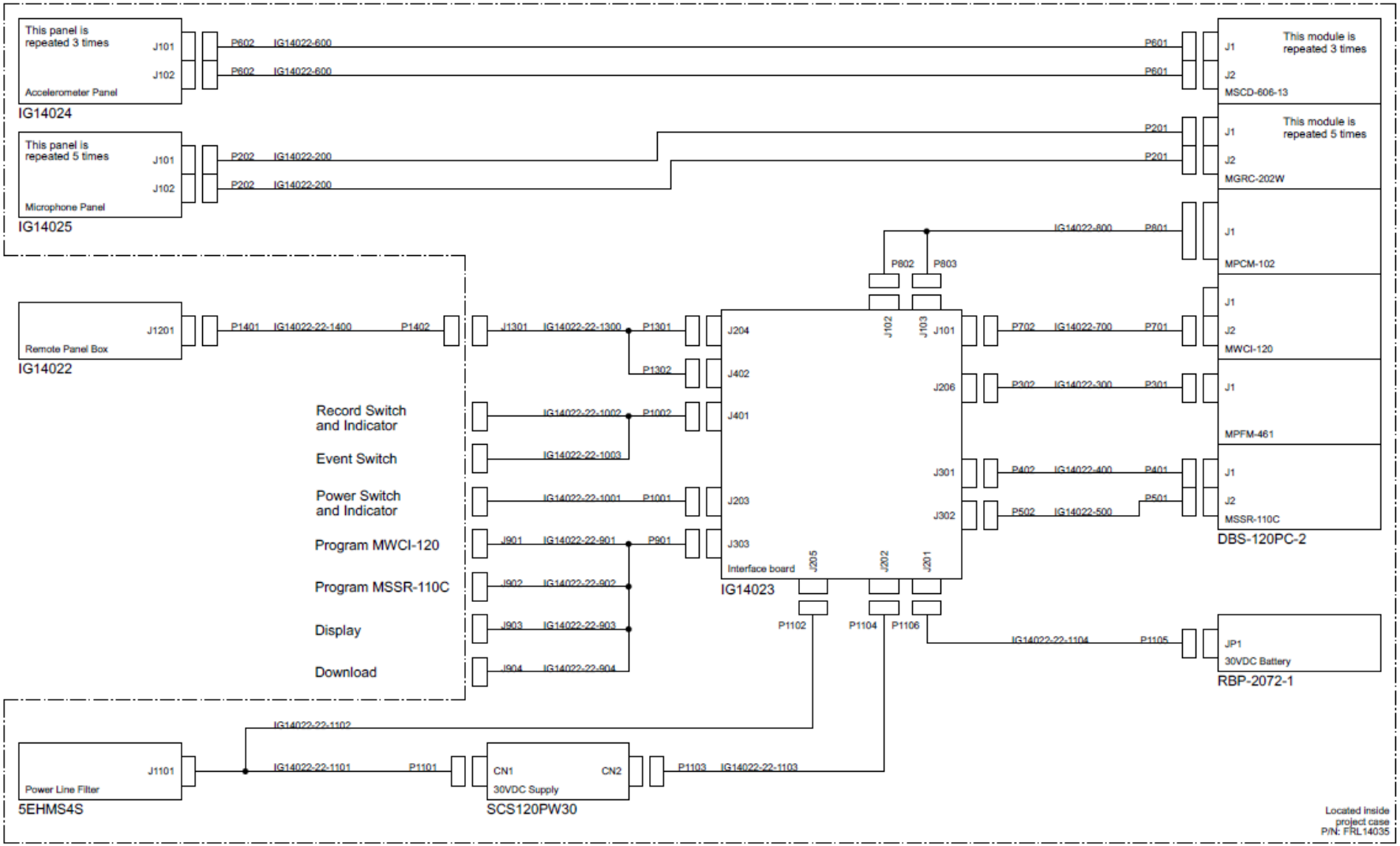

NOTES:

All wiring installed in accordance with AC43.13-1B
All multi conductor wire MIL-27500
All single conductor wire MIL-22759
Schematic label specifies AWG – Wire #
Physically label wires: Document# - AWG – Wire #
The system contains three accelerometer panels and its associated module.
The system contains five microphone panels and its associated module.

Drawn by: J. Araujo			Date: 17-Apr-2014	
Checked by:			Date:	
Approved by: M. Ovenden			Date: 25-June-2014	
Mod Card Number: FRLP1401	PMCN:	Assembly: FRL14035	Drawing Number: IG14022	Sheet: 1/14 Revision: -

NRC·CNRC Flight Research Laboratory

Project: Hearing Protection Evaluation System
System Block Diagram
Project Code: A1-002961

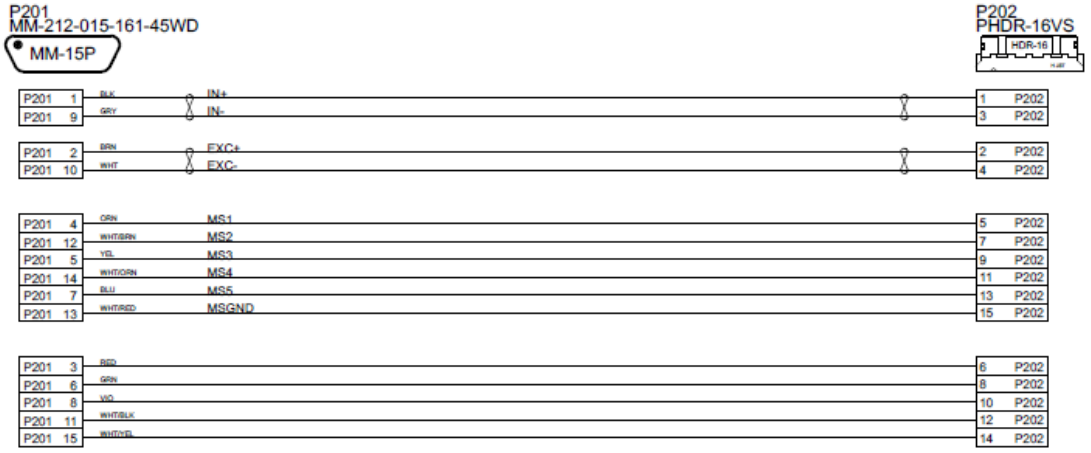

6 X 20 inches
4 X 16 inches

Crimp Tool: 455-2572-ND $601
22-26AWG Contacts: 455-1325-1-ND

NOTES:

All wiring installed in accordance with AC43.13-1B
All multi conductor wire MIL-27500
All single conductor wire MIL-22759
Schematic label specifies AWG – Wire #
Physically label wires: Document# - AWG – Wire #
This wiring harness is repeated 10 times. Five modules with two ports each.

Drawn by: J. Araujo		Date: 17-Apr-2014	NRC·CNRC Flight Research Laboratory		
Checked by:		Date:	Project: Hearing Protection Evaluation System MGRC-202W Wiring Harness	Project Code: A1-002961	
Approved by: M. Ovenden		Date: 25-June-2014			
Mod Card Number: FRLP1401	PMCN:	Assembly: FRL14035	Drawing Number: IG14022	Sheet: 2/14	Revision: -

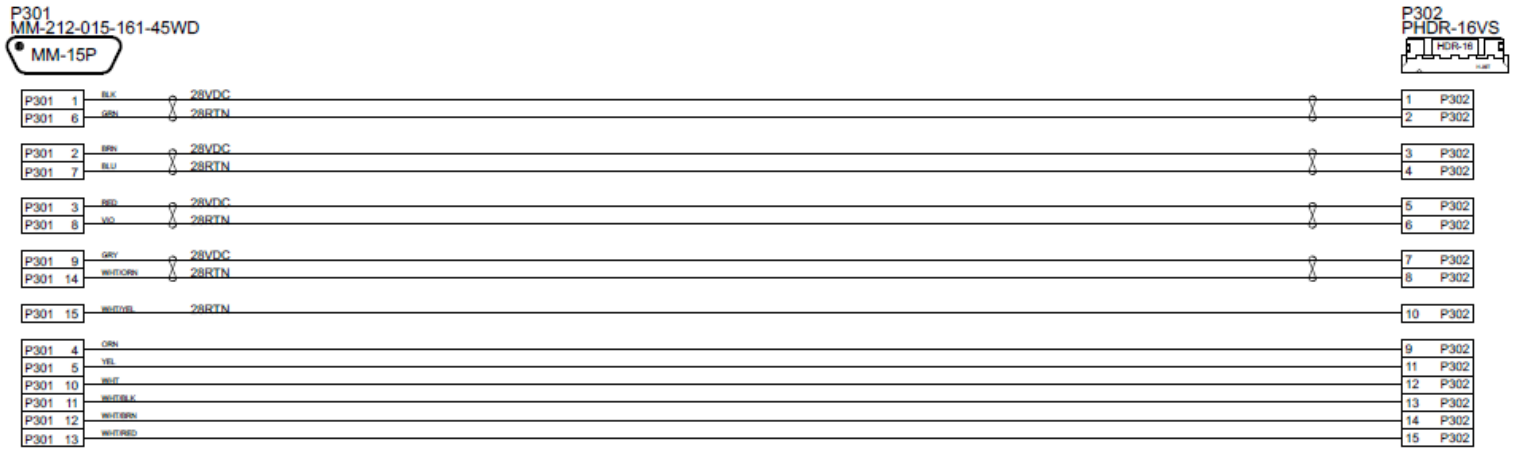

12 " INCHES

NOTES:

All wiring installed in accordance with AC43.13-1B
All multi conductor wire MIL-27500
All single conductor wire MIL-22759
Schematic label specifies AWG – Wire #
Physically label wires: Document# - AWG – Wire #

Drawn by: J. Araujo			Date: 17-Apr-2014	NRC-CNRC Flight Research Laboratory	
Checked by:			Date:	Project: Hearing Protection Evaluation System MPFM-461 Wiring Harness	Project Code: A1-002961
Approved by: M. Ovenden			Date: 25-June-2014		
Mod Card Number: FRLP1401	PMCN:	Assembly: FRL14035		Drawing Number: IG14022	Sheet: 3/14 / Revision: -

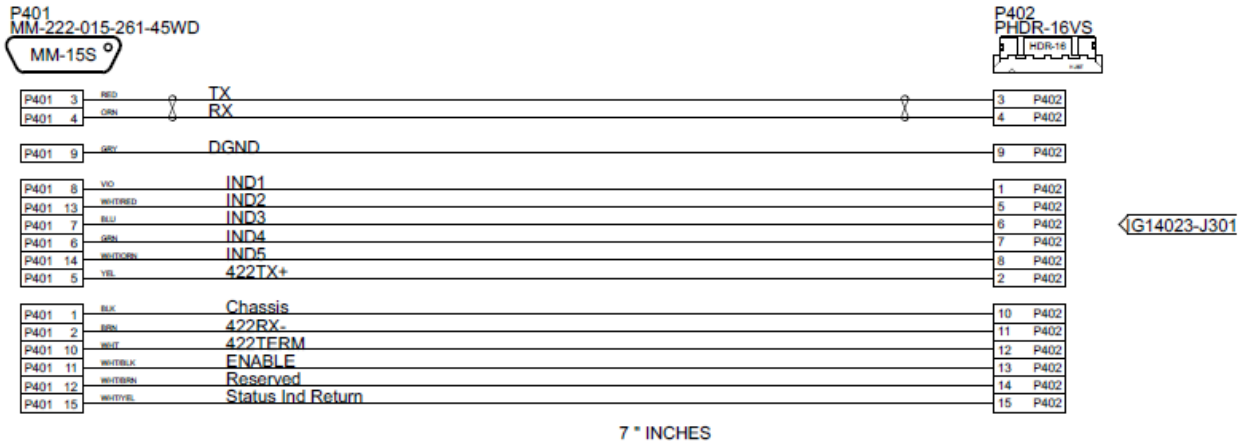

NOTES:

All wiring installed in accordance with AC43.13-1B
All multi conductor wire MIL-27500
All single conductor wire MIL-22759
Schematic label specifies AWG – Wire #
Physically label wires: Document# - AWG – Wire #

Drawn by: J. Araujo		Date: 17-Apr-2014	NRC-CNRC Flight Research Laboratory		
Checked by:		Date:	Project: Hearing Protection Evaluation System MSSR-110C J1 Wiring Harness	Project Code: A1-002961	
Approved by: M. Ovenden		Date: 25-June-2014			
Mod Card Number: FRLP1401	PMCN:	Assembly: FRL14035	Drawing Number: IG14022	Sheet: 4/14	Revision: -

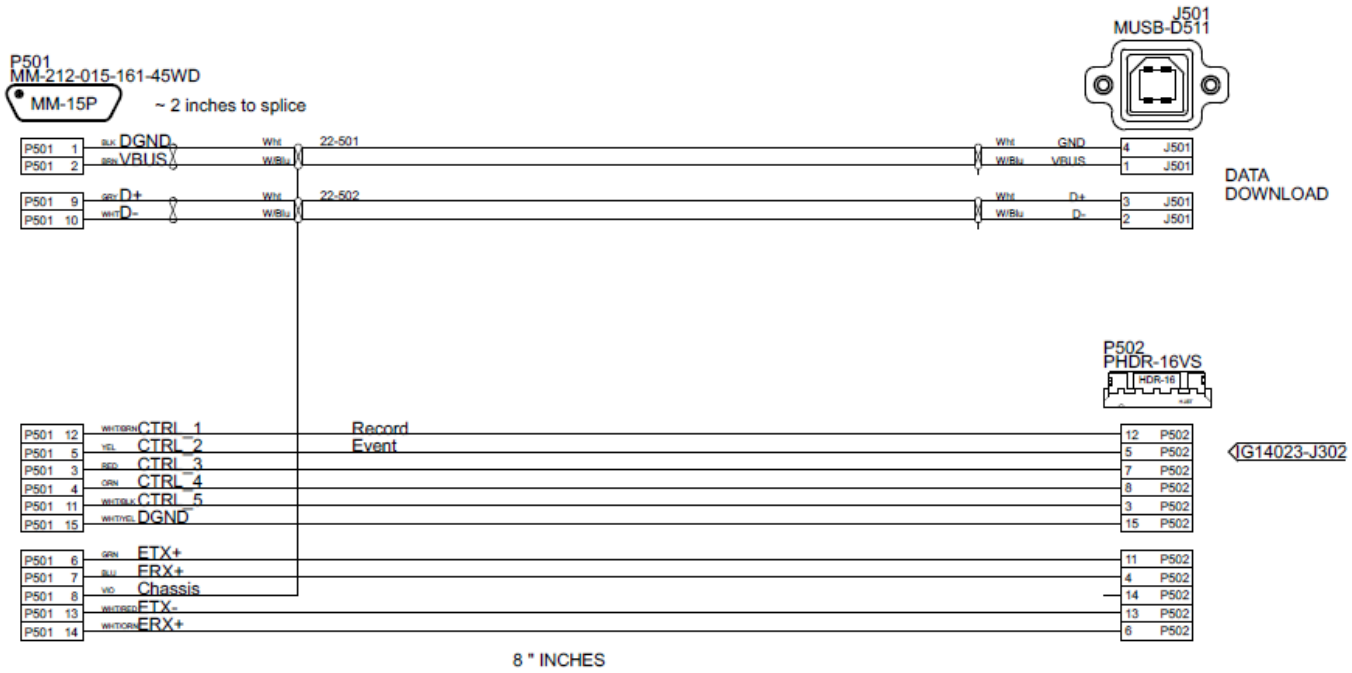

NOTES:

All wiring installed in accordance with AC43.13-1B
All multi conductor wire MIL-27500
All single conductor wire MIL-22759
Schematic label specifies AWG – Wire #
Physically label wires: Document# - AWG – Wire #

Drawn by: J. Araujo		Date: 17-Apr-2014	NRC·CNRC Flight Research Laboratory		
Checked by:		Date:	Project: Hearing Protection Evaluation System MSSR-110C J2 Wiring Harness		Project Code: A1-002961
Approved by: M. Ovenden		Date: 25-June-2014			
Mod Card Number: FRLP1401	PMCN:	Assembly: FRL14035	Drawing Number: IG14022	Sheet: 5/14	Revision: -

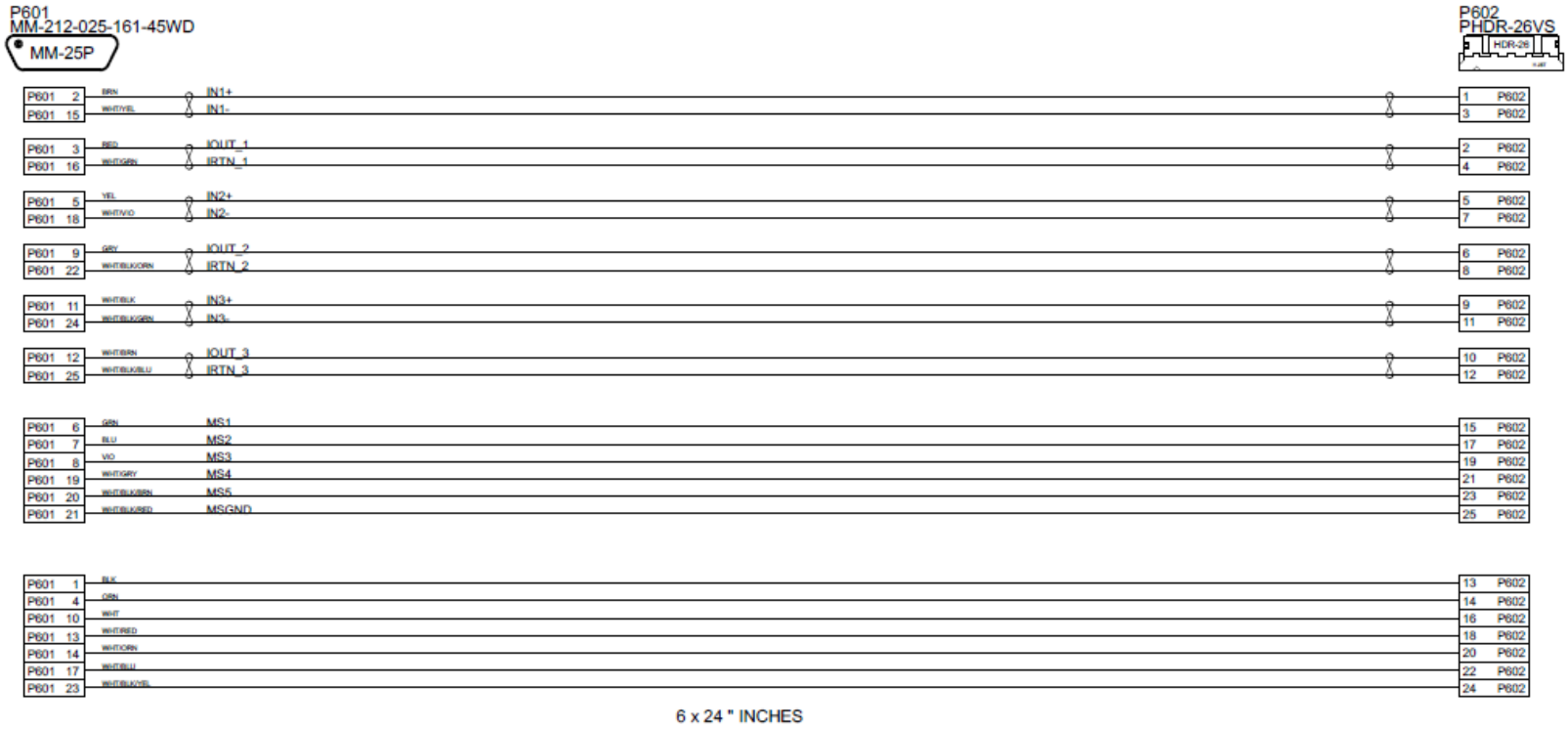

6 x 24 " INCHES

NOTES:

All wiring installed in accordance with AC43.13-1B
All multi conductor wire MIL-27500
All single conductor wire MIL-22759
Schematic label specifies AWG – Wire #
Physically label wires: Document# - AWG – Wire #
This wiring harness is repeated six times. Three modules with two ports each.

Drawn by: J. Araujo			Date: 17-Apr-2014	NRC-CNRC Flight Research Laboratory	
Checked by:			Date:	Project: Hearing Protection Evaluation System MSCD-606-13 Wiring Harness	Project Code: A1-002961
Approved by: M. Ovenden			Date: 25-June-2014		
Mod Card Number: FRLP1401	PMCN:	Assembly: FRL14035		Drawing Number: IG14022	Sheet: 6/14 / Revision: -

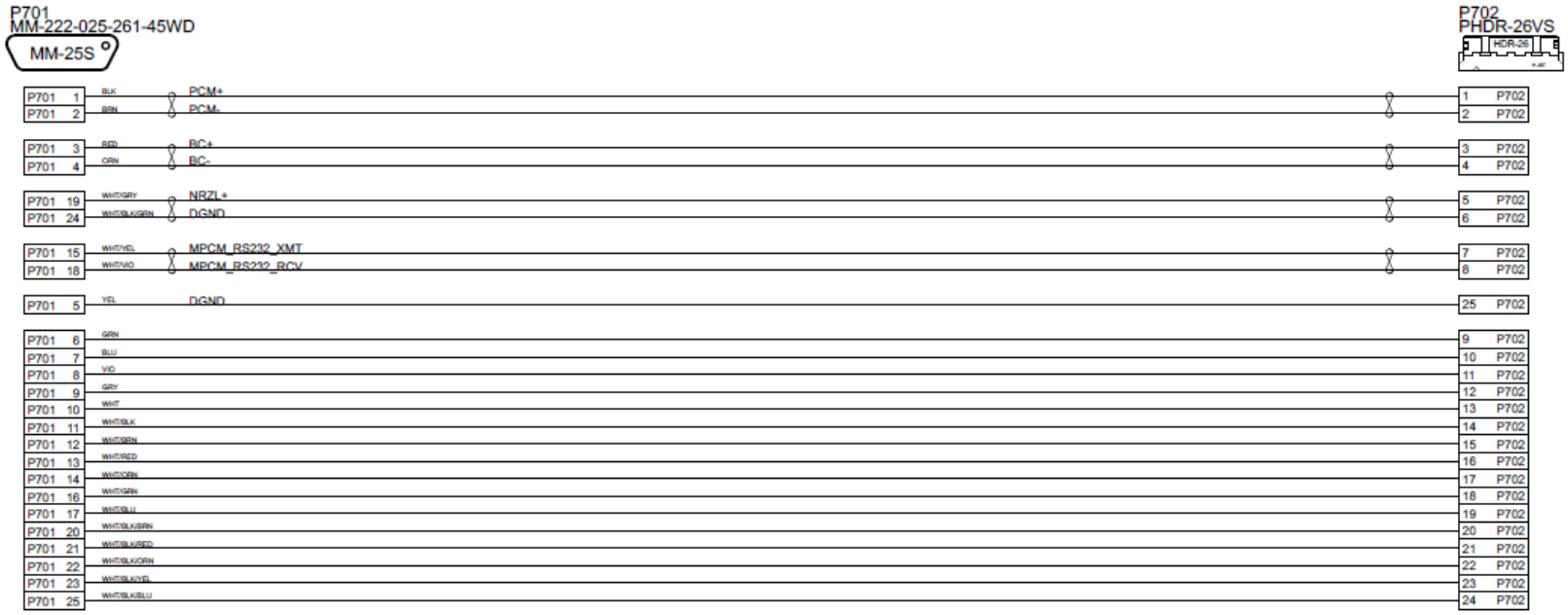

11 inches

NOTES:

All wiring installed in accordance with AC43.13-1B
All multi conductor wire MIL-27500
All single conductor wire MIL-22759
Schematic label specifies AWG – Wire #
Physically label wires: Document# - AWG – Wire #

Drawn by: J. Araujo		Date: 17-Apr-2014	NRC-CNRC Flight Research Laboratory		
Checked by:		Date:	Project: Hearing Protection Evaluation System MWCI-120 J2 Wiring Harness	Project Code: A1-002961	
Approved by: M. Ovenden		Date: 25-June-2014			
Mod Card Number: FRLP1401	PMCN:	Assembly: FRL14035	Drawing Number: IG14022	Sheet: 7/14	Revision: -

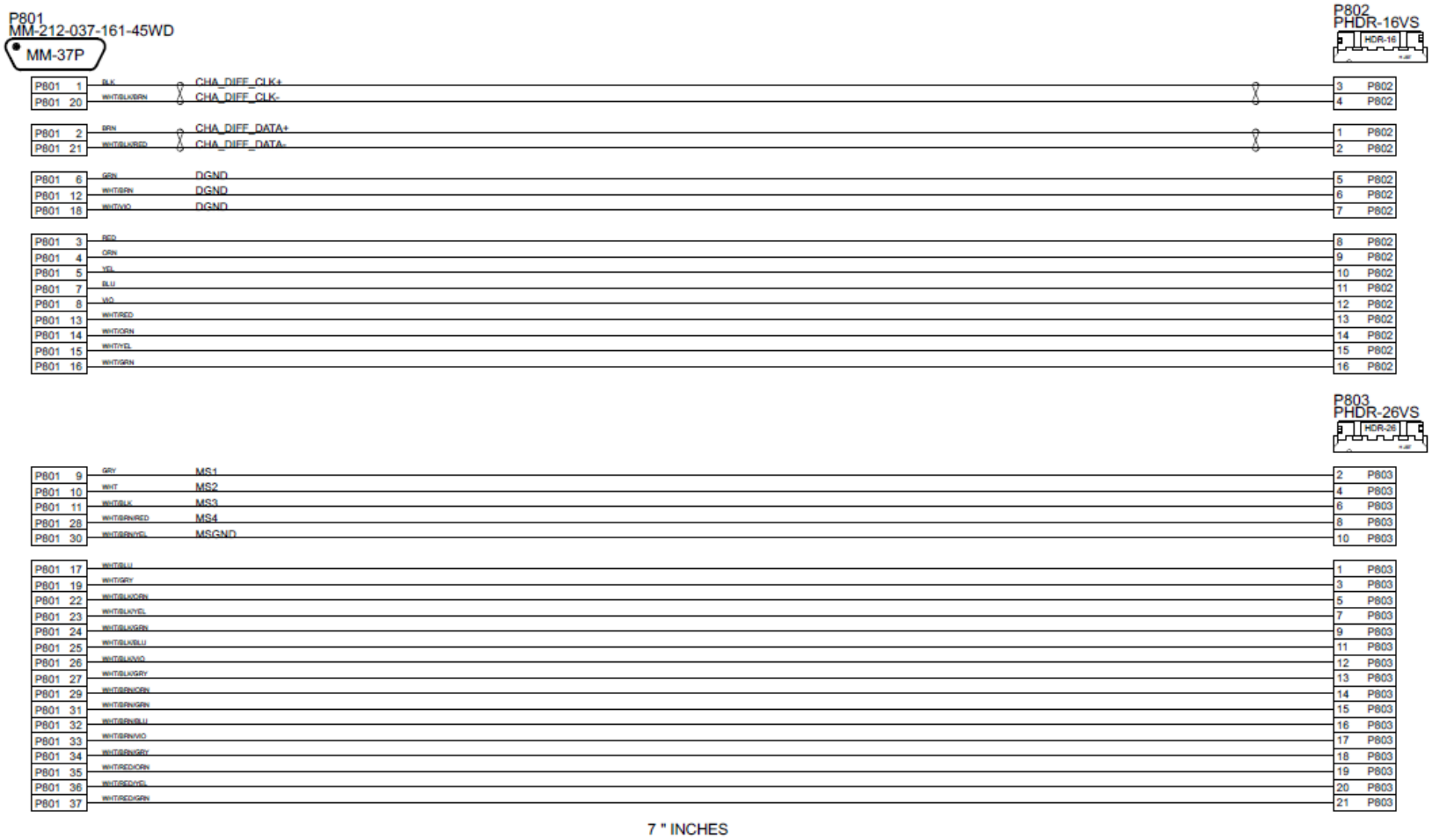

NOTES:

All wiring installed in accordance with AC43.13-1B
All multi conductor wire MIL-27500
All single conductor wire MIL-22759
Schematic label specifies AWG – Wire #
Physically label wires: Document# - AWG – Wire #

Drawn by: J. Araujo		Date: 17-Apr-2014	NRC·CNRC Flight Research Laboratory
Checked by:		Date:	Project: Hearing Protection Evaluation System MPCM-102M Wiring Harness — Project Code: A1-002961
Approved by: M. Ovenden		Date: 25-June-2014	
Mod Card Number: FRLP1401	PMCN:	Assembly: FRL14035	Drawing Number: IG14022 — Sheet: 8/14 — Revision: -

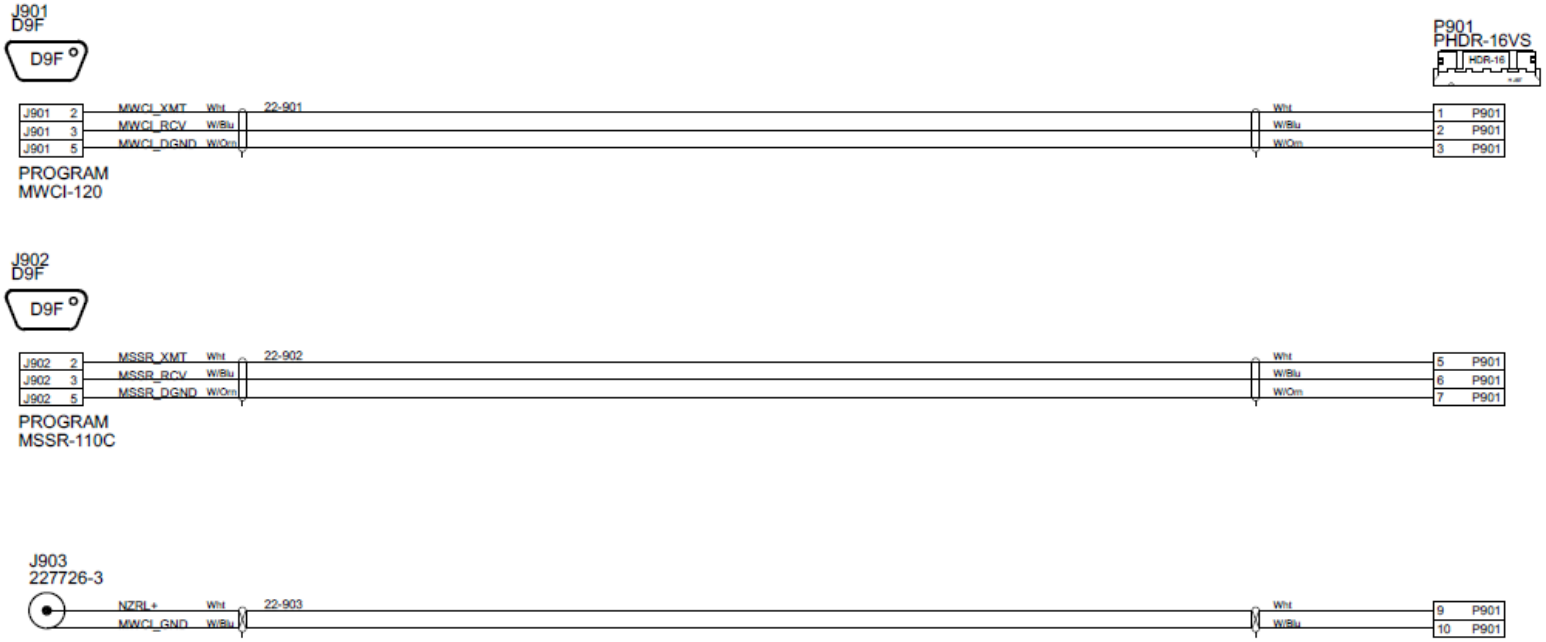

Drawn by: J. Araujo		Date: 17-Apr-2014	NRC·CNRC Flight Research Laboratory		
Checked by:		Date:	Project: Hearing Protection Evaluation System Communication Wiring Harness		Project Code: A1-002961
Approved by: M. Ovenden		Date: 25-June-2014			
Mod Card Number: FRLP1401	PMCN:	Assembly: FRL14035	Drawing Number: IG14022	Sheet: 9/14	Revision: -

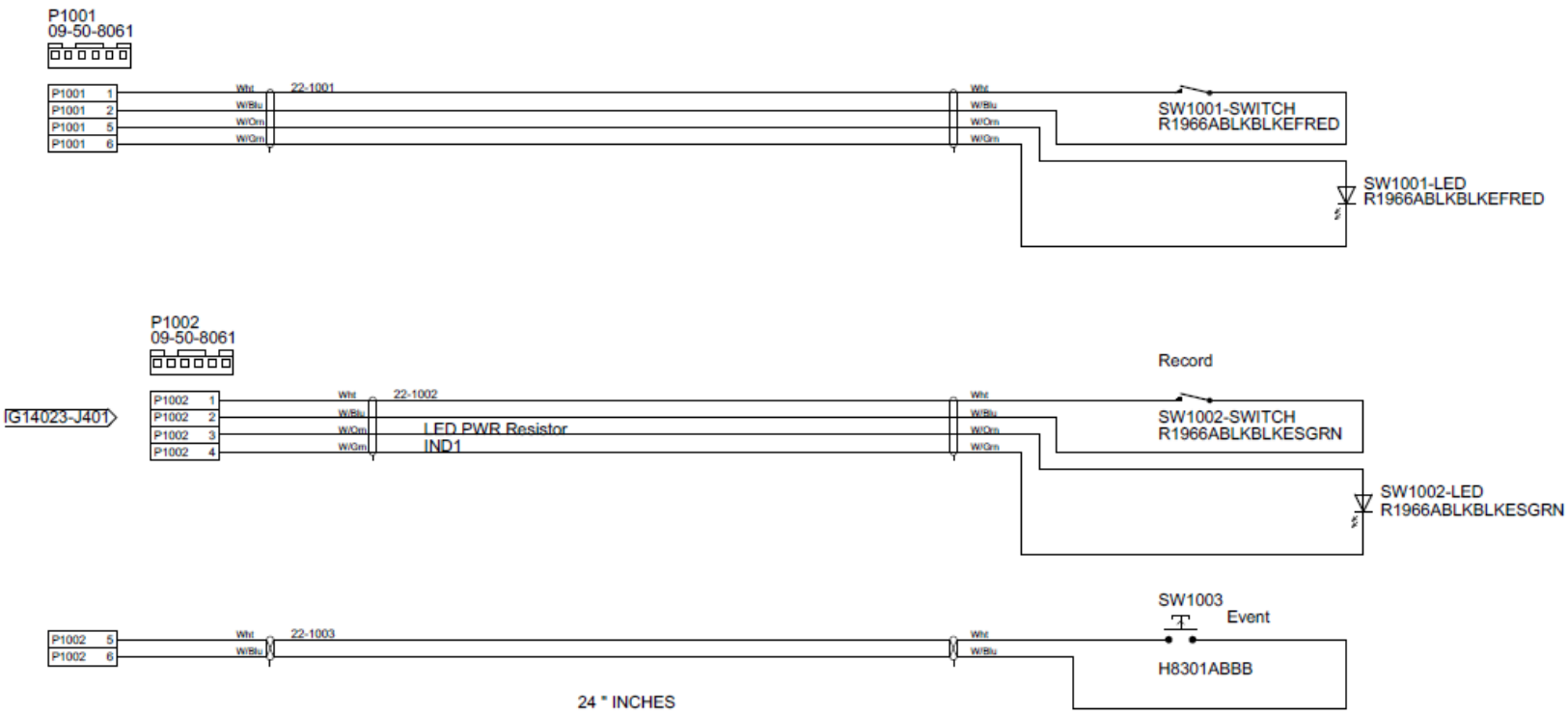

NOTES:

All wiring installed in accordance with AC43.13-1B
All multi conductor wire MIL-27500
All single conductor wire MIL-22759
Schematic label specifies AWG – Wire #
Physically label wires: Document# - AWG – Wire #

Drawn by: J. Araujo		Date: 17-Apr-2014	NRC-CNRC Flight Research Laboratory
Checked by:		Date:	Project: Hearing Protection Evaluation System Switch and Indicator Wiring Harnesses — Project Code: A1-002961
Approved by: M. Ovenden		Date: 25-June-2014	
Mod Card Number: FRLP1401	PMCN:	Assembly: FRL14035	Drawing Number: IG14022 — Sheet: 10/14 — Revision: -

NOTES:

All wiring installed in accordance with AC43.13-1B
All multi conductor wire MIL-27500
All single conductor wire MIL-22759
Schematic label specifies AWG – Wire #
Physically label wires: Document# - AWG – Wire #

Drawn by: J. Araujo		Date: 17-Apr-2014	NRC-CNRC Flight Research Laboratory		
Checked by:		Date:	Project: Hearing Protection Evaluation System Power Wiring Harnesses	Project Code: A1-002961	
Approved by: M. Ovenden		Date: 25-June-2014			
Mod Card Number: FRLP1401	PMCN:	Assembly: FRL14035	Drawing Number: IG14022	Sheet: 11/14	Revision: -

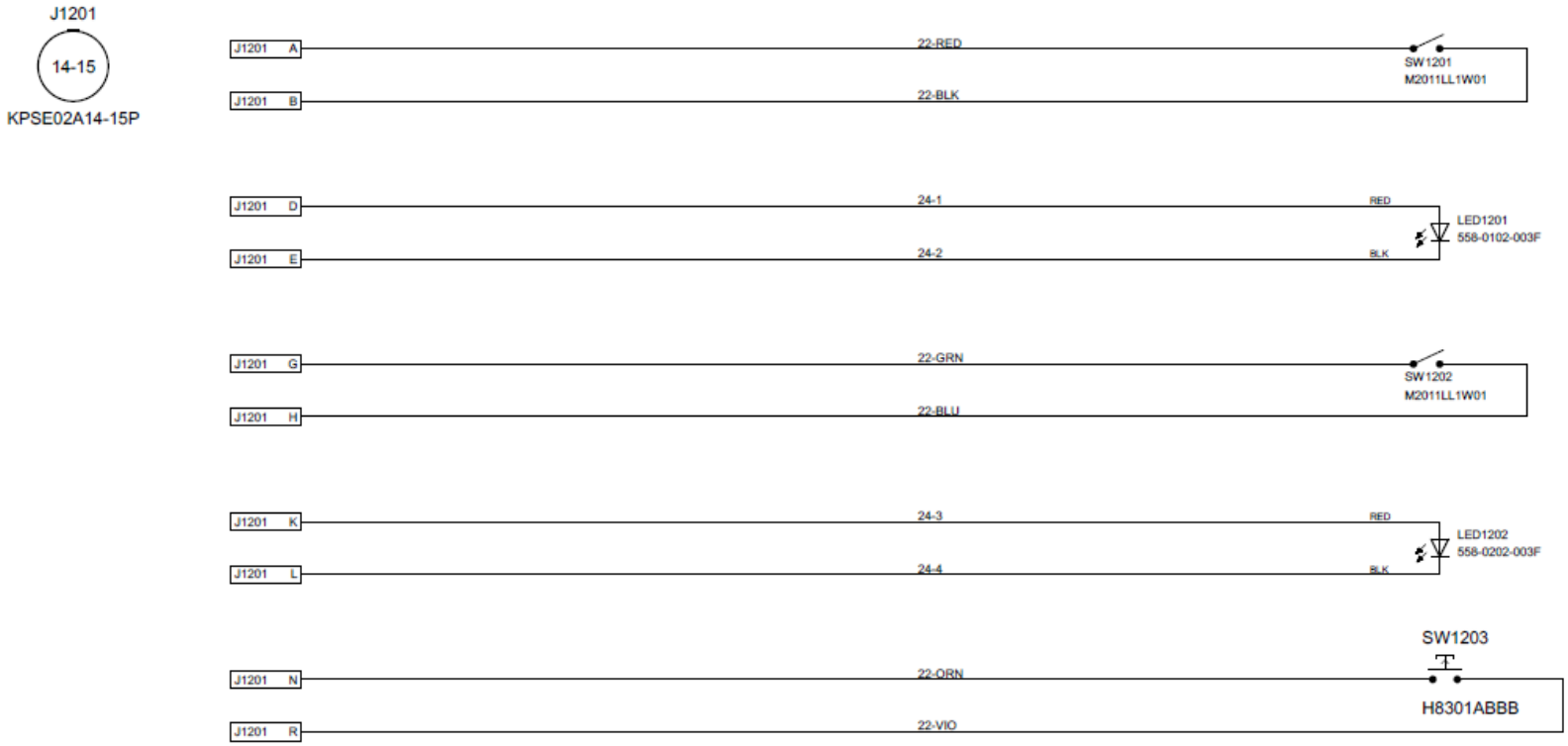

NOTES:

All wiring installed in accordance with AC43.13-1B
All multi conductor wire MIL-27500
All single conductor wire MIL-22759
Schematic label specifies AWG – Wire #
Physically label wires: Document# - AWG – Wire #

Drawn by: J. Araujo		Date: 17-Apr-2014	NRC-CNRC Flight Research Laboratory		
Checked by:		Date:	Project: Hearing Protection Evaluation System Remote Box Internal Wiring		Project Code: A1-002961
Approved by: M. Ovenden		Date: 25-June-2014			
Mod Card Number: FRLP1401	PMCN:	Assembly: FRL14035	Drawing Number: IG14022	Sheet: 12/14	Revision: -

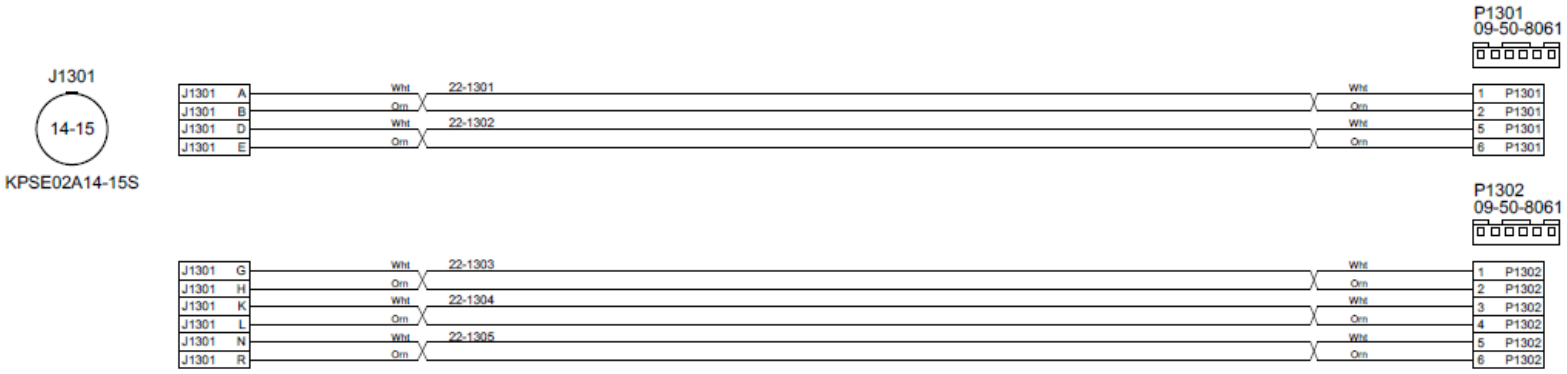

NOTES:

All wiring installed in accordance with AC43.13-1B
All multi conductor wire MIL-27500
All single conductor wire MIL-22759
Schematic label specifies AWG – Wire #
Physically label wires: Document# - AWG – Wire #

Drawn by: J. Araujo		Date: 17-Apr-2014	NRC·CNRC Flight Research Laboratory		
Checked by:		Date:	Project: Hearing Protection Evaluation System Remote Box Adaptor Wiring		Project Code: A1-002961
Approved by: M. Ovenden		Date: 25-June-2014			
Mod Card Number: FRLP1401	PMCN:	Assembly: FRL14035	Drawing Number: IG14022	Sheet: 13/14	Revision: -

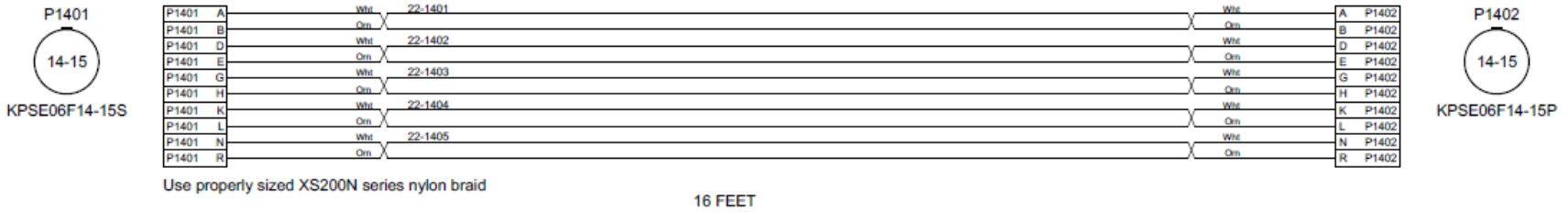

NOTES:

All wiring installed in accordance with AC43.13-1B
All multi conductor wire MIL-27500
All single conductor wire MIL-22759
Schematic label specifies AWG – Wire #
Physically label wires: Document# - AWG – Wire #

Drawn by: J. Araujo		Date: 17-Apr-2014	NRC-CNRC Flight Research Laboratory		
Checked by:		Date:	Project: Hearing Protection Evaluation System Remote Box Extension Cable		Project Code: A1-002961
Approved by: M. Ovenden		Date: 25-June-2014			
Mod Card Number: FRLP1401	PMCN:	Assembly: FRL14035	Drawing Number: IG14022	Sheet: 14/14	Revision: -

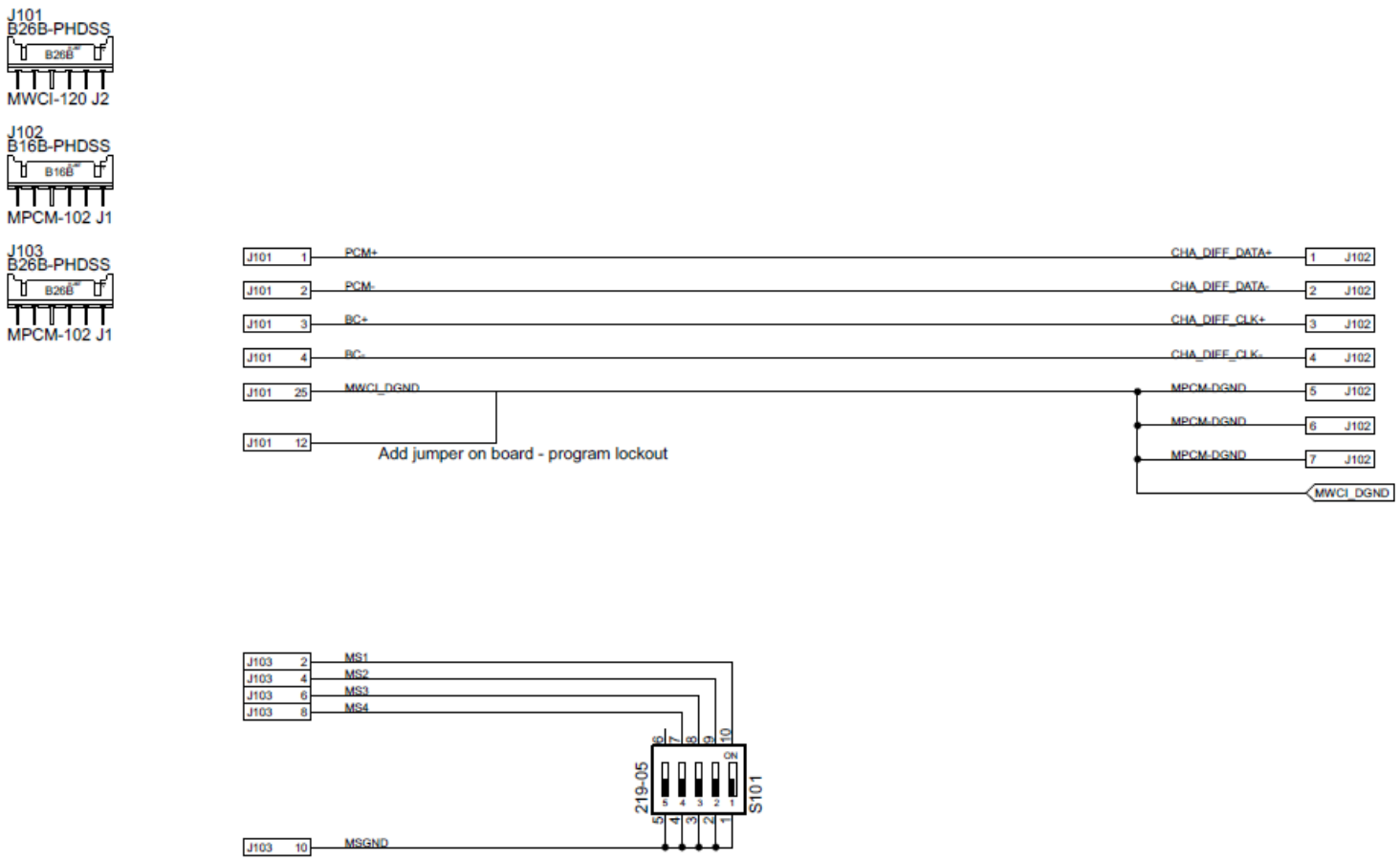

H1 MOUNT-HOLE4.5
H2 MOUNT-HOLE4.5
H3 MOUNT-HOLE4.5
H4 MOUNT-HOLE4.5
LOGO1

Drawn by: J. Araujo		Date: 17-Apr-2014	NRC-CNRC Flight Research Laboratory		
Checked by:		Date: - -	Project: Hearing Protection Main Interface Board MWCI-120 to MPCM-102 Interface Circuit	Project Code: A1-002961	
Approved by: M. Ovenden		Date: 25-June-2014			
Mod Card Number: FRLP1401	PMCN:	Assembly: IG14022	Drawing Number: IG14023	Sheet: 1/4	Revision: -

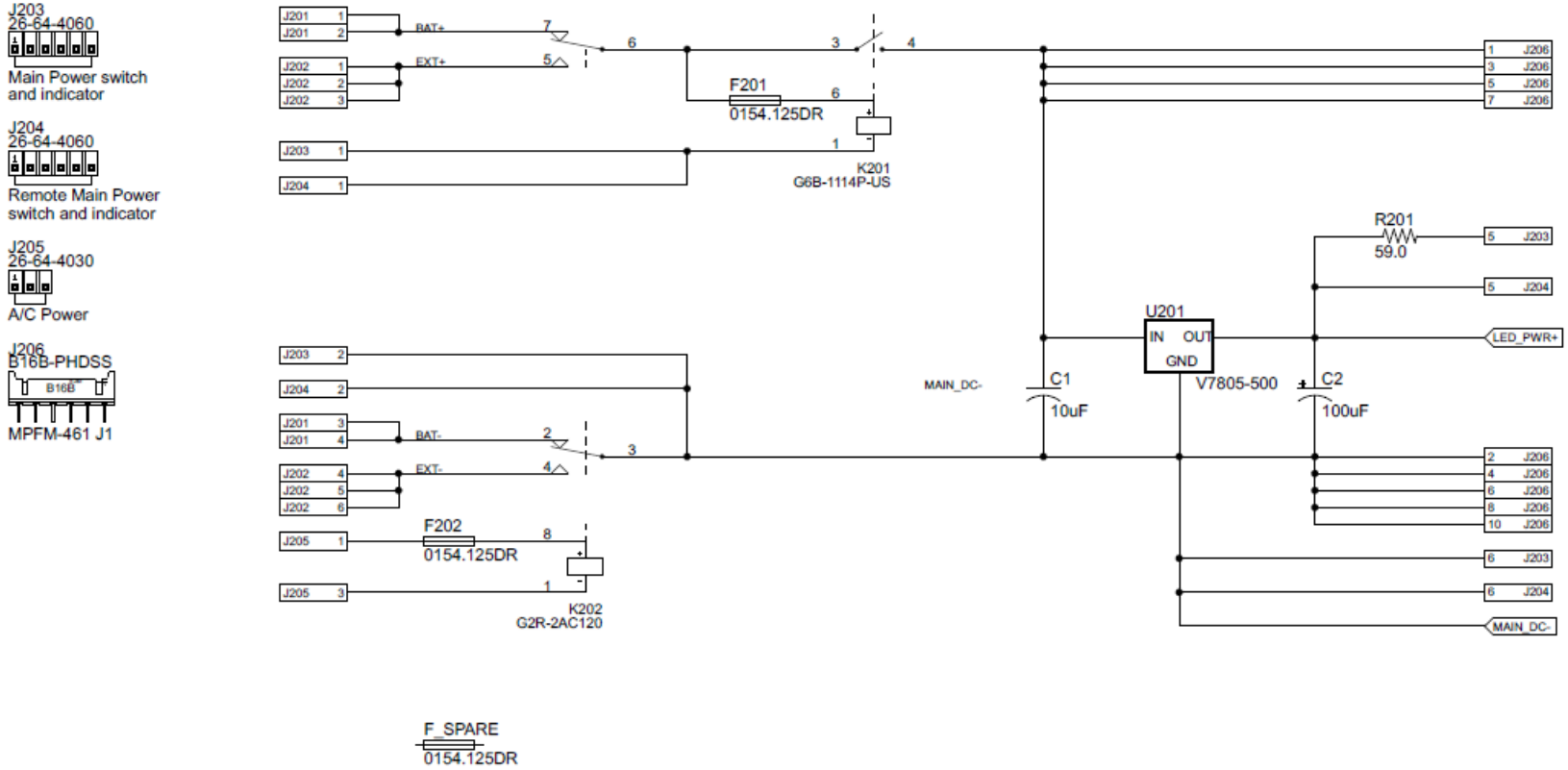

Drawn by: J. Araujo		Date: 17-Apr-2014	NRC-CNRC Flight Research Laboratory		
Checked by:		Date: - -	Project: Hearing Protection Main Interface Board 28 Vdc Power Circuit		Project Code: A1-002961
Approved by: M. Ovenden		Date: 25-June-2014			
Mod Card Number: FRLP1401	PMCN:	Assembly: IG14022	Drawing Number: IG14023	Sheet: 2/4	Revision: -

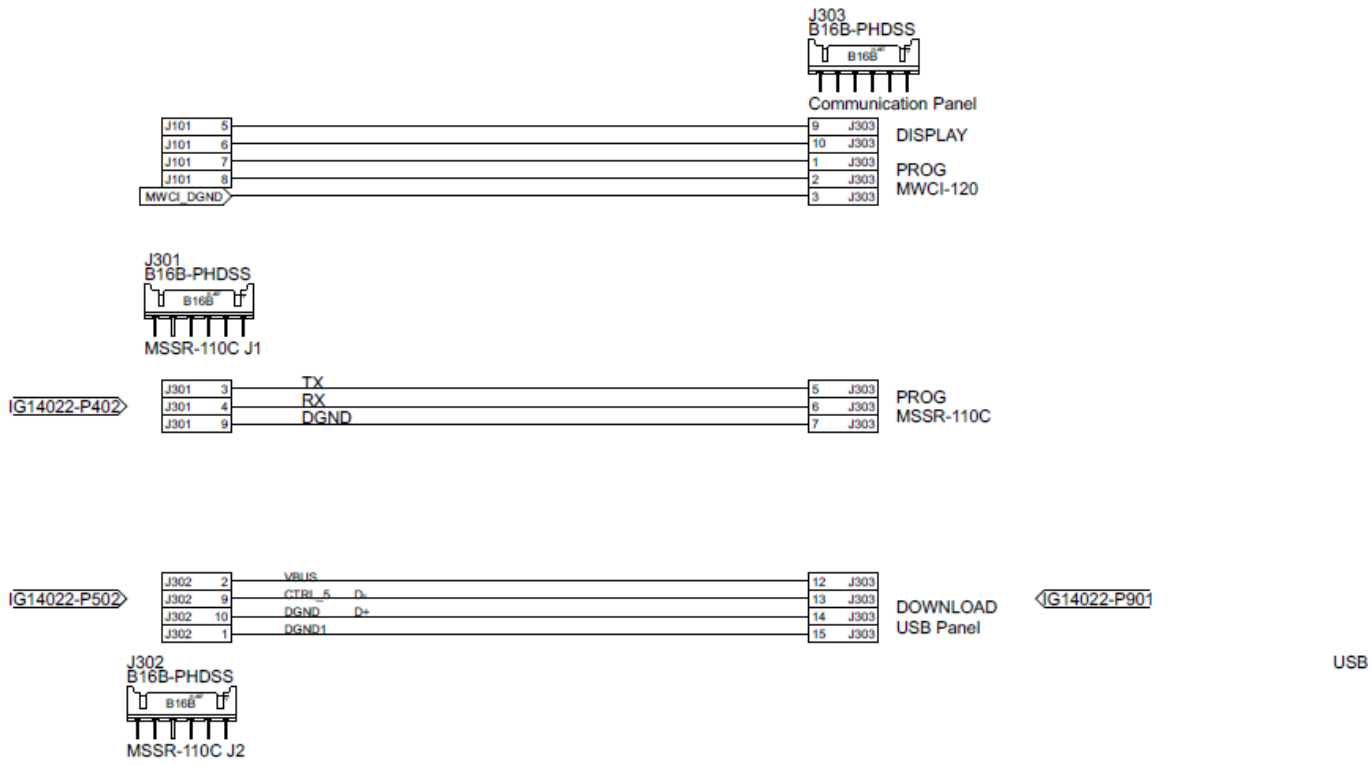

Drawn by: J. Araujo		Date: 17-Apr-2014	NRC-CNRC Flight Research Laboratory		
Checked by:		Date: - -	Project: Hearing Protection Main Interface Board Communication Interface Circuit	Project Code: A1-002961	
Approved by: M. Ovenden		Date: 25-June-2014			
Mod Card Number: FRLP1401	PMCN:	Assembly: IG14022	Drawing Number: IG14023	Sheet: 3/4	Revision: -

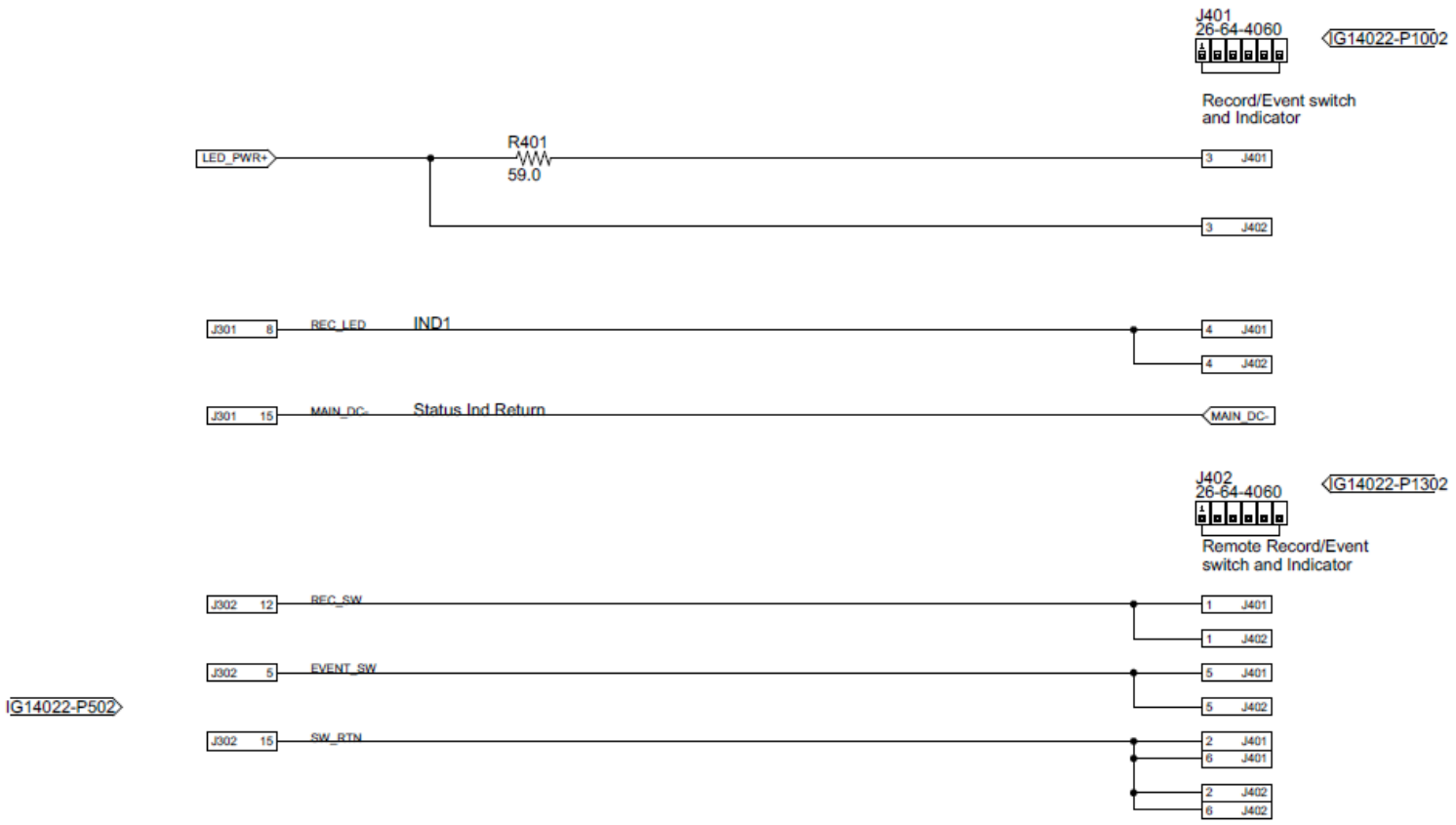

Drawn by: J. Araujo		Date: 17-Apr-2014	NRC-CNRC Flight Research Laboratory		
Checked by:		Date: - -	Project: Hearing Protection Main Interface Board Indicators/Switches Interface Circuit		Project Code: A1-002961
Approved by: M. Ovenden		Date: 25-June-2014			
Mod Card Number: FRLP1401	PMCN:	Assembly: IG14022	Drawing Number: IG14023	Sheet: 4/4	Revision: -

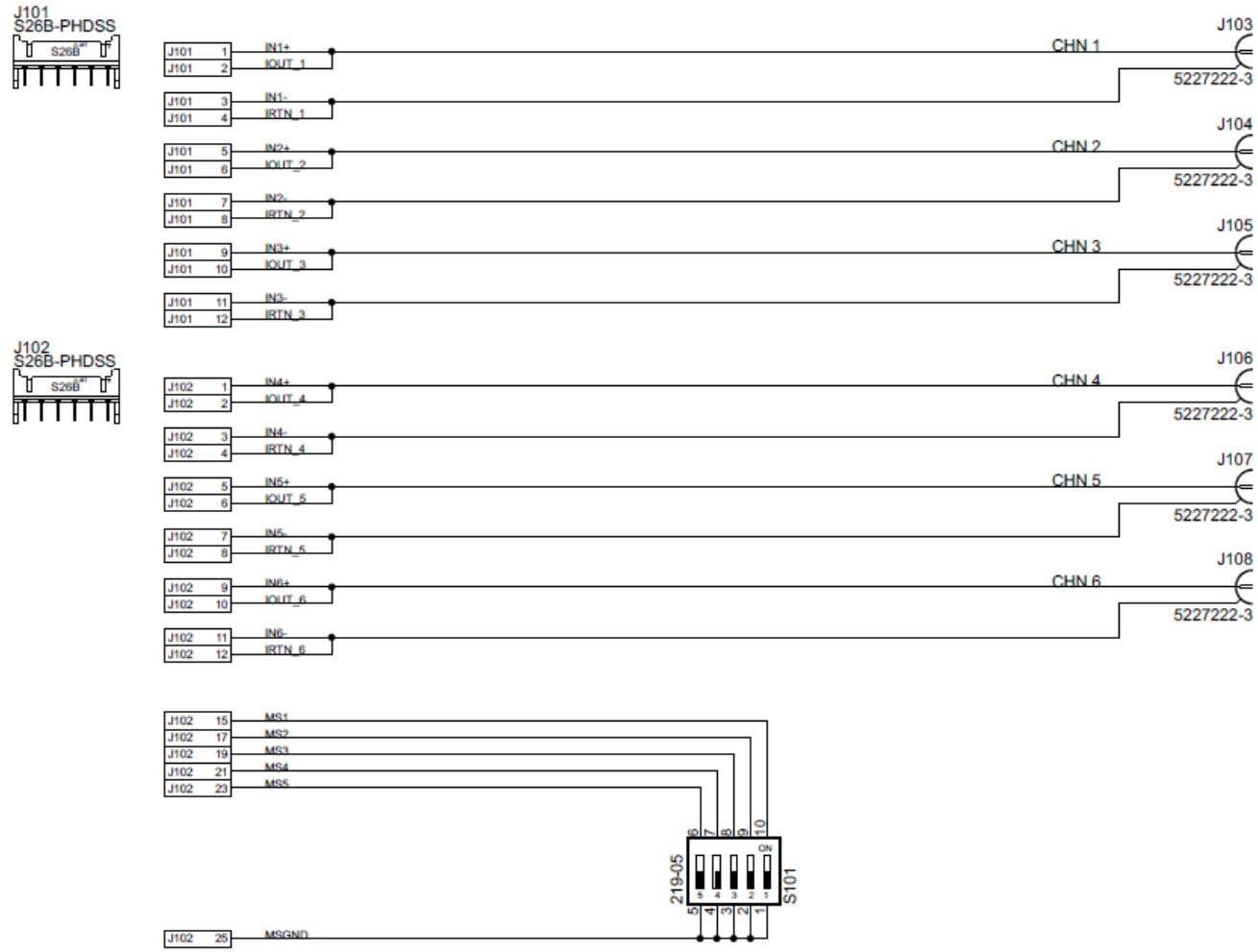

NOTES:

All wiring installed in accordance with AC43.13-1B
All multi conductor wire MIL-27500
All single conductor wire MIL-22759
Schematic label specifies AWG – Wire #
Physically label wires: Document# - AWG – Wire #

Drawn by: J. Araujo		Date: 15-Apr-2014	NRC-CNRC Flight Research Laboratory		
Checked by:		Date: - -	Project: Accelerometer Interface Board Hearing Protection Evaluation System		Project Code: A1-002961
Approved by: M. Ovenden		Date: 25-June-2014			
Mod Card Number: FRLP1401	PMCN:	Assembly: IG14022	Drawing Number: IG14024	Sheet: 1/1	Revision: -

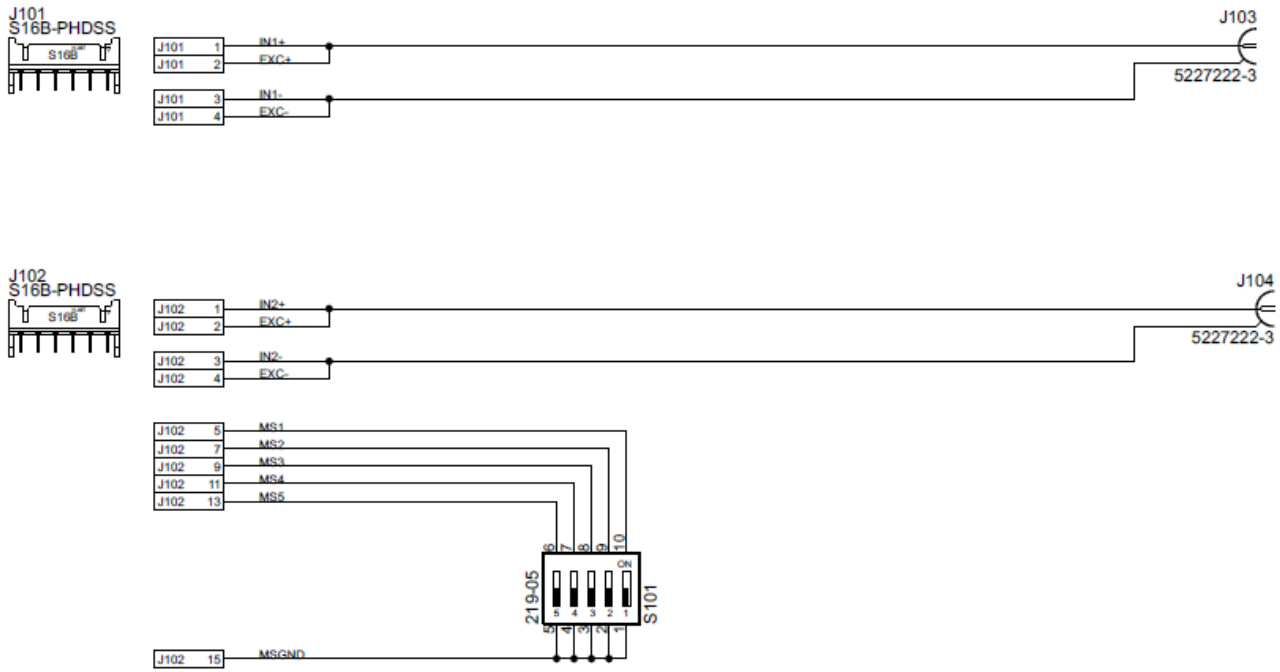

Drawn by: J. Araujo		Date: 9-Apr-2014	NRC·CNRC Flight Research Laboratory		
Checked by:		Date:	Project: Microphone Interface Board Hearing Protection Evaluation System		Project Code: A1-002961
Approved by: M. Ovenden		Date: 25-June-2014			
Mod Card Number: FRLP1401	PMCN:	Assembly: IG14022	Drawing Number: IG14025	Sheet: 1/1	Revision: -

A 2: MATLAB CSV import script <<importPILOTchan.m>>

```
function importPILOTchan(filename, saveNAME)
%Saves Data in 'saveNAME.mat' <--don't forget '.mat'

%Function imports 3 channels of data from GSS csv file and saves to the
%user given variable name 'Data' under the user chosen file name
%'saveNAME.mat'
%Function assumes the data is in 16 bit format and then translates
%'filename.csv' is a string and must be entered between ' '
%'saveNAME.mat' is a string and must be entered between ' '
%sensA is the sensitivity (mV/Pa) of channel Aseat
%sensB is the sensitivity (mV/Pa) of channel Bstand
%sensC is the sensitivity (mV/Pa) of channel Cpilot

%% Import data from text file.
delimiter = ',';

%% Format string for each line of text:
% double (%f)
% string (%s) (%*s means to ignore that field)

formatSpec = '%*s%f%*s%f%*s%f%[^\n\r]';
%\n does not read to the end of the row

%% Open the text file.
fileID = fopen(filename,'r');

%% Read columns of data according to format string.
dataArray = textscan(fileID, formatSpec, inf, 'Delimiter', delimiter, 'EmptyValue',
NaN,'HeaderLines', 1, 'ReturnOnError', false);

%Reads file fileID
%Expects the data in the following formatSpec columns:
%string,double,string,double,string,double (ignores strings)
%Reads until the end of the file (all rows 'inf')
%Separates into columns using the delimiter ','
%Changes all empty cells into 'Not a Number' (NaN)
%Acknowledges that the first row is a header and contains no data
%Does not return the values if there is an error during the read

%% Close the text file.
fclose(fileID);

%% Allocate imported array to column variable names
SeatCAL = dataArray{:, 1};
SeatCAL(isnan(SeatCAL)) = []; %Delete NaN cells

Data(:,1) = SeatCAL;
Header = {'CH147:CAL:+Z'};

%% Convert bit values into Pascals
Data = Data./3276.8; %convert bits to volts
Data = Data - 10; %recenter volts about zero
Data = Data.*1000; %convert volts to mV
Data(:,1) = Data(:,1)./198.8;

save(saveNAME, 'Data', 'Header'); %Save the variable to file
```

A 3: MATLAB Filter Generation

```
function [RMS, RMSav] = RMScal(filename)
%Opens GSS calibration data and determines the RMS value in 3 ways

%Script for treating calibration data files

%First take the calibration data csv and place it in matlab

[Days,Hours,Minutes,Seconds,us,ns,Data] = GSStoMAT(filename);
%This assumes the file is "test.csv" - for future implementation this will
%have to be changed to accept any file name

%Next transform the "Data" into volts centered about zero

Volts = (Data/3276.8) - 10;

%% For this function only the RMS value is required

clearvars Days Hours Minutes Seconds us ns %Data

%% Now find the maximums and minimums

[Max, MaxL] = findpeaks(Volts); %Find maximums
[Min, MinL] = findpeaks(-Volts); %Find minimums
Min = - Min; %Minimums have to be converted back to their original sign

MaxL = uint32(MaxL);
MinL = uint32(MinL);
Max = single(Max);
Min = single(Min);
Volts = single(Volts);

%Each pair of maximum and minimum will make up a period.

%Each period must be recentered about zero.

%Find the systemmatic offsets

offset = single(zeros(length(Max), 1));

for i = 1 : length(Max) - 1 %Complete for each maximum and minimum pair

    offset(i) = single((Max(i) + Min(i))/2);

end

%% Now to offset all of the data

Volts2 = single(Volts);

for i = 1 : length(MaxL) - 1 %For each period

    for j = MaxL(i) : MaxL(i+1) %For every data point within that period

        Volts2(j) = Volts(j) - offset(i);
```

```
    end

end

%Drop the end of the data so that we don't include any data missed by the
%offsetter

Volts = Volts(1:MaxL(end-1));
Volts2 = Volts2(1:MaxL(end-1));

figure(1) %Compare the data
subplot(2,2,1), plot(Volts,'b')
hold on
subplot(2,2,1), plot(Volts2, 'r')
hold off

%% Try the different high pass filters
Volts3 = ybutter(Volts);
Volts4 = ychebyI(Volts);
Volts5 = ychebyII(Volts);

figure(1) %Compare the data
subplot(2,2,2), plot(Volts, 'b')
hold on
subplot(2,2,2), plot(Volts3, 'r')
hold off

figure(1) %Compare the data
subplot(2,2,3), plot(Volts, 'b')
hold on
subplot(2,2,3), plot(Volts4, 'r')
hold off

figure(1) %Compare the data
subplot(2,2,4), plot(Volts, 'b')
hold on
subplot(2,2,4), plot(Volts5, 'r')
hold off

%% Compare the filter data
%% Calculate the RMS
RMS1 = sqrt((1/length(Volts2))*sum(Volts2.^2));
RMS2 = sqrt((1/length(Volts3))*sum(Volts3.^2));
RMS3 = sqrt((1/length(Volts4))*sum(Volts4.^2));
RMS4 = sqrt((1/length(Volts5))*sum(Volts5.^2));
RMS = [RMS1 RMS2 RMS3 RMS4]
RMSav = (RMS1 + RMS2 + RMS3 + RMS4)/4
```

```
function y = ybutter(x)
%YBUTTER Filters input x and returns output y.

% MATLAB Code
% Generated by MATLAB(R) 8.2 and the Signal Processing Toolbox 6.20.
% Generated on: 12-May-2014 16:15:47

persistent Hd;

if isempty(Hd)

    Fstop = 0.005;  % Stopband Frequency
    Fpass = 0.01;   % Passband Frequency
    Astop = 60;     % Stopband Attenuation (dB)
    Apass = 1;      % Passband Ripple (dB)

    h = fdesign.highpass('fst,fp,ast,ap', Fstop, Fpass, Astop, Apass);

    Hd = design(h, 'butter', ...
        'MatchExactly', 'stopband');

    set(Hd,'PersistentMemory',true);

end

y = filter(Hd,x);
```

```
function y = ychebyI(x)
%YCHEBYI Filters input x and returns output y.

% MATLAB Code
% Generated by MATLAB(R) 8.2 and the Signal Processing Toolbox 6.20.
% Generated on: 12-May-2014 16:16:50

persistent Hd;

if isempty(Hd)

    Fstop = 0.005;  % Stopband Frequency
    Fpass = 0.01;   % Passband Frequency
    Astop = 60;     % Stopband Attenuation (dB)
    Apass = 1;      % Passband Ripple (dB)

    h = fdesign.highpass('fst,fp,ast,ap', Fstop, Fpass, Astop, Apass);

    Hd = design(h, 'cheby1', ...
        'MatchExactly', 'passband');

    set(Hd,'PersistentMemory',true);

end

y = filter(Hd,x);
```

```
function y = ychebyII(x)
%YCHEBYII Filters input x and returns output y.

% MATLAB Code
% Generated by MATLAB(R) 8.2 and the Signal Processing Toolbox 6.20.
% Generated on: 12-May-2014 16:17:13

persistent Hd;

if isempty(Hd)

    Fstop = 0.005;  % Stopband Frequency
    Fpass = 0.01;   % Passband Frequency
    Astop = 60;     % Stopband Attenuation (dB)
    Apass = 1;      % Passband Ripple (dB)

    h = fdesign.highpass('fst,fp,ast,ap', Fstop, Fpass, Astop, Apass);

    Hd = design(h, 'cheby2', ...
        'MatchExactly', 'stopband');

    set(Hd,'PersistentMemory',true);

end

y = filter(Hd,x);
```

```
%Script for treating calibration data files

clear

%First take the calibration data csv and place it in matlab

[Days,Hours,Minutes,Seconds,us,ns,Data] = GSStoMAT('PILOTtwo.csv');
%This assumes the file is "test.csv" - for future implementation this will
%have to be changed to accept any file name

%Next transform the "Data" into volts centered about zero

Volts = (Data/3276.8) - 10;

%% For this function only the RMS value is required

clearvars Days Hours Minutes Seconds us ns %Data

%% Now find the maximums and minimums

[Max, MaxL] = findpeaks(Volts); %Find maximums
[Min, MinL] = findpeaks(-Volts); %Find minimums
Min = - Min; %Minimums have to be converted back to their original sign

MaxL = uint32(MaxL);
MinL = uint32(MinL);
Max = single(Max);
Min = single(Min);
Volts = single(Volts);

%Each pair of maximum and minimum will make up a period.

%Each period must be recentered about zero.

%Find the systemmatic offsets

offset = single(zeros(length(Max), 1));

for i = 1 : length(Max) - 1 %Complete for each maximum and minimum pair

    offset(i) = single((Max(i) + Min(i))/2);

end

%% Now to offset all of the data

Volts2 = single(Volts);

for i = 1 : length(MaxL) - 1 %For each period

    for j = MaxL(i) : MaxL(i+1) %For every data point within that period

        Volts2(j) = Volts(j) - offset(i);

    end
```

```
end

%Drop the end of the data so that we don't include any data missed by the
%offsetter

Volts = Volts(1:MaxL(end-1));
Volts2 = Volts2(1:MaxL(end-1));

figure(1) %Compare the data
subplot(2,2,1), plot(Volts,'b')
hold on
subplot(2,2,1), plot(Volts2, 'r')
hold off

%% Try the different high pass filters
Volts3 = ybutter(Volts);
Volts4 = ychebyI(Volts);
Volts5 = ychebyII(Volts);

figure(1) %Compare the data
subplot(2,2,2), plot(Volts,'b')
hold on
subplot(2,2,2), plot(Volts3, 'r')
hold off

figure(1) %Compare the data
subplot(2,2,3), plot(Volts,'b')
hold on
subplot(2,2,3), plot(Volts4, 'r')
hold off

figure(1) %Compare the data
subplot(2,2,4), plot(Volts,'b')
hold on
subplot(2,2,4), plot(Volts5, 'r')
hold off

%% Compare the filter data

%% Calculate the RMS

RMS1 = sqrt((1/length(Volts2))*sum(Volts2.^2));
RMS2 = sqrt((1/length(Volts3))*sum(Volts3.^2));
RMS3 = sqrt((1/length(Volts4))*sum(Volts4.^2));
RMS4 = sqrt((1/length(Volts5))*sum(Volts5.^2));

RMSvalues = [RMS1 RMS2 RMS3 RMS4]
RMSav = (RMS1 + RMS2 + RMS3 + RMS4)/4
```

A 4: Discrete Fourier transform MATLAB implementation

```
%Discrete Fourier Transform Function

%Created by Andrew Price
%May 22, 2014

%*** Not advisable to use this function with long signals
%*** This is not an optimized function

function xj = dft(xk, fs)

%Requires data vector xk
%Requires sampling frequency


N = length(xk);
xj = zeros(size(xk));

for J = 1:N; %for each element (each frequency band)

    temp = 0;

    for k = 1:N; %for each indice of the vector xk

        temp = temp + xk(k)*exp(-2*pi*1i*J*k/N);
        %Euler Identity used to simplify the equation

    end

    xj(J) = temp;

end

%Find the absolute value of the vector before plotting
%Only need to plot the single side of the spectrum
%1 -> 1/2 * length(xj)
```

```
%Windowing of Data before FFT

load('LMS_CD_00.mat')

Seat = Data(:,1);
Stand = Data(:,2);
Pilot = Data(:,3);

clearvars Data Header

%*-*-*-*-*-*

frac = 0.04; %Cutoff frequency, as a fraction of the sampling rate (frac can be anywhere
in 0:0.5)
%1/4 means the cuttoff frequency should be half of the FFT
%0.04 is 2000 Hz cut off (for 50 kHz sampling rate)

%*-*-*-*-*-*

%% Windowing

% I am going to window the signal with a Blackman window

L = length(Seat); %Total number of points in our signal length
Blackman = zeros(L,1);

for count = 1:L;
    Blackman(count) = 0.42 - 0.5*cos(2*pi*count/L) + 0.08*cos(4*pi*count/L);
end

Seat_Window = Blackman.*Seat;

%Compare the FFT of the windowed and not windowed data

Seat_FFT = fft(Seat);
%Normalize the amplitude
Seat_FFT = Seat_FFT/length(Seat);
Seat_Window_FFT = fft(Seat_Window);
%Normalize the amplitude
Seat_Window_FFT = Seat_Window_FFT/length(Seat);

ff = 25000*linspace(0,1,L/2+1);

% Compare the matlab window function

blackman_mat = blackman(L, 'periodic');

Seat_Window_mat = blackman_mat.*Seat;

% Find the error in my window (if there is any)
error = zeros(L,1);
error = Seat_Window - Seat_Window_mat;
%error = abs(error);

%
figure(1)
subplot(3,1,1)
```

```
plot(Seat)
title('Seat Channel')
subplot(3,1,2)
plot(Seat_Window, 'b')
hold on
plot(Seat_Window_mat, 'r')
title('Windowed Seat Channel')
hold off
legend('My window', 'Matlab''s window')
subplot(3,1,3)
plot(error)
title('Difference between my window and Matlab''s window')

figure(2)
loglog(ff, 2*abs(Seat_FFT(1:L/2+1)), 'b',ff, 2*abs(Seat_Window_FFT(1:L/2+1)),'r')
title('Logarithmic Comparison')
legend('No Windowing', 'Windowing')
xlabel('Frequency')
ylabel('Amplitude')

figure(3)
semilogy(ff, 2*abs(Seat_FFT(1:L/2+1)), 'b',ff, 2*abs(Seat_Window_FFT(1:L/2+1)),'r')
title('Semi-Logarithmic Comparison')
legend('No Windowing', 'Windowing')
xlabel('Frequency')
ylabel('Amplitude')
%}

%% Now lets try to reduce the noise level

%First a four segment average (removed in latest run)

%{
a = 1;
b = L/4;
c = L/2;
d = 3*L/4;
e = L;

Seat1 = Seat(a:b+1); %Slight overlap
Seat2 = Seat(b:c);
Seat3 = Seat(c:d);
Seat4 = Seat(d:e);

Seat_FFT1 = fft(Seat1);
Seat_FFT2 = fft(Seat2);
Seat_FFT3 = fft(Seat3);
Seat_FFT4 = fft(Seat4);

ff4 = 25000*linspace(0,1,length(Seat_FFT1)/2+1);

av4 = (abs(Seat_FFT1) + abs(Seat_FFT2) + abs(Seat_FFT3) + abs(Seat_FFT4))/4;

figure(4)
loglog(ff, 2*abs(Seat_FFT(1:L/2+1)), 'b', ff4, 2*(av4(1:length(Seat_FFT1)/2+1)), 'r');
title('No averaging VS 4 averages')
legend('No averaging', '4 averages')
xlabel('Frequency')
```

```
ylabel('Amplitude')

figure(5)
semilogx(ff, 2*abs(Seat_FFT(1:L/2+1)), 'b', ff4, 2*(av4(1:length(Seat_FFT1)/2+1)), 'r');
title('No averaging VS 4 averages')
legend('No averaging', '4 averages')
xlabel('Frequency')
ylabel('Amplitude')
%}

clearvars a b c d e Seat_FFT1 Seat_FFT2 Seat_FFT3 Seat_FFT4
clearvars Seat1 Seat2 Seat3 Seat4

%% Compare Multiple Averaging

L = length(Seat);
av = zeros(length(Seat)/2+1,5);
av_Blackman = av;
ffav = av;
sampleL = zeros(5,1);

for power = 1:5;

    n = 2^power;
    temp2 = 0;
    temp2_Blackman = temp2;

    nL = L/n+1; %Total number of points in our signal length
    Blackman = zeros(floor(nL),1);

    for count = 1:nL;
        Blackman(count) = 0.42 - 0.5*cos(2*pi*count/nL) + 0.08*cos(4*pi*count/nL);
    end

    for count = 1:n;
        if count == 1;
            temp = Seat(1:count*L/n+1);
        else
            temp = Seat((count-1)*L/n: count*L/n);
        end

        temp_Blackman = Blackman.*temp;
        temp = fft(temp);
        temp_Blackman = fft(temp_Blackman);
        temp = abs(temp);
        temp_Blackman = abs(temp_Blackman);
        temp2 = temp2 + temp;
        temp2_Blackman = temp2_Blackman + temp_Blackman;

    end

    sampleL(power) = length(temp2)/2+1;
    av(1:sampleL(power),power) = temp2(1:sampleL(power))/n;
    av_Blackman(1:sampleL(power),power) = temp2_Blackman(1:sampleL(power))/n;
    ffav(1:sampleL(power),power) = 25000*linspace(0,1,sampleL(power));

end
```

```
%
figure(6)
semilogy(ff, 2*abs(Seat_FFT(1:L/2+1)), 'b', ffav(1:sampleL(1),1), 2*av(1:sampleL(1),1),
'r', ffav(1:sampleL(2),2), 2*av(1:sampleL(2),2), 'g', ffav(1:sampleL(3),3),
2*av(1:sampleL(3),3), 'c', ffav(1:sampleL(4),4), 2*av(1:sampleL(4),4), 'm',
ffav(1:sampleL(5),5), 2*av(1:sampleL(5),5), 'y')
title('Averaging Comparison')
legend('No Averaging', '2 Averages', '4 Averages', '8 Averages', '16 Averages', '32
Averages')
xlabel('Frequency')
ylabel('Amplitude')
%}

%% Compare Multiple Averaging with Blackman Windowed Multiple Averaging

%
figure(7)
semilogy(ff, 2*abs(Seat_Window_FFT(1:L/2+1)), 'b', ffav(1:sampleL(1),1),
2*av_Blackman(1:sampleL(1),1), 'r', ffav(1:sampleL(2),2), 2*av_Blackman(1:sampleL(2),2),
'g', ffav(1:sampleL(3),3), 2*av_Blackman(1:sampleL(3),3), 'c', ffav(1:sampleL(4),4),
2*av_Blackman(1:sampleL(4),4), 'm', ffav(1:sampleL(5),5), 2*av_Blackman(1:sampleL(5),5),
'y')
title('Windowed Averaging Comparison')
legend('No Averaging', '2 Averages', '4 Averages', '8 Averages', '16 Averages', '32
Averages')
xlabel('Frequency')
ylabel('Amplitude')
%}

% Compare Windowed and non-Windowed 32 averages

figure(8)
semilogy(ffav(1:sampleL(5),5), 2*av(1:sampleL(5),5), 'b', ffav(1:sampleL(5),5),
2*av_Blackman(1:sampleL(5),5), 'r')
title('non-Windowed VS Windowed 32 Average Comparison')
legend('No Windowing', 'Windowing')
xlabel('Frequency')
ylabel('Amplitude')

%% How much can we reduce this noise?


n = 100;
temp2 = 0;
temp2_Blackman = temp2;

nL = L/n+1; %Total number of points in our signal length
Blackman = zeros(floor(nL),1);

for count = 1:nL;
    Blackman(count) = 0.42 - 0.5*cos(2*pi*count/nL) + 0.08*cos(4*pi*count/nL);
end

for count = 1:n;
    if count == 1;
            temp = Seat(1:count*L/n+1);
    else
            temp = Seat((count-1)*L/n: count*L/n);
```

```
    end

    temp_Blackman = Blackman.*temp;
    temp = fft(temp);
    temp_Blackman = fft(temp_Blackman);
    temp = abs(temp);
    temp_Blackman = abs(temp_Blackman);
    temp2 = temp2 + temp;
    temp2_Blackman = temp2_Blackman + temp_Blackman;

end

sampleL2 = length(temp2)/2+1;
average = zeros(sampleL2,1);
average_Blackman = average;

average = temp2(1:sampleL2)/n;
average_Blackman = temp2_Blackman(1:sampleL2)/n;
ffaverage = 25000*linspace(0,1,sampleL2);

figure(9)
semilogy(ff, 2*abs(Seat_FFT(1:L/2+1)), 'b', ffaverage, 2*abs(average), 'r', ffaverage,
2*abs(average_Blackman), 'g');
title('Noise Reduction Test (33656 averages)')
legend('Raw Data', '100 segment length average', 'Windowed 100 segment length average')
xlabel('Frequency')
ylabel('Amplitude')
```

A 5: Unaltered 3rd octave in-flight data

Note: Standard deviations, microphone adjustments and windscreen adjustments have not been included in these charts.

Closed Door Ground Segment

3rd Octave Center Frequency [Hz]	Run A Seat [dB]	Run A Stand [dB]	Run A Pilot [dB]	Run B Seat [dB]	Run B Stand [dB]	Run B Pilot [dB]
12.5	78.70	78.48	78.31	79.90	79.58	79.44
16	81.55	81.44	81.75	80.71	80.41	80.32
20	94.15	93.75	94.10	93.02	92.19	92.08
25	86.42	84.20	84.29	88.21	85.53	84.16
31.5	80.37	77.44	80.68	80.50	77.32	79.56
40	93.35	92.33	94.36	91.80	90.04	93.69
50	97.97	97.86	92.93	96.37	94.41	92.33
63	90.23	86.38	86.44	89.37	85.86	87.53
80	82.00	86.04	88.39	82.45	85.76	87.60
100	104.98	100.45	102.28	103.66	98.72	100.38
125	91.06	88.02	88.49	91.83	88.47	88.36
160	90.58	90.79	90.54	89.24	90.29	90.29
200	89.03	90.71	88.54	91.88	89.45	88.25
250	86.60	88.55	88.45	85.53	87.32	87.92
315	90.52	89.20	89.46	90.02	89.76	90.75
400	88.23	88.72	84.54	87.28	87.61	84.35
500	95.41	90.28	87.51	92.96	89.97	87.70
630	95.19	89.07	86.49	92.92	88.99	85.11
800	88.59	90.10	83.46	86.50	87.71	82.14
1000	87.73	90.13	83.22	87.72	89.07	82.98
1250	87.56	86.46	82.01	86.53	86.08	81.43
1600	93.68	90.25	85.25	92.19	90.37	85.43
2000	87.34	84.45	80.64	87.59	83.68	80.63
2500	86.57	83.90	79.18	84.85	81.83	78.00
3150	91.19	90.13	84.75	88.91	89.40	83.31
4000	86.38	84.00	79.06	83.90	81.83	77.90
5000	84.21	82.48	77.26	82.61	80.58	76.21
6300	84.29	80.79	76.15	83.34	80.06	75.42
8000	90.94	87.25	82.60	92.45	89.48	86.01
10000	77.44	74.21	69.65	78.12	75.06	70.61
12500	65.27	61.64	59.19	65.47	61.87	59.58
16000	54.70	51.59	48.27	54.83	51.72	48.46
20000	44.17	43.64	44.33	44.42	43.79	44.40

Closed Door Hover Segment

3rd Octave Center Frequency [Hz]	Run A Seat [dB]	Run A Stand [dB]	Run A Pilot [dB]	Run B Seat [dB]	Run B Stand [dB]	Run B Pilot [dB]
12.5	82.91	82.82	82.96	79.45	79.39	79.60
16	81.38	81.04	81.15	78.68	78.46	79.36
20	96.17	96.43	98.55	100.26	99.50	99.23
25	87.83	85.52	83.43	89.28	86.56	82.59
31.5	84.41	81.19	83.03	85.45	81.48	82.37
40	93.08	89.85	89.18	91.88	87.07	93.43
50	96.42	92.07	86.83	97.04	92.93	86.79
63	89.32	87.26	86.91	89.73	86.94	90.10
80	85.35	85.98	88.29	86.61	86.41	88.24
100	103.74	100.51	100.54	106.08	102.48	99.43
125	89.72	88.87	87.25	90.07	90.37	87.72
160	88.04	88.51	84.18	87.96	88.09	84.55
200	87.87	89.01	88.00	89.45	89.38	90.18
250	82.43	83.75	83.44	82.90	83.97	85.27
315	86.99	87.09	85.86	85.04	91.74	85.46
400	84.45	83.08	80.03	84.97	83.84	81.37
500	93.35	85.90	86.87	92.86	87.98	87.82
630	88.65	87.68	86.79	89.40	91.67	89.35
800	88.49	86.02	81.15	87.50	86.08	81.32
1000	86.04	88.23	81.26	87.11	87.11	81.81
1250	86.91	85.93	82.60	87.28	85.88	81.61
1600	89.10	87.48	88.85	90.33	87.92	87.14
2000	88.63	84.79	83.24	87.98	85.99	82.61
2500	85.06	85.55	78.41	84.86	84.20	78.77
3150	95.00	96.05	86.11	96.41	95.51	88.45
4000	84.39	82.51	78.91	84.78	85.25	79.84
5000	85.21	79.34	75.16	84.25	79.85	75.31
6300	80.01	77.56	72.15	80.57	78.43	72.91
8000	80.84	78.49	74.03	81.66	78.75	73.98
10000	94.38	90.41	85.72	93.37	93.61	85.38
12500	63.83	60.49	56.75	63.93	60.45	56.95
16000	51.27	48.60	45.77	51.86	48.55	45.96
20000	50.01	46.75	45.88	49.70	46.78	45.75

Closed Door Climb Segment

3rd Octave Center Frequency [Hz]	Run A Seat [dB]	Run A Stand [dB]	Run A Pilot [dB]	Run B Seat [dB]	Run B Stand [dB]	Run B Pilot [dB]
12.5	80.15	79.50	78.81	80.32	79.56	78.84
16	81.37	80.86	82.33	82.24	81.76	83.32
20	92.54	93.83	95.91	93.50	94.58	96.20
25	87.32	84.93	83.77	86.12	83.94	82.02
31.5	90.30	86.07	89.26	90.50	86.02	86.50
40	94.31	90.75	91.49	92.31	90.04	92.48
50	97.80	95.31	91.90	97.77	95.69	92.12
63	89.58	87.13	87.34	88.28	87.56	90.21
80	83.67	88.00	87.88	83.15	87.78	86.92
100	103.62	100.64	101.56	105.91	101.20	99.75
125	91.44	88.28	87.34	90.58	88.33	87.29
160	89.05	88.35	87.10	89.37	88.40	86.91
200	87.04	87.51	87.53	88.93	88.08	88.70
250	83.15	85.14	84.04	83.54	85.65	84.59
315	86.63	86.78	85.58	85.58	89.99	85.35
400	85.13	82.53	78.41	84.82	82.94	78.40
500	94.34	84.68	87.54	94.09	86.29	86.06
630	91.86	86.57	87.72	92.19	88.76	89.43
800	87.29	84.55	79.89	86.55	83.76	79.42
1000	84.94	86.33	79.20	84.50	85.23	79.21
1250	85.80	84.22	80.51	86.04	84.88	80.02
1600	88.53	88.20	81.12	90.19	88.16	82.97
2000	86.47	84.75	80.84	87.06	84.37	80.14
2500	84.32	84.13	78.07	84.93	83.88	78.21
3150	95.59	96.65	87.64	97.85	92.47	88.49
4000	85.56	83.05	78.62	84.11	82.60	77.68
5000	81.62	79.56	73.65	82.22	79.02	73.13
6300	80.26	78.39	72.69	80.28	76.99	72.13
8000	82.00	79.27	74.49	81.89	79.88	74.74
10000	91.27	90.60	84.68	90.64	89.88	83.90
12500	65.00	61.45	58.11	65.54	62.23	58.68
16000	52.15	49.25	46.15	52.40	49.23	46.45
20000	49.26	46.23	45.19	49.80	46.75	45.42

Closed Door Steady Level Flight (100 knots) Segment

3rd Octave Center Frequency [Hz]	Run A Seat [dB]	Run A Stand [dB]	Run A Pilot [dB]	Run B Seat [dB]	Run B Stand [dB]	Run B Pilot [dB]
12.5	83.36	82.71	82.37	81.92	81.28	80.95
16	82.94	82.63	83.25	82.14	81.48	81.59
20	99.15	92.40	101.57	97.82	88.82	99.79
25	90.17	86.12	89.91	89.02	85.34	86.26
31.5	95.55	92.51	92.03	97.71	94.84	91.91
40	102.53	101.79	104.18	99.25	99.42	103.99
50	98.20	97.68	95.44	97.80	97.04	95.22
63	97.48	99.55	101.26	96.92	98.19	100.23
80	90.13	96.04	94.77	89.33	95.21	95.56
100	104.74	102.02	101.50	106.83	102.32	100.41
125	94.76	92.67	92.75	94.50	91.80	92.41
160	93.19	94.35	89.89	94.36	94.64	89.89
200	91.31	94.16	91.18	92.12	95.27	91.03
250	90.61	93.72	90.31	90.05	93.24	90.15
315	91.25	92.10	89.38	90.93	92.38	90.36
400	89.99	88.77	86.98	90.07	90.26	86.98
500	95.34	90.06	88.19	94.44	90.07	87.06
630	93.65	88.87	89.79	94.49	90.16	90.53
800	88.10	86.32	81.99	88.02	86.10	82.15
1000	86.01	86.84	82.26	85.95	86.61	81.94
1250	86.97	85.39	81.77	86.87	85.40	81.68
1600	89.12	88.46	83.25	89.23	88.59	83.40
2000	87.03	86.33	82.26	86.57	85.60	82.08
2500	86.28	83.89	80.51	85.76	83.72	79.89
3150	93.77	99.00	87.49	98.03	94.37	88.07
4000	84.61	82.49	78.73	84.84	84.12	78.86
5000	81.72	78.68	76.31	81.74	77.67	76.53
6300	81.55	77.26	74.36	81.97	77.04	73.64
8000	83.50	81.79	77.92	82.49	79.91	75.43
10000	90.57	88.85	82.32	90.45	91.63	83.23
12500	64.72	62.04	59.95	64.94	62.04	60.11
16000	52.11	48.91	46.70	52.67	49.23	46.99
20000	50.05	47.17	45.31	50.24	47.23	45.59

Closed Door Steady Level Flight (120 knots) Segment

3rd Octave Center Frequency [Hz]	Run A Seat [dB]	Run A Stand [dB]	Run A Pilot [dB]	Run B Seat [dB]	Run B Stand [dB]	Run B Pilot [dB]
12.5	83.52	82.79	82.22	82.44	81.85	81.52
16	86.35	85.70	84.76	86.40	85.96	85.19
20	105.33	100.70	98.24	104.68	99.68	98.61
25	91.97	88.59	87.83	92.58	89.23	88.77
31.5	99.50	96.30	93.88	99.96	96.95	94.90
40	108.70	109.35	108.22	106.24	107.60	107.73
50	101.53	99.83	96.14	101.07	99.97	96.40
63	102.13	101.59	102.89	102.00	101.15	102.22
80	93.74	99.94	97.41	94.56	100.14	97.77
100	105.46	102.53	102.22	105.28	102.31	102.11
125	97.45	96.11	96.66	97.61	96.19	96.65
160	96.16	98.61	93.33	96.69	98.52	93.82
200	94.49	97.15	94.06	95.41	97.87	94.52
250	93.63	96.03	92.91	94.22	96.49	93.45
315	93.22	95.64	91.23	93.90	95.57	91.45
400	91.58	90.87	87.79	92.15	91.32	88.06
500	95.24	91.88	89.40	94.76	92.27	89.86
630	94.10	90.56	90.58	95.08	91.49	91.22
800	89.99	88.68	84.95	90.02	89.12	84.96
1000	88.52	90.18	85.08	88.65	89.35	85.18
1250	89.07	88.24	84.79	88.74	88.16	84.99
1600	93.43	89.21	86.77	93.12	89.78	85.42
2000	87.90	87.33	84.65	87.72	87.27	84.60
2500	87.39	88.93	83.61	86.57	87.69	83.09
3150	96.36	94.93	86.63	96.35	92.64	88.55
4000	85.64	84.37	81.82	85.13	84.68	81.75
5000	82.65	79.86	79.85	83.72	80.88	79.99
6300	80.36	78.05	76.90	80.33	77.77	76.84
8000	81.02	78.67	75.86	80.65	78.22	75.35
10000	92.83	87.99	83.22	89.62	88.88	83.11
12500	63.35	61.19	60.89	63.77	61.77	61.03
16000	51.51	48.50	47.48	51.83	48.99	48.02
20000	49.90	46.96	45.33	49.55	46.63	45.37

Closed Door Descent Segment

3rd Octave Center Frequency [Hz]	Run A Seat [dB]	Run A Stand [dB]	Run A Pilot [dB]	Run B Seat [dB]	Run B Stand [dB]	Run B Pilot [dB]
12.5	83.71	83.34	83.68	84.07	83.72	83.82
16	83.81	83.21	83.39	83.94	83.34	83.45
20	105.03	99.26	103.62	105.22	99.04	104.13
25	93.26	90.95	87.25	92.77	90.56	87.22
31.5	101.17	97.77	96.92	100.76	97.24	96.47
40	109.28	109.10	106.50	104.13	105.01	104.31
50	102.75	103.05	98.71	103.17	103.38	99.23
63	104.44	102.69	102.94	104.24	102.35	103.13
80	95.80	101.60	99.85	95.81	101.42	100.42
100	105.10	102.70	100.70	105.42	102.74	101.92
125	100.77	99.16	100.74	101.01	99.39	100.72
160	99.18	102.04	97.24	99.41	101.96	97.00
200	98.06	100.88	98.20	97.98	100.63	97.74
250	97.48	99.90	97.07	97.56	99.88	96.91
315	97.03	99.02	95.17	97.00	98.59	95.00
400	95.28	95.04	93.02	95.21	94.97	92.46
500	97.29	94.94	92.41	96.86	94.56	92.39
630	95.52	93.98	92.93	96.26	94.40	93.36
800	92.96	92.73	89.52	93.12	92.67	89.27
1000	91.59	92.46	88.58	91.73	91.99	88.63
1250	91.14	90.61	88.68	91.19	90.63	88.66
1600	93.94	90.88	88.73	93.81	90.90	88.29
2000	89.91	89.71	87.82	89.77	89.82	87.74
2500	88.70	89.66	86.88	88.62	88.98	86.74
3150	96.43	93.06	88.65	96.00	91.53	89.08
4000	86.41	85.24	85.38	86.67	85.56	85.26
5000	83.29	82.00	83.32	85.63	83.98	84.52
6300	82.35	79.89	81.24	82.04	80.27	81.14
8000	81.08	79.14	78.21	80.56	78.92	77.87
10000	90.38	88.22	84.03	89.86	88.17	83.76
12500	64.79	62.82	63.57	65.10	62.92	63.42
16000	52.66	50.22	50.17	52.65	50.42	50.10
20000	49.74	46.87	45.57	48.98	46.57	45.40

Closed Door Landing Segment

3rd Octave Center Frequency [Hz]	Run A Seat [dB]	Run A Stand [dB]	Run A Pilot [dB]	Run B Seat [dB]	Run B Stand [dB]	Run B Pilot [dB]
12.5	82.79	82.58	82.40	83.62	83.36	83.19
16	83.19	82.86	83.07	81.33	80.97	80.90
20	96.55	96.22	97.08	99.52	98.64	98.69
25	89.68	87.96	87.31	91.10	88.80	86.96
31.5	85.73	82.07	83.48	85.96	82.28	84.22
40	92.76	90.17	92.24	94.44	91.35	95.60
50	95.47	91.62	87.93	97.18	93.22	88.49
63	94.06	92.70	90.49	94.83	92.95	91.53
80	85.81	87.73	89.73	86.93	88.90	91.13
100	103.29	99.79	99.55	105.71	101.62	99.14
125	100.90	96.80	90.15	100.10	97.08	90.08
160	89.68	90.50	88.54	90.06	90.00	87.92
200	87.33	89.06	88.87	88.67	88.81	89.41
250	86.47	86.65	86.26	86.02	85.86	86.73
315	89.06	89.01	87.00	87.88	91.31	86.61
400	85.97	85.27	82.27	86.14	85.26	82.17
500	96.64	87.26	86.90	96.45	87.84	87.64
630	89.96	87.97	86.80	89.35	90.25	88.29
800	88.27	85.98	81.63	87.40	85.96	81.31
1000	86.56	87.92	81.30	86.79	86.86	81.43
1250	86.66	85.80	81.62	86.96	85.78	81.11
1600	89.34	89.02	87.30	89.78	87.73	86.97
2000	87.62	85.52	82.32	87.45	86.21	81.80
2500	85.19	84.29	78.12	84.95	83.52	78.44
3150	95.69	95.35	89.08	95.28	96.03	87.83
4000	85.13	82.93	78.80	85.13	84.08	79.24
5000	84.16	79.37	74.83	84.18	79.57	75.07
6300	81.12	78.34	73.59	81.23	78.33	73.69
8000	85.08	82.98	78.28	85.08	83.32	78.94
10000	92.98	89.44	85.33	92.11	89.96	85.64
12500	64.89	61.41	58.25	65.13	61.58	58.38
16000	52.65	49.72	46.58	52.71	49.59	46.59
20000	49.45	46.50	45.60	49.58	46.58	45.63

Open Door Ground Segment

3rd Octave Center Frequency [Hz]	Run A Seat [dB]	Run A Stand [dB]	Run A Pilot [dB]	Run B Seat [dB]	Run B Stand [dB]	Run B Pilot [dB]
12.5	82.87	83.51	84.19	81.85	82.11	83.22
16	87.85	89.27	91.75	88.56	89.81	91.96
20	100.98	102.71	106.51	95.77	97.83	101.69
25	89.01	90.17	94.54	87.42	88.25	92.16
31.5	79.21	78.62	81.47	80.07	79.37	81.35
40	95.94	94.63	95.93	94.74	93.17	91.40
50	109.66	110.07	106.69	109.86	110.51	107.86
63	94.93	93.26	90.79	93.70	92.87	91.04
80	90.71	88.90	90.68	90.25	87.55	89.26
100	103.45	104.27	103.96	104.19	104.62	103.14
125	95.50	92.66	91.81	94.44	91.63	90.71
160	99.24	99.01	96.84	98.53	98.14	97.48
200	95.65	96.05	94.03	95.05	96.70	93.43
250	94.81	95.14	92.11	95.69	95.08	92.60
315	97.65	95.50	92.11	97.43	95.93	91.91
400	95.26	96.80	88.15	96.07	96.97	87.99
500	97.24	98.08	89.00	97.52	98.60	89.02
630	96.09	94.89	90.17	96.66	95.25	89.22
800	94.89	93.74	88.66	95.44	94.79	89.74
1000	96.83	95.56	88.33	97.99	96.51	88.93
1250	95.02	95.17	87.49	95.63	95.93	87.79
1600	94.15	93.61	86.94	93.05	93.85	87.04
2000	91.19	89.95	84.66	91.42	90.27	85.20
2500	89.24	87.34	82.59	89.22	87.93	83.10
3150	91.25	88.93	85.04	91.72	88.09	84.29
4000	85.76	84.92	79.56	85.63	85.25	79.96
5000	84.48	82.85	77.68	84.52	83.15	78.01
6300	85.68	84.31	78.02	85.71	84.34	78.34
8000	90.75	90.49	83.39	93.20	89.65	84.83
10000	79.59	77.83	72.02	80.50	78.59	73.14
12500	66.81	65.01	60.90	67.14	65.50	62.03
16000	55.38	52.96	48.86	55.63	53.46	49.12
20000	44.42	43.92	44.42	44.52	44.01	44.46

Open Door Hover Segment

3rd Octave Center Frequency [Hz]	Run A Seat [dB]	Run A Stand [dB]	Run A Pilot [dB]	Run B Seat [dB]	Run B Stand [dB]	Run B Pilot [dB]
12.5	93.50	91.24	91.47	91.53	91.20	91.28
16	93.41	92.31	94.76	92.36	91.52	94.36
20	104.93	107.05	110.86	103.36	105.50	108.78
25	90.88	90.47	95.52	89.19	89.73	94.32
31.5	87.81	85.67	87.73	86.27	84.09	86.58
40	94.82	93.48	94.55	94.65	93.01	91.95
50	101.79	103.31	102.17	102.06	103.53	102.55
63	95.15	94.19	94.77	93.40	92.43	92.80
80	92.24	89.31	93.32	91.21	88.02	92.02
100	100.63	100.04	103.52	100.22	98.19	102.84
125	91.52	89.72	89.25	89.97	88.27	89.10
160	93.95	94.85	91.44	93.24	93.68	92.18
200	91.54	93.82	89.65	90.99	93.57	88.49
250	88.97	87.47	87.43	88.08	86.91	85.60
315	91.16	90.68	88.05	90.37	90.05	87.31
400	89.12	89.88	84.83	88.23	88.74	83.78
500	93.01	93.57	86.55	92.46	92.16	86.18
630	94.25	93.42	87.86	92.87	92.04	88.33
800	94.39	92.34	86.17	93.96	91.68	85.64
1000	92.66	92.06	86.49	92.91	91.34	86.30
1250	91.22	90.85	85.15	90.55	90.26	84.31
1600	93.25	90.51	85.93	92.80	89.95	84.83
2000	90.22	88.45	84.56	89.75	87.92	83.87
2500	88.70	85.55	81.36	88.51	85.37	81.05
3150	94.81	90.13	86.65	95.81	91.56	86.84
4000	85.62	83.50	79.00	86.14	83.98	79.00
5000	82.76	81.06	76.22	82.12	80.92	75.63
6300	83.14	80.63	76.45	83.48	81.39	77.02
8000	82.69	81.01	76.80	83.25	81.67	77.38
10000	90.33	90.41	84.53	90.78	88.59	84.84
12500	63.75	61.44	57.90	64.46	62.31	58.81
16000	51.45	48.92	46.24	52.06	49.46	46.49
20000	48.83	46.21	45.47	48.94	46.23	45.37

Open Door Climb Segment

3rd Octave Center Frequency [Hz]	Run A Seat [dB]	Run A Stand [dB]	Run A Pilot [dB]	Run B Seat [dB]	Run B Stand [dB]	Run B Pilot [dB]
12.5	94.11	92.95	89.47	94.90	93.06	91.03
16	97.63	94.55	95.65	97.27	94.60	96.64
20	105.74	108.31	111.00	104.00	108.18	111.18
25	93.82	92.14	96.89	93.67	92.91	98.20
31.5	92.93	91.04	93.78	94.12	92.78	94.77
40	97.06	93.50	92.46	97.98	95.67	92.43
50	102.65	103.67	102.08	102.48	103.48	101.95
63	94.34	93.21	92.17	94.52	93.07	92.38
80	93.24	89.90	92.23	93.21	89.88	93.03
100	99.78	99.73	103.76	98.91	99.01	102.59
125	92.23	89.93	88.90	91.76	89.59	89.20
160	93.48	93.59	91.78	94.21	93.45	91.80
200	90.46	91.18	88.48	90.40	92.21	88.20
250	86.89	86.81	85.75	87.31	87.63	85.30
315	87.97	89.53	87.28	89.10	90.37	87.93
400	84.12	83.99	80.40	84.20	84.13	80.22
500	90.32	91.27	83.75	90.20	89.92	84.21
630	92.63	88.83	86.87	92.55	87.46	87.06
800	87.55	84.19	79.60	87.73	84.24	79.64
1000	86.86	84.54	81.31	88.69	84.89	81.54
1250	87.52	84.39	79.81	87.78	85.00	80.31
1600	92.89	87.05	82.21	92.04	86.83	82.70
2000	88.48	85.38	79.84	88.48	85.28	80.26
2500	86.30	82.23	78.31	86.92	83.03	78.86
3150	94.59	92.34	90.85	95.08	92.57	89.10
4000	84.97	81.46	77.83	84.37	82.37	77.38
5000	82.01	81.34	74.26	81.12	78.83	74.50
6300	82.41	79.13	73.78	82.08	78.80	73.68
8000	83.68	81.77	77.24	85.14	83.17	78.16
10000	91.47	89.41	83.21	91.74	88.43	82.97
12500	65.67	63.66	59.98	65.96	63.88	60.21
16000	52.66	49.46	46.51	52.35	49.44	46.41
20000	48.73	45.99	45.04	48.76	46.01	45.06

Open Door Steady Level Flight (60 knots) Segment

3rd Octave Center Frequency [Hz]	Run A Seat [dB]	Run A Stand [dB]	Run A Pilot [dB]	Run B Seat [dB]	Run B Stand [dB]	Run B Pilot [dB]
12.5	98.17	93.78	93.52	100.26	94.49	94.29
16	103.73	98.14	100.78	102.25	96.83	99.43
20	103.78	108.62	112.89	104.32	108.47	113.57
25	93.75	94.10	96.96	93.07	95.60	99.37
31.5	92.41	92.28	91.45	91.63	92.20	91.18
40	102.94	101.85	101.53	102.45	101.65	101.57
50	104.42	105.20	103.21	103.69	104.61	102.91
63	97.40	95.82	95.63	96.67	95.82	95.80
80	98.93	96.19	95.52	95.36	93.14	93.64
100	103.59	101.57	102.53	104.07	101.98	99.65
125	96.35	92.74	90.56	93.29	90.73	89.23
160	97.73	97.13	94.48	97.61	96.18	93.87
200	97.99	99.80	91.25	97.01	99.12	90.55
250	93.29	96.33	91.77	92.36	94.76	90.59
315	94.40	93.34	90.99	94.50	93.27	90.44
400	92.72	93.24	88.87	90.96	91.79	86.50
500	93.02	93.59	87.07	93.23	92.22	85.66
630	92.63	90.53	86.57	92.25	89.44	85.57
800	91.54	90.46	84.91	91.59	90.24	84.26
1000	92.35	90.03	85.13	92.30	90.07	84.63
1250	89.17	88.31	82.41	89.50	88.50	81.79
1600	90.94	89.02	84.15	91.89	88.69	84.33
2000	88.16	86.98	82.32	88.52	86.20	82.21
2500	86.96	84.76	80.75	87.19	84.60	80.44
3150	91.17	91.23	84.60	93.86	88.97	87.76
4000	84.73	83.15	77.13	84.71	83.56	77.18
5000	81.53	78.69	74.65	81.52	78.92	74.61
6300	82.33	79.25	74.06	82.27	79.38	74.03
8000	91.02	87.52	82.21	92.09	87.95	82.85
10000	79.38	77.80	73.76	80.06	78.39	74.17
12500	65.42	63.37	59.73	65.75	63.62	60.02
16000	53.88	50.54	47.03	54.09	50.64	47.15
20000	44.67	43.91	44.42	44.76	43.98	44.43

Open Door Steady Level Flight (80 knots) Segment

3rd Octave Center Frequency [Hz]	Run A Seat [dB]	Run A Stand [dB]	Run A Pilot [dB]	Run B Seat [dB]	Run B Stand [dB]	Run B Pilot [dB]
12.5	98.87	98.25	96.58	99.93	98.42	97.17
16	102.03	98.40	99.03	102.13	98.52	99.33
20	116.75	115.38	119.66	118.30	114.65	119.26
25	106.82	98.52	103.74	107.75	99.54	104.58
31.5	101.71	98.74	95.65	103.17	98.95	96.35
40	101.11	99.81	99.17	101.55	100.08	98.20
50	106.36	107.11	104.66	106.23	106.91	104.73
63	100.60	99.04	99.21	100.93	99.22	99.69
80	100.55	97.87	98.38	100.82	98.08	98.34
100	101.02	101.30	103.56	101.67	101.72	102.66
125	95.51	92.07	91.15	95.59	92.11	91.00
160	96.86	96.96	95.46	96.29	96.63	96.22
200	95.94	97.58	91.02	96.38	97.59	91.38
250	93.18	93.56	91.62	92.97	93.58	91.30
315	92.54	92.89	91.61	93.29	93.38	90.59
400	90.80	91.38	85.66	90.99	91.59	85.27
500	92.38	93.00	86.43	92.81	91.95	85.81
630	93.05	90.66	86.91	93.13	90.33	86.36
800	92.41	91.21	85.06	92.43	91.14	84.99
1000	93.09	90.94	85.74	93.36	91.18	85.72
1250	90.96	90.29	84.23	91.26	90.44	84.17
1600	92.22	89.64	85.49	92.08	89.08	85.71
2000	90.07	88.43	83.80	89.59	87.52	84.08
2500	88.30	86.48	82.22	88.54	86.46	82.49
3150	91.84	91.55	86.16	93.86	89.55	88.40
4000	85.46	84.52	78.72	85.07	85.05	79.31
5000	82.14	79.77	75.87	82.13	79.98	75.98
6300	82.28	79.50	74.36	82.34	79.65	74.51
8000	89.54	87.32	81.89	90.11	87.54	81.80
10000	81.68	80.10	75.70	82.34	80.52	76.18
12500	66.53	64.98	61.61	66.84	65.16	61.88
16000	54.74	50.64	47.53	55.88	50.51	47.56
20000	47.81	44.35	44.78	50.49	44.39	44.80

Open Door Descent Segment

3rd Octave Center Frequency [Hz]	Run A Seat [dB]	Run A Stand [dB]	Run A Pilot [dB]	Run B Seat [dB]	Run B Stand [dB]	Run B Pilot [dB]
12.5	98.29	97.50	95.40	98.55	97.01	95.68
16	101.71	98.86	98.25	101.77	98.40	97.48
20	112.39	113.22	119.92	111.48	112.26	118.52
25	107.94	101.61	107.97	106.06	101.56	107.67
31.5	103.82	99.20	96.84	102.33	99.98	97.78
40	108.08	106.49	101.08	110.05	108.23	100.64
50	107.26	107.64	105.44	105.67	106.02	103.91
63	102.90	102.56	103.77	104.95	105.16	106.99
80	102.84	99.61	100.13	103.61	100.80	100.27
100	103.95	102.68	101.25	103.96	101.80	100.65
125	101.05	97.92	92.38	99.97	98.32	94.01
160	103.16	102.26	96.30	103.85	103.09	97.10
200	105.05	105.89	97.90	105.07	106.09	98.73
250	100.20	101.40	94.37	102.01	103.82	95.83
315	96.44	98.30	94.37	97.76	99.28	95.00
400	96.27	96.54	93.64	97.36	97.57	95.42
500	96.42	95.79	89.39	97.33	96.07	90.90
630	93.77	93.17	88.58	94.04	92.87	88.25
800	92.55	92.24	87.36	93.12	92.59	87.40
1000	92.75	90.65	86.28	93.00	90.79	86.99
1250	90.05	88.83	84.59	90.30	89.05	84.67
1600	91.33	88.44	85.28	91.95	87.67	84.44
2000	88.47	86.47	83.39	89.10	86.74	83.81
2500	87.34	84.88	81.06	87.22	84.31	81.14
3150	91.11	88.73	85.31	90.44	89.17	88.99
4000	85.00	82.72	78.10	84.44	82.85	78.10
5000	82.97	80.25	76.08	82.54	80.12	76.25
6300	83.84	80.10	75.17	83.48	79.89	75.26
8000	90.71	87.05	81.73	90.94	87.73	82.21
10000	78.89	77.70	73.41	79.12	77.98	73.82
12500	65.86	64.07	60.71	65.90	64.50	61.06
16000	54.86	51.00	48.50	54.72	51.31	48.16
20000	46.87	44.70	45.35	46.59	44.87	44.92

Open Door Landing Segment

3rd Octave Center Frequency [Hz]	Run A Seat [dB]	Run A Stand [dB]	Run A Pilot [dB]	Run B Seat [dB]	Run B Stand [dB]	Run B Pilot [dB]
12.5	90.09	88.81	88.75	91.03	88.77	89.89
16	91.39	90.73	92.71	91.12	91.12	93.40
20	103.83	106.18	109.75	103.68	105.80	109.62
25	91.36	92.05	96.55	91.49	92.42	97.07
31.5	85.95	84.35	87.00	86.06	84.58	87.27
40	96.53	95.30	95.66	95.33	94.17	94.85
50	104.14	105.09	103.05	101.90	103.16	101.85
63	99.40	99.85	98.91	100.37	101.39	100.60
80	94.34	91.71	93.24	92.93	89.93	92.01
100	101.41	100.48	103.66	101.87	100.23	101.96
125	96.52	95.17	91.91	98.44	97.27	92.00
160	96.40	96.74	94.37	96.20	96.92	95.85
200	93.25	95.33	91.63	93.38	94.66	91.45
250	92.18	91.64	89.85	91.65	91.98	89.15
315	93.90	92.91	89.56	93.47	92.56	88.96
400	91.99	92.73	86.35	90.83	92.16	85.35
500	94.48	95.41	87.61	94.91	94.94	87.42
630	94.50	93.42	88.63	94.38	92.57	88.33
800	94.35	92.38	86.77	94.35	92.70	86.76
1000	94.25	93.14	86.50	94.84	93.42	86.92
1250	92.44	91.94	85.34	92.09	92.26	85.39
1600	92.96	91.36	85.72	92.69	90.86	85.74
2000	90.67	88.63	84.12	90.53	88.55	84.43
2500	88.32	85.75	81.30	88.44	85.95	81.50
3150	95.44	91.46	86.86	96.39	92.83	87.72
4000	85.42	84.15	79.17	85.52	84.27	79.09
5000	83.17	81.53	76.74	83.08	81.73	76.53
6300	84.13	81.92	77.03	84.31	82.32	77.34
8000	85.32	84.20	79.01	85.91	84.83	79.66
10000	90.56	89.66	83.77	90.60	88.41	84.10
12500	65.16	63.16	59.40	65.56	63.59	60.05
16000	52.80	50.56	46.99	53.10	50.81	47.08
20000	48.50	46.10	45.35	48.73	46.13	45.30